

UNCLASSIFIED

AD NUMBER
ADB045250
NEW LIMITATION CHANGE
TO Approved for public release, distribution unlimited
FROM Distribution authorized to U.S. Gov't. agencies only; Test and Evaluation; Dec 1979. Other requests shall be referred to Air Force Materials Lab., Polymar Branch, Wright-Patterson AFB, OH 45433.
AUTHORITY
AFWAL ltr, 3 Aug 1983

THIS PAGE IS UNCLASSIFIED

AFML-TR-79-4182

ADB045250

MECHANISMS OF POLYMER CURING AND THERMAL DEGRADATION

E. G. JONES

J. M. PICKARD

D. L. PEDRICK

RESEARCH APPLICATIONS DIVISION

SYSTEMS RESEARCH LABORATORIES, INC.

2800 INDIAN RIPPLE ROAD

DAYTON, OH 45440

DECEMBER 1979

TECHNICAL REPORT AFML-TR-79-4182

Interim Report for period June 1978 — June 1979

Distribution limited to U. S. Government agencies only.

AIR FORCE MATERIALS LABORATORY

AIR FORCE WRIGHT AERONAUTICAL LABORATORIES

AIR FORCE SYSTEMS COMMAND

WRIGHT-PATTERSON AIR FORCE BASE, OHIO 45433

BEST AVAILABLE COPY

200 4022 4077

NOTICE


When Government drawings, specifications, or other data are used for any purpose other than in connection with a definitely related Government procurement operation, the United States Government thereby incurs no responsibility nor any obligation whatsoever; and the fact that the government may have formulated, furnished, or in any way supplied the said drawings, specifications, or other data, is not to be regarded by implication or otherwise as in any manner licensing the holder or any other person or corporation, or conveying any rights or permission to manufacture, use, or sell any patented invention that may in any way be related thereto.

This report has been reviewed by the Information Office (OI) and is releasable to the National Technical Information Service (NTIS). At NTIS, it will be available to the general public, including foreign nations.

This technical report has been reviewed and is approved for publication.

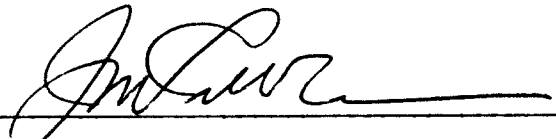


IVAN J. GOLDFARB
Project Monitor



R. L. VAN DEUSEN, Chief
Polymer Branch
Nonmetallic Materials Division

FOR THE COMMANDER



J. M. KELBLE, Chief
Nonmetallic Materials Division

"If your address has changed, if you wish to be removed from our mailing list, or if the addressee is no longer employed by your organization please notify AFML/MBP, W-PAFB, OH 45433 to help us maintain a current mailing list".

Copies of this report should not be returned unless return is required by security considerations, contractual obligations, or notice on a specific document.

REPORT DOCUMENTATION PAGE		READ INSTRUCTIONS BEFORE COMPLETING FORM
1. REPORT NUMBER AFML-TR-79-4182	2. GOVT ACCESSION NO.	3. RECIPIENT'S CATALOG NUMBER
4. TITLE (and Subtitle) MECHANISMS OF POLYMER CURING AND THERMAL DEGRADATION	5. TYPE OF REPORT & PERIOD COVERED June 1978-June 1979	
	6. PERFORMING ORG. REPORT NUMBER	
7. AUTHOR(s) E. G. Jones, J. M. Pickard, and D. L. Pedrick	8. CONTRACT OR GRANT NUMBER(s) F33615-77-C-5175	
9. PERFORMING ORGANIZATION NAME AND ADDRESS Systems Research Laboratories, Inc. 2800 Indian Ripple Road Dayton, OH 45440	10. PROGRAM ELEMENT, PROJECT, TASK AREA & WORK UNIT NUMBERS 2419 04 04	
11. CONTROLLING OFFICE NAME AND ADDRESS Air Force Materials Laboratory (MBP) Wright-Patterson Air Force Base, OH 45433	12. REPORT DATE December 1979	
	13. NUMBER OF PAGES 124	
14. MONITORING AGENCY NAME & ADDRESS (if different from Controlling Office)	15. SECURITY CLASS. (of this report) Unclassified	
	15a. DECLASSIFICATION/DOWNGRADING SCHEDULE	
16. DISTRIBUTION STATEMENT (of this Report) Distribution limited to U. S. Government agencies only; (test and evaluation). Other requests for this document must be referred to the Air Force Materials Laboratory, Nonmetallic Materials Division, Polymer Branch, AFML/MBP, Wright- Patterson Air Force Base, OH 45433		
17. DISTRIBUTION STATEMENT (of the abstract entered in Block 20, if different from Report)		
18. SUPPLEMENTARY NOTES		
19. KEY WORDS (Continue on reverse side if necessary and identify by block number) Bis[4-3(3-Ethynylphenoxy)Phenyl]Sulfone Thermochemistry Thermogravimetry Acetylene-Terminated Oligomers Kinetic Chain Length Mass Spectra Polymer Kinetics Molecular Weight Differential Scanning Calorimetry Polymer Degradation Polymerization Mechanisms Polymer Analysis 4-(3-Ethynylphenoxy)Phenyl Phenyl Sulfone		
20. ABSTRACT (Continue on reverse side if necessary and identify by block number) The results of a TGMS analysis of a series of polymers are presented. Sample weight loss and volatile gas evolution during programmed heating of polymers are correlated in order to investigate thermal stability and the mechanism of thermal degradation. Thermal polymerization at 434 K of bis[4-(3- ethynylphenoxy)phenyl]sulfone (I) in the initial stages of reaction and of 4-(3-ethynylphenoxy)phenyl phenyl sulfone (II) up to 90% conversion was found to yield polymers with number-average molecular weights approaching 3000. The IR spectrum of polymer (I) contains a band at 3300 cm ⁻¹ , indicating		

20. Abstract continued

the presence of free ethynyl moieties in the polymer. Both polymers exhibit weak bands in the region of 950 cm^{-1} , indicative of trans-unsaturation. The existence of trans-unsaturation in the polymer backbone is confirmed by ^1H NMR for both polymers and by ^{13}C NMR for polymer (II) from analysis of spectral perturbations induced by the addition of a shift reagent, $\text{Eu}(\text{fod})_3$. The kinetics of polymerization of Oligomer (I) were determined using differential scanning calorimetry over the range of 467 to 533 K. Least-squares analysis of the rate data was used to obtain an apparent activation energy, $E = 24.2 \pm 0.7\text{ kcal/mol}$, and logarithm of the pre-exponential factor, $\log (A/\text{s}^{-1}) = 8.5 \pm 0.6$. In the pre-gel stages of polymerization at constant conversion, the number-average molecular weight of the polymer exhibited a small exponential temperature dependence. These data are examined in terms of a free-radical chain mechanism in which molecular weight is controlled by a first-order termination reaction.

PREFACE

This report was prepared by Drs. E. Grant Jones and James M. Pickard with the assistance of Mr. Donald L. Pedrick. Work was performed under contract F33615-77-C-5175 by the Research Applications Division of Systems Research Laboratories, Inc., 2800 Indian Ripple Road, Dayton, OH 45440. The contract was administered under the direction of the Air Force Materials Laboratory (AFML/MBP), Wright-Patterson Air Force Base, OH, with Dr. Ivan J. Goldfarb as Project Monitor.

Studies were conducted during the period June 1978 through June 1979 jointly at the Systems Research Laboratories Polymer Facility and at the Air Force Materials Laboratory.

The authors would like to acknowledge the editorial assistance of Mrs. Marian M. Whitaker in the report preparation.

Valuable discussions with the Polymer Scientists at the Air Force Materials Laboratory are appreciated.

TABLE OF CONTENTS

SECTION	PAGE
I INTRODUCTION	1
II EXPERIMENTAL	3
Polymer Characterization and Synthesis	3
TGMS Apparatus	3
Polymer Synthesis	3
NMR and IR Spectra	4
Molecular Weights	5
Polymer Kinetics	5
Thermochemistry	6
III RESULTS AND DISCUSSION	7
Polymer Characterization	7
TGMS Analysis	7
IR Spectra	29
¹ H NMR Spectra	33
¹³ C NMR Spectra	36
Polymer Kinetics and Thermochemistry	42
DSC Kinetics	42
Effect of Reaction Variables on Molecular Weight	46
Proposed Reaction Mechanism	50
IV SUMMARY, CONCLUSIONS, AND RECOMMENDATIONS	57
Summary and Conclusions	57
Recommendations	58
REFERENCES	59
APPENDIX - PUBLICATIONS AND PRESENTATIONS UNDER CONTRACT F33615-77-C-5175 FOR PERIOD JUNE 1978 - JUNE 1979	61
"The Kinetics and Mechanism of the Bulk Thermal Polymerization of (3-Phenoxyphenyl)Acetylene"	62

TABLE OF CONTENTS Continued

SECTION	PAGE
"The Polymerization of Bis[4-(3-Ethynylphenoxy)Phenyl] Sulfone and 4-(3-Ethynylphenoxy)Phenyl Phenyl Sulfone"	104
"The Kinetics and Mechanism of the Bulk Thermal Polymerization of Bis[4-(3-Ethynylphenoxy)Phenyl]-Sulfone"	105

LIST OF ILLUSTRATIONS

FIGURE		PAGE
1	Ion Intensity as Function of Temperature for Tri ϕ PBT.	20
2	Ion Intensity as Function of Temperature for Tri ϕ PBO.	21
3	Ion Intensity as Function of Temperature for PBT.	23
4	Ion Intensity as Function of Temperature for PBO .	24
5	Ion Intensity as Function of Temperature for DAPI .	28
6	IR Spectrum of Bis[4-(3-Ethynylphenoxy)Phenyl]Sulfone (a) Oligomer Film NaCl Plate; (b) Polymer, KBr Matrix.	30
7	IR Spectrum of Bis[4-(3-Dideuterioethynylphenoxy)Phenyl]- Sulfone (a) Oligomer; (b) Polymer.	31
8	IR Spectrum of 4-(3-Ethynylphenoxy)Phenyl Phenyl Sulfone (a) Oligomer; (b) Polymer.	32
9	¹ H NMR Spectrum of Bis(4-(3-Ethynylphenoxy)Phenyl]Sulfone from 3 to 8 ppm Relative to TMS; (a) Oligomer 0.2 M in CDCl ₃ ; (b) Polymer 0.05 g/ml with 0.07 M Eu(fod) ₃ in CDCl ₃ .	34
10	¹ H NMR Spectrum for 4-(3-Ethynylphenoxy)Phenyl Phenyl Sulfone from 3 to 8 ppm Relative to TMS; (a) Oligomer, 0.2 M in CDCl ₃ ; (b) Polymer, 0.05 g/ml with 0.05 M Eu(fod) ₃ in CDCl ₃ .	35
11	¹³ C Spectrum at 4-(3-Ethynylphenoxy)Phenyl Phenyl Sulfone, δ vs [Eu(fod) ₃].	39
12	¹³ C Spectrum of Poly[4-(3-Ethynylphenoxy)Phenyl Phenyl Sulfone], δ vs [Eu(fod) ₃].	40
13	Dynamic DSC Exotherms for Bis[4-(3-Ethynylphenoxy) Phenyl] Sulfone. Heat Rate in (K/min): \circ , 80; Δ , 40; +, 20; x, 10; \square , 5 .	43
14	Arrhenius Plot for Thermal Reaction of Bis[4-(3-Ethynylphenoxy) Phenyl]Sulfone from 467 to 533 K .	45
15	Cummulative Differential Molecular Weight Distributions for Thermal Polymerizations of Oligomers at 434 K (a) Oligomer (I); (b) Oligomer (II).	48
16	Influence of Conversion upon the Ratio M_w/M_n at 434 K for Bis[4-(3-Ethynylphenoxy)Phenyl]Sulfone.	49

LIST OF ILLUSTRATIONS (cont'd)

FIGURE		PAGE
17	Temperature Dependence of Number-Average Molecular Weight at 25% Conversion.	51
18	Proposed Reaction Mechanism for Thermal Polymerization of Bis[4-(3-Ethynylphenoxy) Phenyl]Sulfone.	53
19	Temperature Dependence of the Number-Average Degree of Polymerization at Constant Conversion.	56

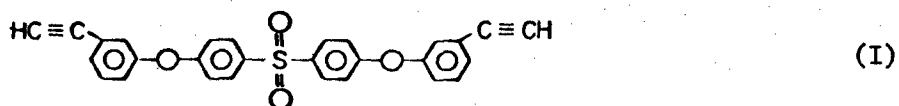
LIST OF TABLES

TABLE		PAGE
1	Comparison at Thermal Degradation of PBO and Tri ϕ PBO	16
2	Comparison of Thermal Degradation of PBT and Tri ϕ PBT	18
3	Summary of ^1H NMR Data	37
4	Summary of ^{13}C NMR Data	38
5	Summary of Dynamic DSC Data	44
6	Heat of Polymerization of Bis[4-(3-Ethynylphenoxy)Phenyl] Sulfone	47
7	Effect of Temperature upon Number-Average Molecular Weight at Constant Conversion	52

SECTION I

INTRODUCTION

In recent years, extensive research has been directed toward synthesis and characterization of acetylene-terminated oligomers consisting of sulfones, imides, and quinoxalines having potential for use as adhesives and composites in high-temperature aerospace environments [1]. The oligomers, for example, bis[4-(3-ethynylphenoxy)phenyl]sulfone



cure by the reaction of the terminal ethynyl moieties without evolution of volatile products, thereby avoiding the cavitation problem encountered with more conventional resin systems.

In the polymer curing reaction, knowledge of the mechanism of chain initiation, the resultant degree of polymerization, degree of cross linking, and mode of chain termination are important kinetic parameters that may be correlated with the desired mechanical properties and thermal stabilities. In this vein, 4-(3-ethynylphenoxy)phenyl phenyl sulfone,



would be expected to possess a reactivity comparable to that of simple arylacetylenes as well as that of the acetylene-terminated oligomer indicated by Structure (I).

Detailed kinetic studies of the polymer curing reaction, coupled with knowledge related to the degradation mechanism which may be obtained from thermogravimetric-mass spectrometric analysis of the cured resins, may be used to guide the design and synthesis of new polymers and insure adherence to rigid quality-control standards required for optimum performance under extreme environmental conditions.

This report summarizes TGMS analyses for a series of acetylene-terminated and related oligomers and kinetic and mechanistic investigations of the curing reaction of oligomers (I) and (II).

SECTION II

EXPERIMENTAL

POLYMER CHARACTERIZATION AND SYNTHESIS

TGMS Apparatus

During the report period the following modifications to the TGMS apparatus were completed

- a) installed new support for furnace
- b) mounted temperature controller, DVM, and Hewlett-Packard counter in panels
- c) installed three-station variac to regulate heating tapes
- d) installed Nupro cut-off valves for the fine roughing and gas-purging lines
- e) relocated TGMS apparatus.

Thermal-degradation studies involved monitoring sample weight and mass spectra of volatile gases evolved during a programmed heating in vacuum from room temperature to 1000°C.

Polymer Synthesis

Samples of bis[4-(3-ethynylphenoxy)phenyl]sulfone (I) and 4-(3-ethynylphenoxy)-phenyl phenyl sulfone (II), obtained from the Polymer Branch of the Air Force Materials Laboratory, were purified by recrystallization from hexane prior to use.

Deuteration of oligomer (I) was conducted in dry THF at -40°C by reaction of 4 g with excess butyl lithium followed by hydrolysis of the resultant lithium salt with excess D₂O. After removal of THF, the deuterated oligomer was purified by three repetitive recrystallizations from dry hexane. ¹H NMR analysis of the oligomer indicated an isotopic composition of 98.1 mol % D.

Thermal polymerizations of the oligomers were conducted in sealed tubes at 434 K under a nitrogen atmosphere. Reaction times for oligomer (I) and the deuterated analogue were limited to 0.75 hr (~25% conversion) in order to minimize the formation of the crosslinked polymer. Oligomer II was reacted 3 hr to obtain a conversion approaching 90%. The reaction products of each polymerization were dissolved in CH_2Cl_2 , and the polymers were isolated by addition of methanol. Analysis of the protonated polymers by vapor-phase osmometry revealed that the number-average molecular weight of polymers I and II were 2785 and 2620, respectively.

NMR and IR Spectra

Infrared spectra of the polymers and oligomers were obtained with a Perkin-Elmer 521 infrared spectrophotometer in KBr matrices unless otherwise stated.

Nuclear magnetic resonance spectra were obtained with a Varian XL 100/15 NMR interfaced with a Varian VFT-100 computer and gyrocode decoupler. Proton spectra of the oligomers (0.2 M in CDCl_3) and polymers (0.05 g/ml in CDCl_3) as well as those obtained in the presence of 0.01 to 0.07 M concentrations of a shift reagent, $\text{Eu}(\text{fod})_3$, were recorded in the CW mode at 100.1 MHz. Chemical shifts were measured relative to internal TMS.

Pulsed FT ^{13}C spectra at 25.2 MHz for oligomer and polymer (I) were obtained in 1.7-mm tubes, while the spectra for oligomer and polymer (II) were obtained in 12-mm tubes. Proton-noise decoupled spectra of the oligomers were obtained using a 65° pulse and repetition time of 4.8 sec, while those of the polymers along with decoupled spectra were obtained with a 25° pulse and repetition time of 0.8 sec.

Molecular Weights

Molecular-weight data were obtained with a Waters Model 244 Liquid Chromatograph (GPC) using 10^4 , 10^3 , $2(5 \times 10^2)$, and 10^2 Å μ -STYRAGEL columns with THF as the solvent at a flow rate of 1 ml/min. Calibration of the GPC columns was based upon isolated fractions of a polymer of known molecular weight determined with a Mecrolab vapor-phase osmometer. Examination of the GPC trace of the reaction products revealed the presence of the polymers as well as two oligomeric fractions. Weight- and number-average molecular weights of the product distribution, including the oligomeric fractions, were determined as functions of conversion and temperature from the areas of the GPC curves using the relation

$$M = \frac{\sum_i N_i M_i^b}{\sum_i N_i M_i^{b-1}} \quad (1)$$

In Eq. (1), $b=1$ for the number-average molecular weight, M_n , while $b=2$ for the weight average, i.e., $M = M_w$. The symbol N_i refers to the number of species with molecular weight M_i .

Polymer Kinetics

For kinetic studies, conversion data were determined from dynamic Differential Scanning Calorimetry (DSC) using a Perkin-Elmer DSC-II calibrated against lead and indium at heating rates of 80, 40, 20, 10 and 5 K/min. The disappearance of monomer was determined from Eq. (2)

$$-\frac{1}{W_0} \left(\frac{dW}{dt} \right) = \frac{1}{Q} \left(\frac{dq}{dt} \right) = A 10^{-E/\theta} F(W) \quad (2)$$

where dq/dt is the differential power output in mcal/sec, Q is total heat of reaction in mcal, W_0 is the initial weight of monomer, and W is the weight of residual monomer at time, t . The variables A and E are the usual Arrhenius parameters and $\theta = 2.303 RT$ kcal/mol.

The quantity $F(W)$ in Eq. (1) represents a concentration variable of the form

$$F(W) = (W/W_0)^n = (1 - \alpha)^n \quad (3)$$

where n is reaction order and α is the conversion at time t . The apparent rate constant, k_{ap} , is $A10^{-E/\theta}$ so that Eqs. (1) and (2) may be combined to obtain

$$\frac{d\alpha}{dt} = k_{ap} (1 - \alpha)^n \quad (4)$$

Thermochemistry

The enthalpy change of the reaction in kcal/mol was determined from

$$\Delta H_p = \Delta H_s (A_m/A_s) (W_s/W_m) \quad (5)$$

where ΔH_s is the heat of fusion of an indium standard, A_m and A_s are areas of the exotherms, and W_m and W_s are weights of the monomer and standard.

In a typical DSC, samples of monomer (2-4 mg) were weighed into standard DSC sample pans and scanned at 80, 40, 20, 10, and 5 K/min. under a nitrogen atmosphere. Data reduction and analysis were performed with computer programs previously described [2].

SECTION III

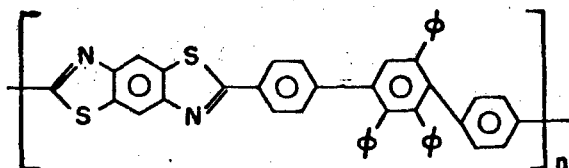
RESULTS AND DISCUSSION

POLYMER CHARACTERIZATION

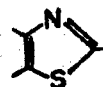
TGMS Analysis

During the course of this work, fifteen reports were submitted on the analysis of outgassing products from polymers at elevated temperatures. Abbreviated versions of these reports follow.

TRI ϕ PBT

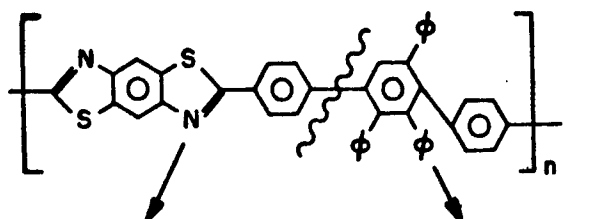


1. Sample Weight 6.13 mg
Weight Loss (30-980°C) 2.5 mg ~ 41%
2. Weight Loss Onset 570°C
Total Ionization Onset 475°C
Primary Maximum 606°C
Secondary Maximum 734°C
3. In the vicinity of 300°C, methanol is released in low abundance.
4. Benzene is evolved as the principal product.
Onset 503°C
Maximum 600°C FWHM ~ 50°C
Completion 734°C
5. Hydrogen sulfide, H₂S, is released at two distinct temperatures. The first maximizes at 625°C, the second at 745°C. Approximately equal amounts are released at each time; these distinct processes probably correspond to the two distinct environments of sulfur in the molecule.
6. Hydrogen cyanide, HCN, is produced in fairly large abundance in the same temperature interval as H₂S; however, there is no sharp delineation of two maxima for HCN production. The maximum rate occurs at 745°C. Production of H₂S and HCN indicate decomposition of the



ring.

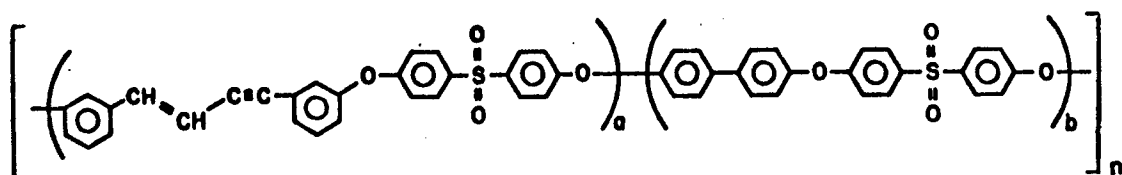
7. Traces of higher-molecular-weight unsaturated hydrocarbons (cf., m/e 103, ϕCN^+) were detected along with benzene.
8. Based on the mass spectral information and percentage weight loss, it appears that at 1000°C the overall effect was to cleave as shown below.



ϕH
 H_2S (2 eliminations)
 HCN
 NH_3

Residue

ENYNE POLYSULFONE COPOLYMER (50:50)

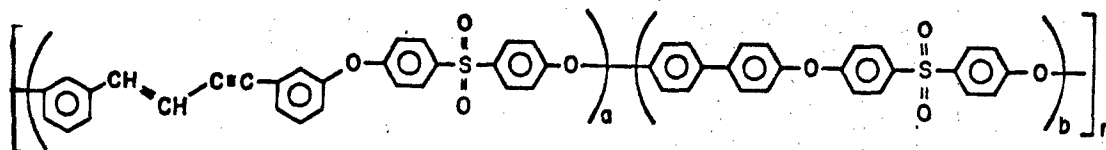


1. Sample Weight 3.88 g
Weight Loss ($30-900^\circ\text{C}$) 218 g ~ 56%
2. Weight Loss Onset 228°C
Total Ionization - three major peaks with maxima at 119, 459, and 573,
and shoulder at 725°C .
3. Production of hydrogen could not be studied in this analysis because the computer sampled only $m/e < 12$. The mass-spectral-scan-voltage range must be lowered to collect m/e 1, 2.

4. The following products were detected:

- Solvent (principally acetone) with onset at 68°C and maximum rate at 118°C
- Water (H₂O) with onset at 525°C and maximum rate at 540°C
- Sulfur dioxide (SO₂) with onset at 314°C and maximum rate at 460°C (asymmetric peak)
- Phenol (φOH) displaying two maxima at 469 and 518°C
- Benzene (φH) maximizing at 583°C
- m/e 171, C₁₂H₁₁O⁺ possibly an isomeric ion from the aromatic ether

ENYNE POLYSULFONE COPOLYMER (50:50) (RERUN)



1. Total ionization is identical in shape with previous run, with three major peaks at 127°C, 460°C, and 573°C, and shoulder at 718°C.
2. Hydrogen evolution onset at 559°C and maximum rate at 761°C.
3. Solvent onset at 82°C peaking at 139°C. The best match is with methyl butyl ketone.

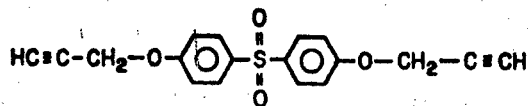
m/e	Present Run 6950-7	Previous Run 6950-4	MBK (iso-) Table	MBK (n-) Table
43	1000	1000	1000	1000
58	325	313	323	323
57	202	200	191	180
41	303	291	192	178
29	156	168	149	120
85	89	85	100	108
100	81	74	105	86
39	125	126	120	84
27	130	142	134	83
42	61	65	62	48

Series of aromatic products maximizing at 587°C. Some of the identifiable ions are $C_7H_7^+$, $-\phi-O-\phi^+$, $-\phi-CH_2-\phi-O^+$ and $-\phi-\phi-C^+$.

$$\text{HC}\equiv\text{C}-\text{CH}_2-\text{O}-\text{C}_6\text{H}_4-\text{S}(=\text{O})_2-\text{C}_6\text{H}_4-\text{O}-\text{CH}_2-\text{C}\equiv\text{CH}$$

- 10

PATS XI-3 (RERUN)

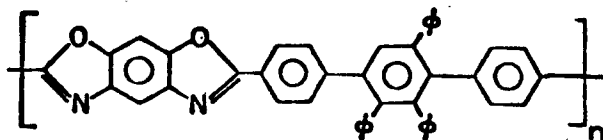


Sample Weight 8.81 mg

Weight Loss 8.5 mg i.e., > 95% weight lost
(Temperature range RT - 500°C)

1. Essentially the information for this run confirms all conclusions from previous report. At a temperature of ~ 180°C, almost the entire sample sublimes from the weighing region. Toluene is the only volatile product observed at the sublimation temperature. Scans on this run included m/3 1 and 2 which confirms that no hydrogen is evolved.
2. At ~500°C there is evidence for the onset of volatile products. These may arise from thermal degradation of the residue or from creeping of the PATS XI-3 sample to the ionization region.
3. Note that this apparatus was designed with no line of sight between the sample and ionizing regions to ensure that only volatile products are detected. Hence, it discriminates strongly against the detection of samples that upon slow heating tend to volatilize rather than thermally degrade. It is recommended that samples such as this one be studied with rapid-heating techniques more akin to pyrolysis studies or placed directly on the solids probe of a high-resolution mass spectrometer. In TG-MS studies a minimum of 5 mg of sample is required for good weight-loss measurements; however, each run of sample such as the present requires the subsequent scrubbing of the hang-down tube and weighing wire region in order to routinely remove the sample.

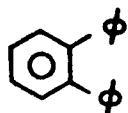
TRI ϕ PBO



1. Sample Weight 6.66 mg
Weight Loss 2.69 mg, i.e., 40%
2. Total Ionization Onset 73°C broad plateau
Maximum 609°C
Second Maximum 794°C

No attempt to identify products above 680°C because of memory from previous sample that sublimed in run up to 550°C. Identification of sample is based on m/e 48 and 64 from SO⁺ and SO₂ characteristic of previous sample.

3. At 126°C small amounts of solvent are observed. This appears to be a mixture of solvents (m/e 16, 17, 41, 55, 56, and 86).
4. The temperature profile has a FWHM of ~47°C. The initial onset is 435°C with a sharp increase at 498°C. Benzene evolution maximizes at 595°C and is complete at 670°C.
5. Accompanying the evolution of benzene but lagging by ~10°C is a series of products consisting of unstaured hydrocarbons,



AND

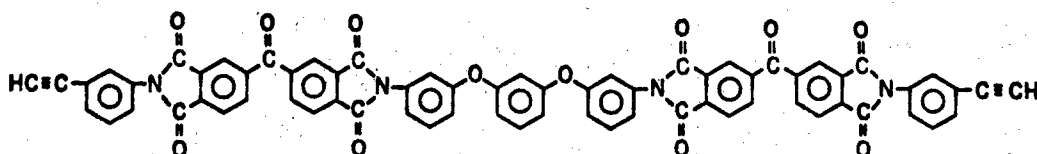


,

corresponding to the breakup of the triphenyl-substituted ring as well as phenol and benzonitrile.

6. H₂O is released at 600°C.
7. HCN is evolved in abundance at 600 and 740°C.

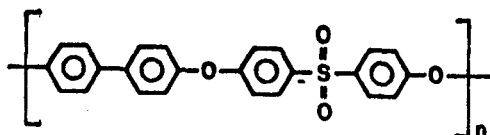
POLYIMIDE DIMER (THERMID)



1. Sample Weight 5.43 mg
Weight Loss (to 980°C) 1.94 mg, i.e., 36%
2. The weight-loss and first-derivative curves indicate two temperatures 280°C, 630°C where weight is lost with a maximum rate. The first-derivative curve and the total-ionization curves are in excellent agreement indicating no sign of sublimation.
3. The peak at 280°C corresponding to ~10% of the weight loss is ethanol.
4. At 450°C there are traces of fluorocarbon products, e.g., CF_3^+ , HF^+ , CF^+ , but no CFO^+ .
5. Starting at 500°C, the sample commences degradation with the following products identified:

Carbon Dioxide	Major peak at 630°C, shoulder at 580°C
Carbon Monoxide	680°C
Water	640°C
Benzene	650°C
Benzonitrile	640°C
Substituted Benzenes	640°C
Hydrogen Cyanide	680°C
6. At higher temperature ~820°C there is evidence for hydrogen evolution.
7. The computer scaling for several peaks including m/e 38, 50, 53, 55, 63, 65, 69, 186, 129, and 170 failed to operate correctly, necessitating analysis based on the spectra rather than the mass-temperature profiles.

RADEL

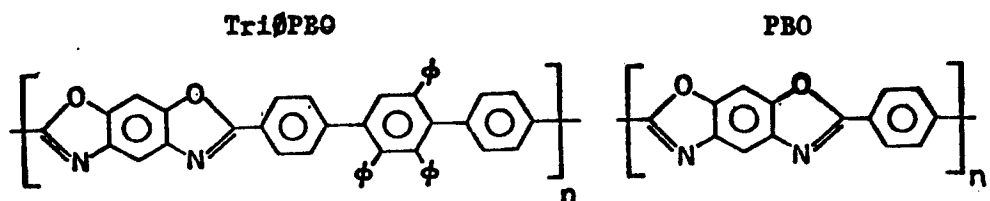


1. Sample Weight 4.35 mg
 Weight Loss (to 1000°C) 2.79 mg i.e., 64%
 Compare 56% in enyne polysulfone copolymer
2. The first derivative of the weight-loss and the total-ionization curves are in excellent agreement showing a major peak at 570°C with a FWHM of 50-60°C and a very small peak at 724°C.
3. This is a very clean sample with no solvent observed.
4. The major degradation products observed at 570°C are water, sulfur dioxide, phenol, and benzene. In addition, several ions of high molecular weight corresponding to $\text{C}_{12}\text{H}_{11}\text{O}^+$ (m/e 171), $\text{C}_{12}\text{H}_{11}\text{O}_2^+$ (m/e = 187), and $\text{C}_{18}\text{H}_{16}\text{O}_2^+$ (m/e 264) are observed.
5. Carbon monoxide is detected at higher temperatures and accounts for the small peak in the total ionization at 724°C.
6. Basically, comparing the present sample with the enyne polysulfone copolymer
 - a) same products are observed but with different temperature profiles
 - b) no solvents or degradation before 430°C in present sample
 - c) sulfur dioxide is released in the present sample along with . all the other degradation products. In the enyne polysulfone copolymer, its production maximized at 460°C, approximately 100°C lower than the present sample
 - d) phenol evolution displayed only one maximum in the present sample contrasted with two maxima in the exyne polysulfone copolymer.

PBO AND TRI ϕ PBO COMPARISON

1. The analysis is presented as a comparison of PBO and Tri ϕ PBO as outlined in Table 1.
2. Some points worthy of note are:
 - a) relative amounts of benzene evolved
 - b) overall abundance of carbon monoxide and hydrogen cyanide
 - c) apparent production of ammonia in each sample
 - d) lower-temperature (543°C) evolution of carbon dioxide from PBO (trapped gas?)
 - e) relative weight loss
 - f) absence of significant amounts of phenol and benzonitrile from PBO
 - g) excellent agreement of total ionization and derivative of weight-loss profiles for PBO
 - h) relative abundance of water from Tri ϕ PBO
 - i) low temperature (~600°C) for benzene evolution from Tri ϕ PBO.

TABLE 1
COMPARISON OF THERMAL DEGRADATION OF PBO AND TRI ϕ PBO



Weight Loss (%) RT-1000°C	40	28
Total Ionization	<u>609(2)</u> ^{a, b} 794(1)	551(1) <u>663(10)</u>
Derivative of Wt. Loss	Excessive Noise	551(1) <u>663(10)</u>
Solvents	126 m/e 16, 17, 41, 55, 56, 86	190 m/e 41, 43, 56, 57, 85

<u>Products</u>	<u>Intensity</u> ^c	<u>Temp For Max.. Rate (°C)</u>	<u>Intensity</u> ^c	<u>Temp For Max. Rate (°C)</u>
Benzene	100	595	3	670
Carbon Monoxide	52	<u>610</u> 777	100	670
Hydrogen Cyanide	40	670 <u>750</u>	53	670
Water	31	610	9	660
Benzonitrile	17	620	<1	650
Ammonia	17	630	12	660
Carbon Dioxide	8	600	56	543 <u>660</u>
Phenol	7	790	<1	650
Unidentified	<5		<5	

^a Relative peak height shown in parenthesis.

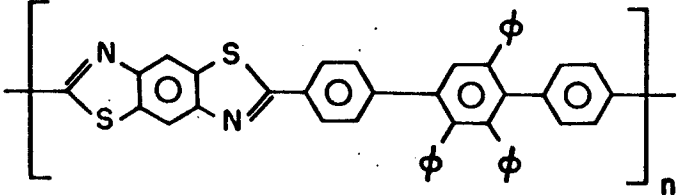
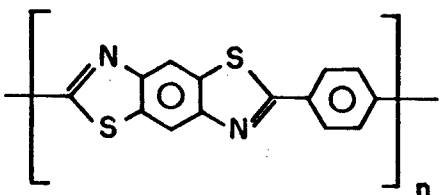
^b Temperature corresponding to next intense peak is underlined.

^c Estimated on basis of peak height and fragmentation pattern. No account is taken for differences in shape of temperature profiles or differences in total-ionization cross sections.

PBT (2122-38A) AND TRI ϕ PBT COMPARISON

1. The analysis is presented as a comparison of PBT and Tri ϕ PBT as outlined in Table 2.
2. Interesting features from Table 2 are:
 - a) relative amounts of benzene evolved
 - b) percentage weight loss in each case correlates very well with the PBO, Tri ϕ PBO analogues
 - c) ammonia is evolved in both samples
 - d) note carbon-disulphide production in PBT analogous to carbon dioxide in PBO (negligible amounts in the Tri ϕ analogues)
 - e) lowest-temperature process in Tri ϕ PBT--precisely the same behavior is observed with Tri ϕ PBO
 - f) aromatic products make a negligible total contribution in PBT and PBO, whereas benzene is the major product for the Tri ϕ analogues in each case.

TABLE 2
COMPARISON OF THERMAL DEGRADATION OF PBT AND TRI ϕ PBT

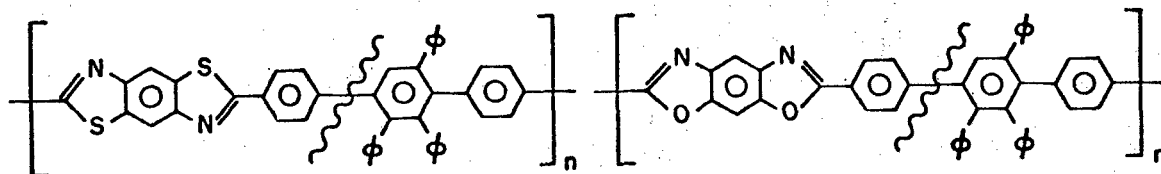
	TRI ϕ PBT	PBT
		
Weight Loss (%) RT-1000°C	41	28
Total Ionization	606(2)	743(1) 690
Derivative of Weight Loss	Excessive Noise	690
Solvents	300, CH ₃ OH	97 m/e 73, 44, 43, 42 240 m/e 73, 68, 66, 55, 54, 53, 44, 43, 42, 41, 39 284 H ₂ O, N ₂ (tentative)

<u>Products</u>	<u>Intensity</u> ^a	<u>Temp For Max. Rate (°C)</u>	<u>Intensity</u>	<u>Temp For Max. Rate (°C)</u>
Benzene	100	600	-	-
Hydrogen Sulphide	75 ^b	625 745	100	690
Hydrogen Cyanide	33	~624 <u>742</u>	51	707
Carbon Disulphide	-	Masked by Benzene	34	760
Ammonia	12 ^b	625 750	3	690
Benzonitrile	9	615	3	680

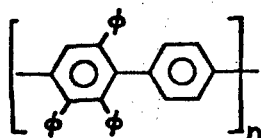
^aEstimated on basis of peak height and fragmentation pattern. No account taken for area under temperature profile or correction for total-ionization cross sections.

^bIn this case the temperature profile indicated two approximately equal rates of production; therefore, the peak intensity was multiplied X2.

TRI ϕ PBO AND TRI ϕ PBT COMPARISON

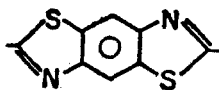


1. Overall weight loss is 41 and 40% for Tri ϕ PBT and Tri ϕ PBO, respectively. As was suggested in a previous report, the weight-loss and mass-spectrometric data suggest that the residue is



That is, the degradation involves the cleavage as shown above accompanied by elimination of benzene occurring with a maximum rate at about 600°C. Based on this cleavage, the expected residue would be 41 and 39% for Tri ϕ PBT and Tri ϕ PBO, respectively. This is an excellent accord with the observed weight loss.

2. The temperature profiles for the major products are shown in Figs. 1 and 2. Note the close correspondence of benzene and hydrogen cyanide profiles for each sample.
3. In Fig. 1, benzene is released at the lowest temperature followed by the release of hydrogen cyanide and hydrogen sulfide. The latter two products display two fairly distinct maxima possibly corresponding to the two heterocyclic rings. The existence of two maxima suggests that one of the five-membered rings opens during the release of benzene.



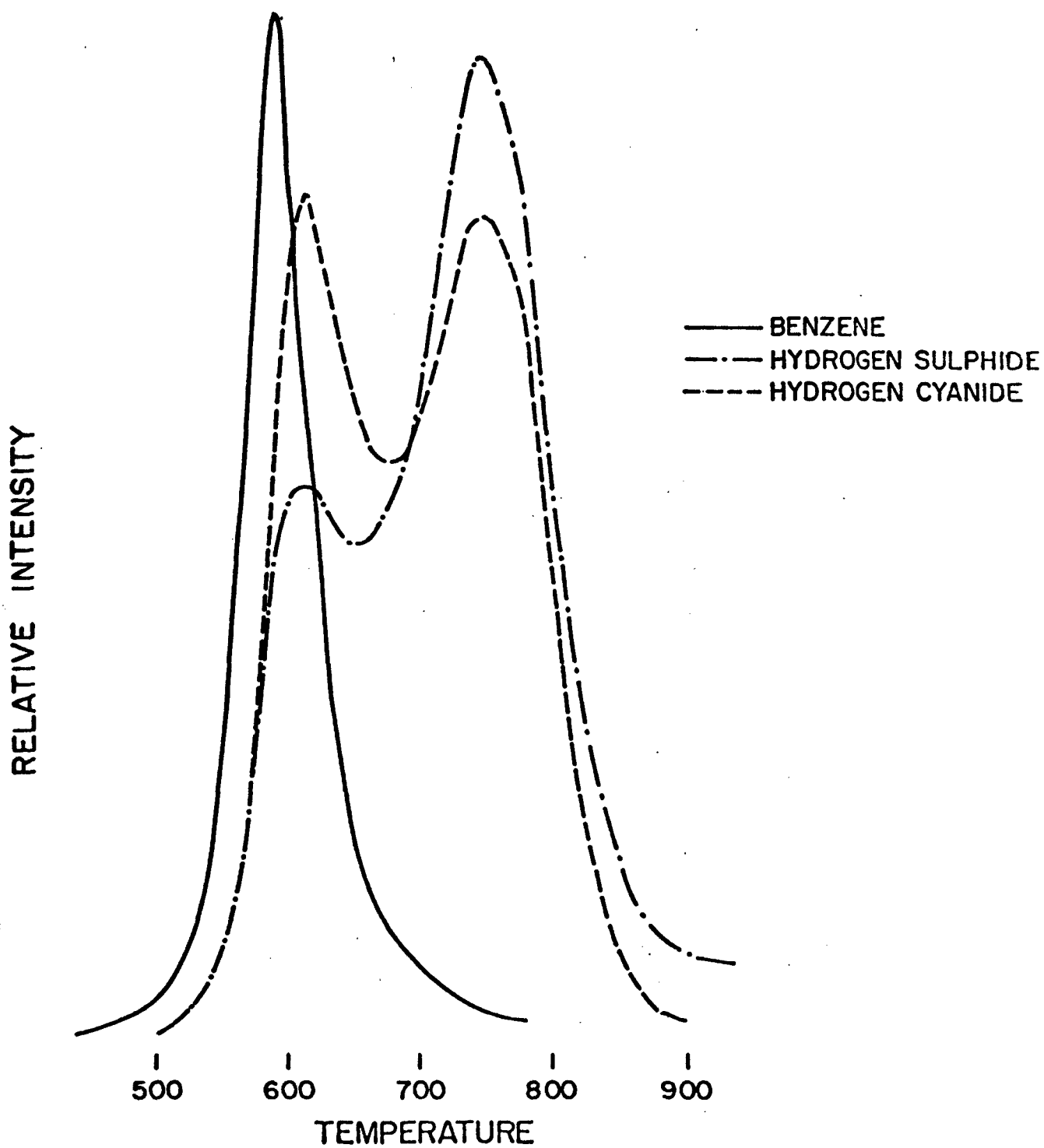


Fig. 1. Ion Intensity as Function of Temperature for Tri ϕ PBT.

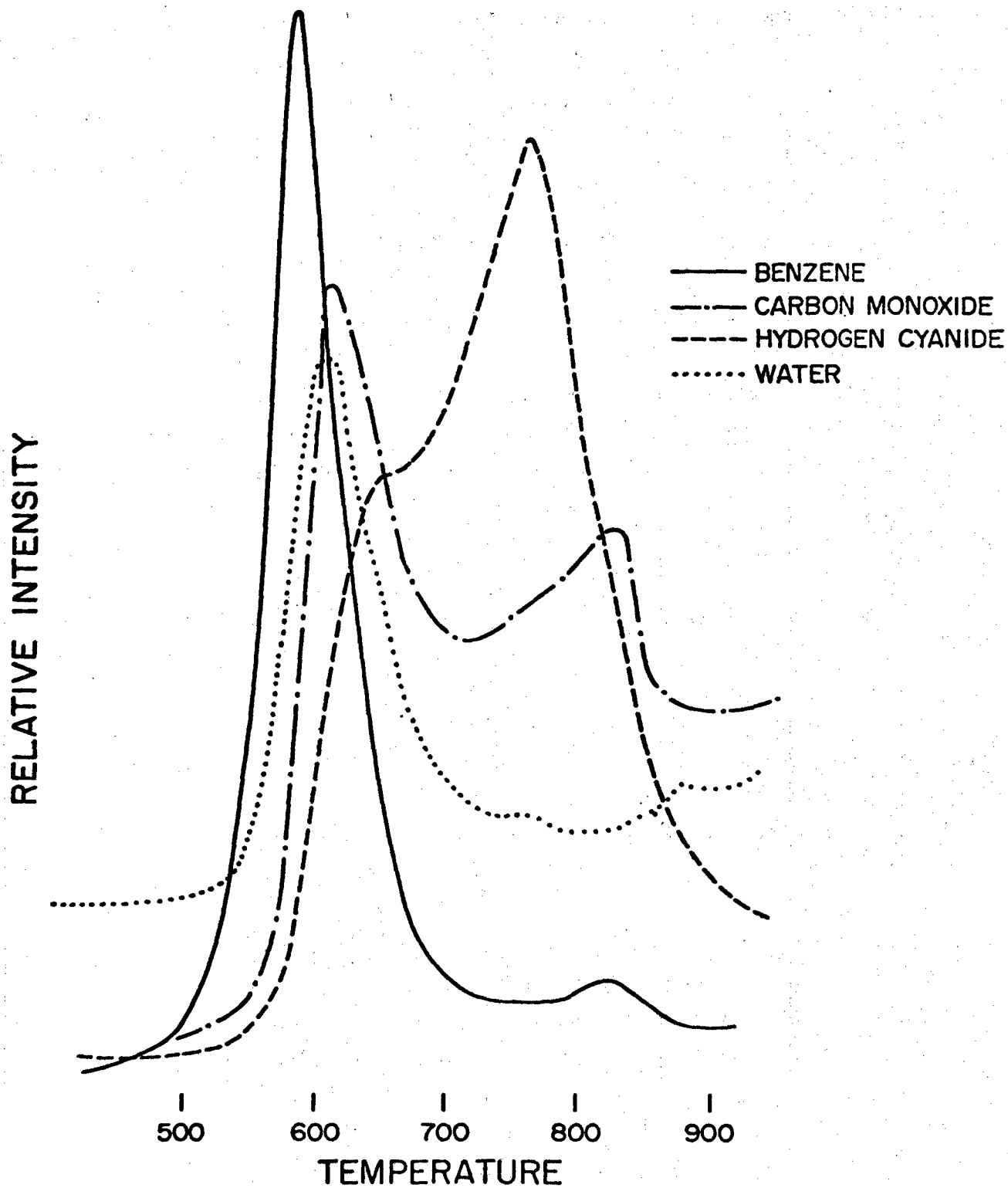
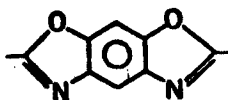


Fig. 2. Ion Intensity as Function of Temperature for Tri ϕ PBO.

4. In Fig. 2, benzene is evolved at the lowest temperature followed shortly by carbon monoxide, hydrogen cyanide, and water.



Many of these processes are competing with the other less important routes producing ϕCN , NH_3 , CO_2 and ϕOH .

PBO (292-12) AND PBT (2122-38A) COMPARISON

1. The basic thermal degradation is completely distinct from the triphenyl-substituted analogues. There is no evidence for benzene evolution indicating initial decomposition of the fused-ring moiety.
2. Temperature profiles of the major products are given in Figs. 3 and 4. In the PBT sample, hydrogen sulfide production is the lowest energy process indicating an opening of one of the five membered rings. As expected, this is closely followed by hydrogen cyanide evolution. At slightly higher temperatures carbon disulfide is evolved over a broad temperature range. It is clear from Fig. 3 that even at 1000°C , the production of CS_2 is still not complete.
3. It appears that only one of the five membered rings is involved in the primary degradation and that CS_2 is driven off from the resultant char. The observed weight loss of 28% is consistent with the loss of 1 H_2S , 1 HCN , and $1/4$ CS_2 from each unit.
4. PBT degradation occurs at temperatures at least 50° above thermal degradation of the triphenyl-substituted species.
5. In PBO, carbon dioxide displays two maxima in its temperature profile. This is somewhat surprising considering the profile for CS_2 in PBT. Conceivably, the lower-temperature peak may not be associated with primary thermal degradation, but this would have to be checked independently. The higher-temperature profiles for carbon dioxide, carbon monoxide, and hydrogen cyanide all peak at about the same temperature.
6. The observed weight loss of 28% is consistent with the loss of 1 CO , 1 HCN , and $1/4$ CO_2 from each unit.

RELATIVE INTENSITY

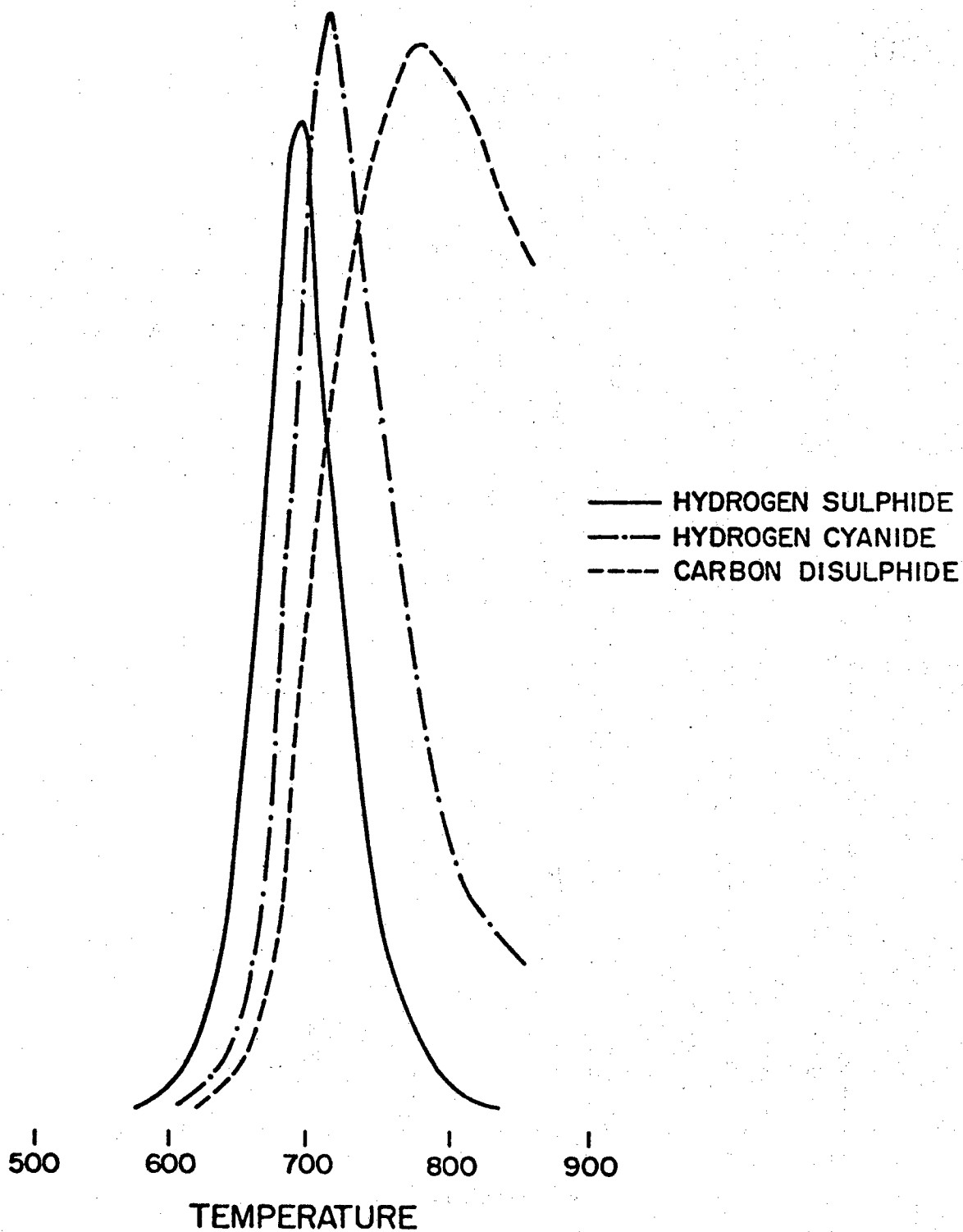


Fig. 3. Ion Intensity as Function of Temperature for PBT.

PBO

RELATIVE INTENSITY

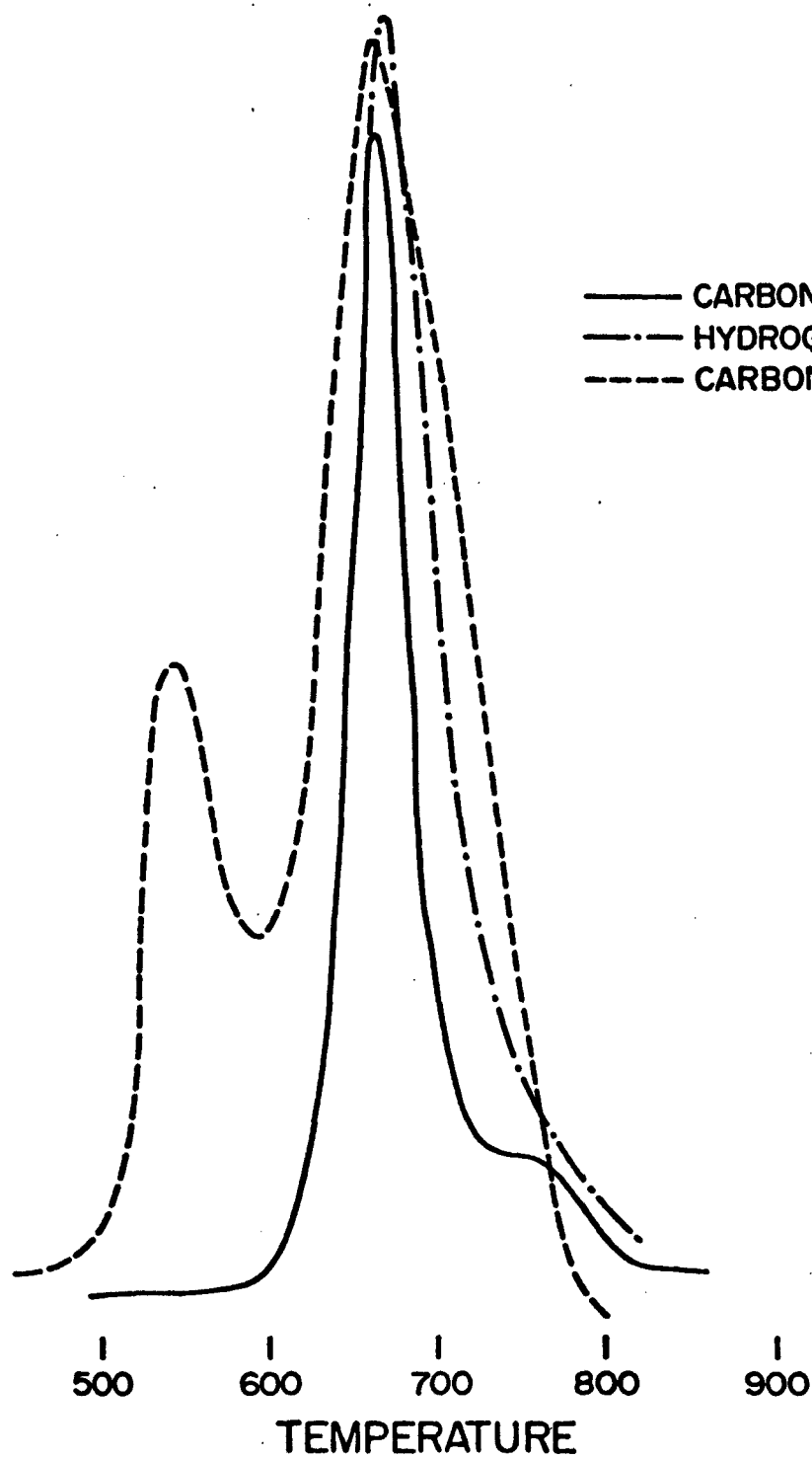
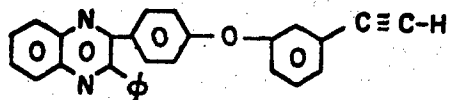


Fig. 4. Ion Intensity as Function of Temperature for Tri ϕ PBO.

7. Neglecting the CO₂ profile at lower temperatures, all profiles for PBO and PBT display one temperature region for evolution consistent with the weight-loss information of decomposition of essentially one of the five membered rings. This can be contrasted with the triphenyl-substituted analogues in which both weight-loss and mass-spectral information indicate decomposition of the entire fused-ring system.

BATQ MODEL COMPOUND

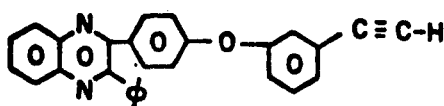


1. Initial weight 4.61 mg
Weight loss (RT-1000°C) 3.16 mg, i.e., 69%
2. The first derivative of the weight-loss and total-ionization temperature profiles do not correlate well. There are strong indications that the sample sublimes from the hot zone prior to thermal degradation. For example, the rate of weight loss peaks at ~490°C, whereas the total ionization curve displays a maximum at 550°C. Also, the FWHM of the latter curve is ~100°C, whereas that of the former is ~170°C.
3. The major products are the following in order of increasing temperature for their detection at maximum rate:

Toluene	~535°C	
Benzonitrile	540	
Benzene	560	
Phenol	~565	
Water	580	
Hydrogen cyanide	710	
Carbon monoxide	720	
Solvent	~380	-ketone

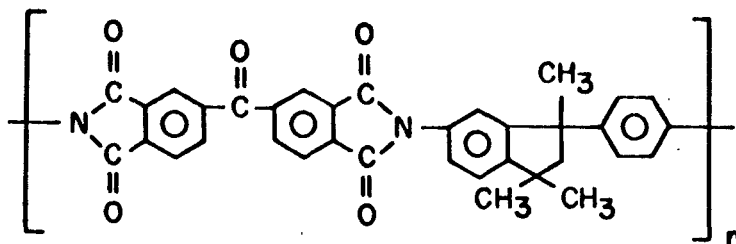
4. In addition, there are some higher-molecular-weight products evolving at ~530°C. Ions up to m/e 282 are observed in low abundance. Some of the more intense ions are m/e 170, 194, and 206.

BATQ MODEL COMPD. (RERUN)



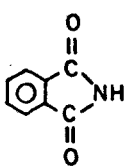
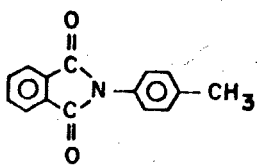
1. Initial Weight 5.85 mg
Final Weight 1.22 mg Weight Loss 78%
2. The analyzed volatile products from this sample are identical with those observed in BATQ II or previous ATQ samples. That is, the major products are toluene, benzonitrile, benzene, phenol, water, hydrogen cyanide, and carbon monoxide. In addition, the temperature profiles and relative abundance of the products are very similar for both samples.
3. This sample contains some carbon tetrachloride which is detected with maximum abundance at 130°C.
4. There are some subtle differences in the ionic distribution of the higher-molecular-weight products; however, the low intensity of these ions precludes any definitive comparison.
5. As in the previous sample, difficulties with the competition between sample sublimation and thermal degradation limit the interpretation of the mass-spectral data.

DAPI



1. Initial Weight 7.5 mg
Final Weight (1000°C) 3.46 mg
Weight Loss 54%
2. The total-ionization curve and first derivative of the weight-loss curve agree quite well. The thermal decomposition exhibits two maxima occurring at 500°C and 590°C.
3. Traces of solvent are detected with maximum intensity in the temperature interval 250-300°C.

4. The polymer is stable with respect to thermal degradation up to a temperature of 430°C; then a wide range of products is detected. The products are listed in the following along with the temperature corresponding to the maximum rate of evolution. The listed order corresponds to decreasing relative abundance.

<u>Product</u>	<u>Temperature (°C)</u>		<u>Comments</u>
CO	500	590	See Fig. 5
H ₂ O	500		Follows Profile A
CH ₄	500	(590)	Follows Profile A
CO ₂	500	580	See Fig. 5
HCN		640	See Fig. 5
NH ₃		590	Follows Profile B
C ₆ H ₆		580	Follows Profile B
C ₇ H ₈		570	Follows Profile B
ØCN		580	
ØNH ₂ (?)	490		
	520	560	
	500		

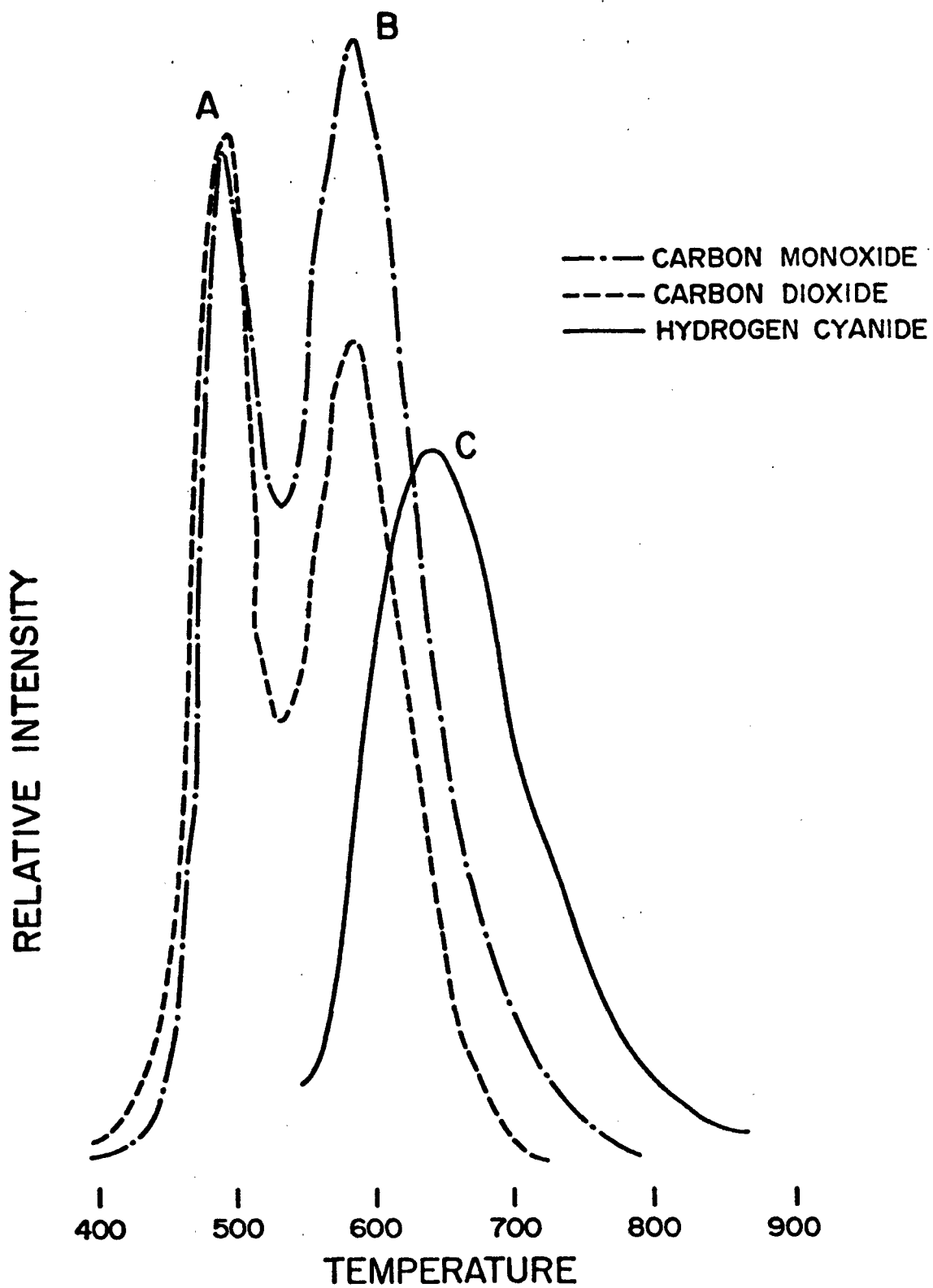
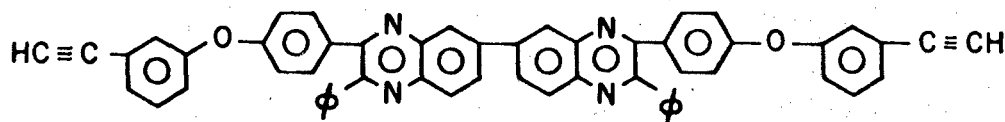


Fig. 5. Ion Intensity as Function of Temperature for DAPI.

BADABA



1. Initial Weight 4.49 mg
 Final Weight 3.66 mg
 Weight Loss 18% (to 1000°C)
2. Only 18% of the sample weight was lost at temperatures up to 1000°C. The maximum rate of weight loss and largest total ion current were observed at approximately 530°C. Some temperature instability was occurring during the evolution of volatile products; therefore, the precise temperature is uncertain $\pm 20^\circ\text{C}$.
3. Below 460°C no volatile products could be detected. Apparently any solvent evolution was below the detectable limits of this experiment.
4. At 530°C a series of aromatic products such as benzene and toluene was observed in maximum abundance. Also included but with considerably lower abundance were phenol and benzonitrile.
5. In the vicinity of 600°C, principally carbon monoxide and water were observed.
6. Above 700°C hydrogen cyanide, ammonia, and carbon monoxide were observed.

IR Spectra

Infrared spectra of oligomer (I), the deuterio-analogue, oligomer (II), and the corresponding polymers isolated after thermal reaction at 434 K are shown in Figs. 6-8, respectively. The structural complexity and inherent lack of high symmetry rule out the use of detailed group theoretical analysis; however, some qualitative assignments are easily discerned. The spectra of the protonated oligomers, Figs. 6a and 8a, possess intense bands in the region of 3300 cm^{-1} and weak bands at 2100 cm^{-1} which are characteristic of C-H and $\text{C}\equiv\text{C}$ stretching motions of the ethynyl moiety [3]. In the deuterated spectra, Fig. 7, the corresponding bands associated with the $-\text{C}\equiv\text{CD}$ moiety occur at 2560 and 1970 cm^{-1} , respectively.

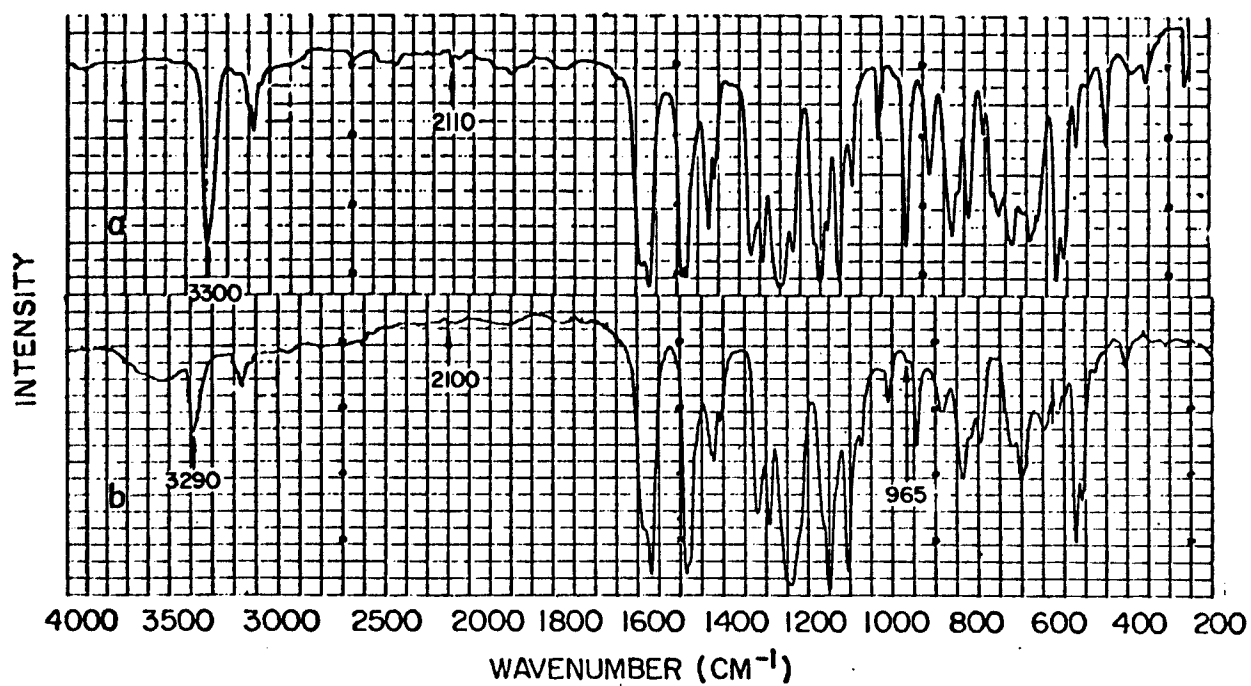


Fig. 6. IR Spectrum of Bis[4-(3-Ethynylphenoxy)Phenyl]Sulfone
(a) Oligomer Film NaCl Plate; (b) Polymer, KBr Matrix.

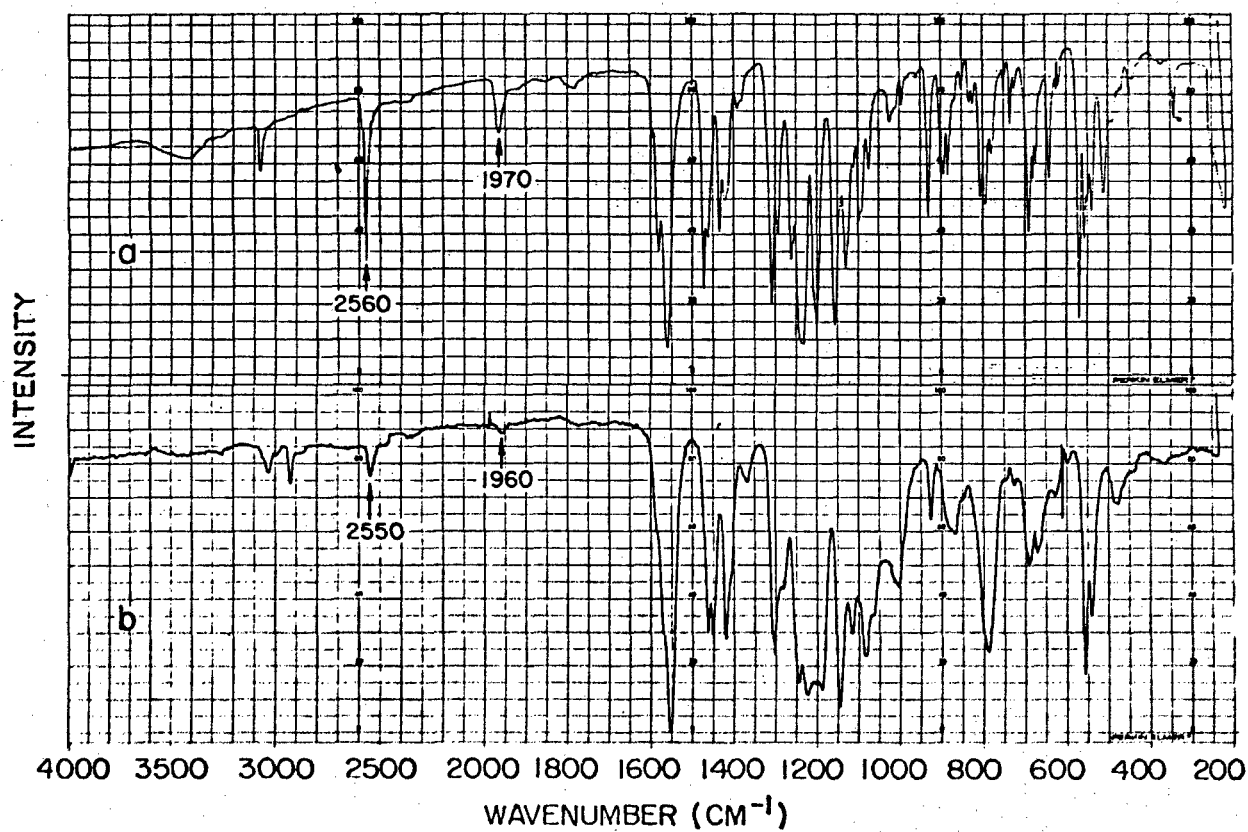


Fig. 7. IR Spectrum of Bis[4-(3-Dideuterioethynylphenoxy)Phenyl]-Sulfone (a) Oligomer; (b) Polymer.

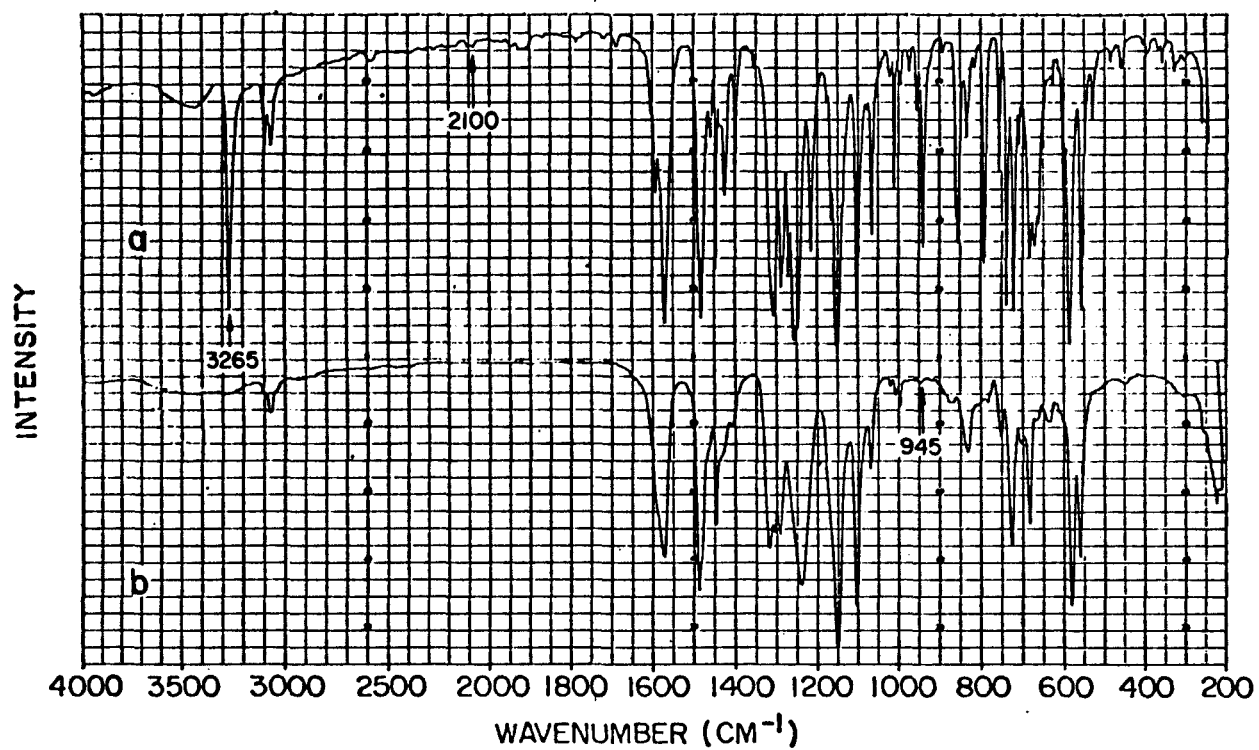


Fig. 8. IR Spectrum of 4-(3-Ethynylphenoxy)Phenyl Phenyl Sulfone
(a) Oligomer; (b) Polymer.

In the spectrum of poly[4-(3-ethynylphenoxy)phenyl phenyl sulfone], Fig. 8b, the C-H stretching motion of the ethynyl moiety is absent and contrasts sharply with the spectra given in Figs. 6b and 7b for poly[Bis[4-(3-ethynylphenoxy)phenyl]sulfone] which indicate that the intensities of the bands associated with the $\text{C}\equiv\text{CH}$ and $\text{C}\equiv\text{C-D}$ moieties are about one-half those observed in the initial oligomers.

The frequencies of the intense bands in all monomers in the $1350\text{--}1200\text{ cm}^{-1}$ and $1150\text{--}1060\text{ cm}^{-1}$ regions associated with symmetric and antisymmetric stretching motions of the aryl ether and sulfone moieties [4] are relatively unperturbed by polymerization.

By analogy with simple conjugated polyenes, the protonated polymers, in particular that of the model compound in Fig. 8b, exhibit weak bands at $960\text{--}940\text{ cm}^{-1}$ indicative of trans-unsaturation [5]. These can be assigned as olefinic C-H deformation modes by comparison with the deuterated polymer in Fig. 8b. In Fig. 7b the band at 940 in the protonated polymer is absent and, therefore, presumably may be associated with unsaturation.

^1H NMR Spectra

The proton spectra in the region 3-8 ppm for polymers (I) and (II) and changes induced by addition of the shift reagent, Eu(fod)_3 , are given in Figs. 9 and 10. Both of these figures show characteristic broad absorption in the region 6-8 ppm which is analogous to the spectra of polyarylacetylenes [5].

Polymer (I) in Fig. 9a shows broad absorption at 7.9, 7.5 (CHCl_3 impurity), and 7.0 ppm with half-bandwidths, i.e., $\Delta\nu_{1/2}$, of 35, 10, and 35 Hz, respectively. The absorption at 7.0 ppm is asymmetric and decreases toward the baseline at 6.0 ppm. There is also a resonance with $\Delta\nu_{1/2}=4\text{ Hz}$ centered at 3.1 ppm, indicative of pendant ethynyl groups. The relative intensities of the ethynyl and aromatic protons are consistent with the polyene structure for polymer (I) and correlate with the intensity ratios

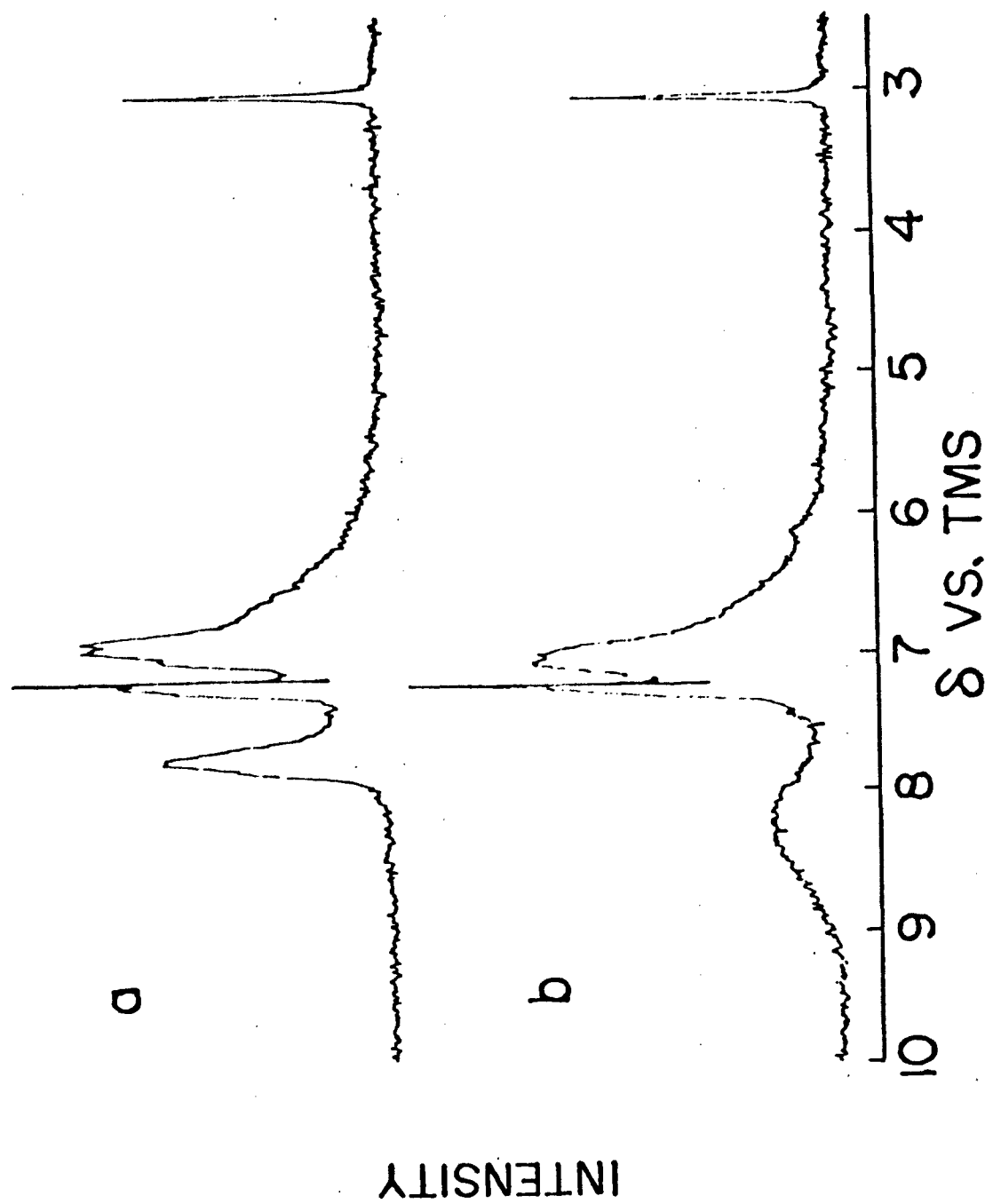


Fig. 9. ¹H Spectrum of Bis[(3-Ethynylphenoxy)Phenyl]Sulfone from 3 to 8 ppm Relative to TMS (a) Oligomer 0.2 M in CDCl₃; (b) Polymer 0.05 g/ml with 0.07 M Eu(fod)₃ in CDCl₃.

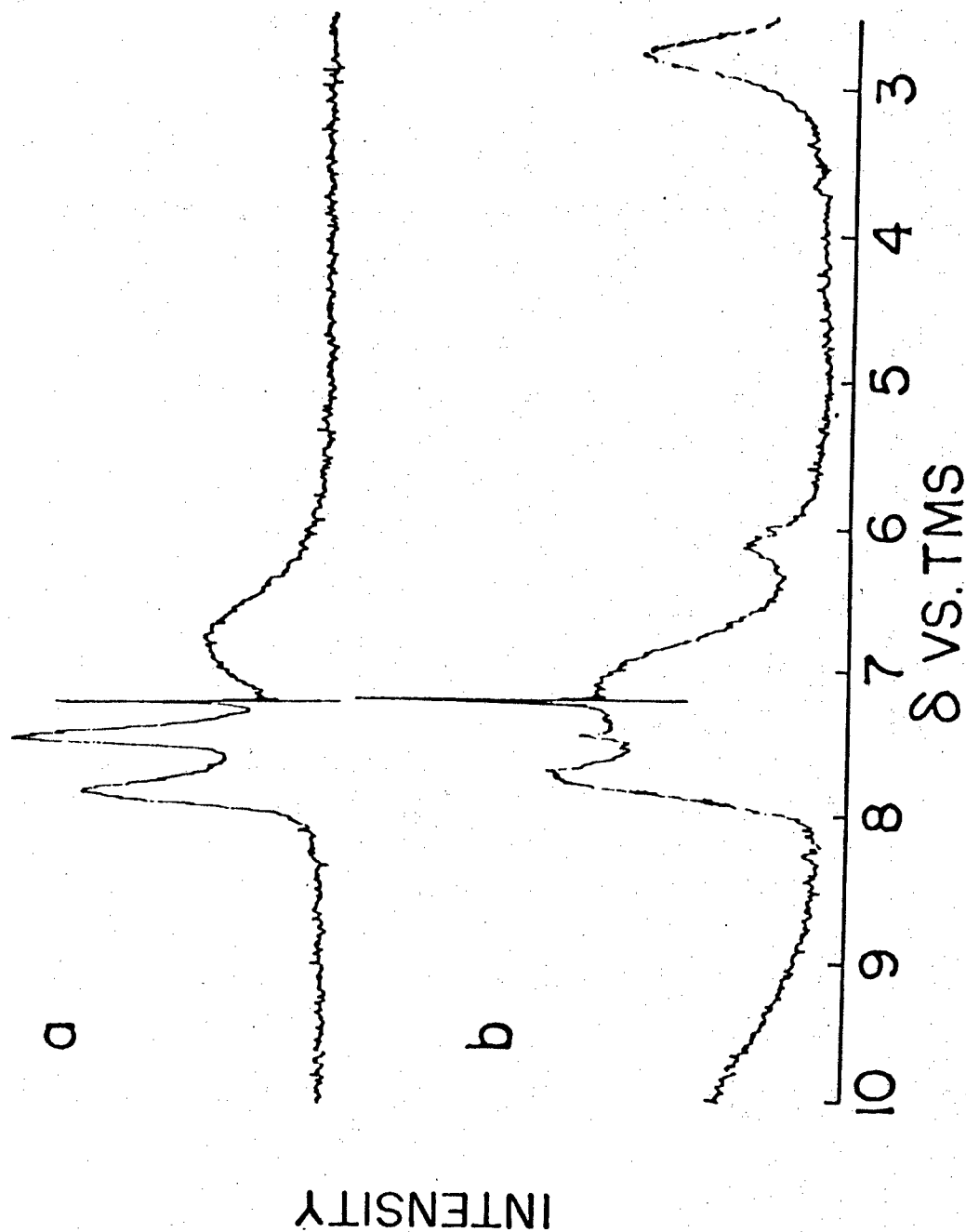


Fig. 10. ^1H NMR Spectrum for 4-(3-Ethynylphenoxy)Phenyl Sulfone from 3 to 8 ppm Relative to TMS (a) Oligomer, 0.2 M in CDCl_3 ; (b) Polymer, 0.05 g/ml with 0.05 M Eu(fod)_3 in CDCl_3 .

observed in the IR spectrum. Polymer (II) in Fig. 10a exhibits broad absorption from 6 to 7.2 ppm, with $\Delta\nu_{1/2} \approx 80$ Hz, a sharp CHCl_3 impurity at 7.2 ppm, and broad absorptions with $\Delta\nu_{1/2} \approx 20$ Hz at 7.2 and 7.9 ppm. Assignments for the proton spectra based upon a first-order analysis of the multiplets are summarized in Table 3.

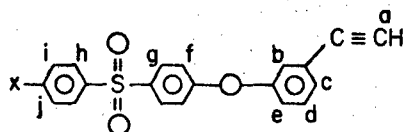
Coordination of the shift reagent with the polymers would be expected to occur at the sulfone nucleus, which is supported experimentally by the spectral changes shown in Figs. 9 and 10. Figure 10 for polymer (II) shows clearly that the aromatic protons shift downfield, revealing a broad resonance at 6.2 ppm. Similar behavior, but less intense due to more extensive line broadening, is observed in the spectrum of polymer (I) in Fig. 9. The resonance in both polymers at 6.2 ppm is in the region reported for the olefinic protons of the trans-cisoidal isomer of polyphenylacetylene [5].

^{13}C NMR Spectra

Assignments for ^{13}C spectra were based upon intensity considerations and additivity rules for substituted benzenes [6,7]. In the oligomers, chemical shifts for the carbon atoms in the ethynylbenzene moiety were derived from substituent constants for a p-sulfonylphenoxy group and empirical parameters given for ethynylbenzene [6]. Chemical shifts for the aromatic carbons in the polymers, based upon parameters for phenylacetylene and styrene [6], were estimated from the chemical shifts of the oligomers and the assumption that the ethynyl group is converted to an ethene linkage by polymerization. The observed ^{13}C spectra are summarized in Table 4, and the reasonable agreement between the observed and estimated chemical shifts supports the polyene structure assumed for each polymer.

Changes in ^{13}C spectra induced by the addition of $\text{Eu}(\text{fod})_3$ to oligomer and polymer (II) are illustrated in Figs. 11 and 12, respectively. Figure 11 reveals that the largest downfield shifts of the aromatic carbons in the oligomer occur at positions l and m which are directly bonded to the sulfone nucleus. In Fig. 11 the ethynyl carbons at 78.3 and 82.2 ppm are unchanged by the addition of $\text{Eu}(\text{fod})_3$.

TABLE 3. SUMMARY OF ^1H NMR DATA



$\frac{\text{X}}{\text{H}}$	Oligomer ^a		Polymer	
	Obs. δ (ppm)	Assign ^b	Obs. δ (ppm)	Assign ^b
	7.9, 8.0	g, h	7.8	g, h
	7.5	i, e	7.5	i, c, l
	7.3	b, e	6.0-7.2	b, d, f, j, =CH
	7.2	d		
	7.0	f, j		
	3.1	a		
	7.9	g	7.9	g
	7.3	b, e	7.4	b, e
	7.1	d	6.0-7.1	c, d, f, =CH
	7.0	f, c	3.1	a
	3.1	a		

^aFor X \neq H, g=h, f=i

^bBased on first-order analysis of multiplets.

TABLE 4. SUMMARY OF ^{13}C NMR DATA

$\frac{\text{X}}{\text{H}}$	Oligomer ^a			Polymer		
	Obs. δ^b (ppm)	Calc. δ (ppm)	Assign.	Obs. δ^b (ppm)	Calc. δ (ppm)	Assign.
	78.3		a	109		a,b
	82.2		b			
	117.5		j	117.2, 117.4	117.3	d j
	120.4	119.9	g	118-120	120.1	g
	123.1	123.9	d			
	123.6	123.5	c			
	126.9		n	126.9		n
	128.1	128.3	e			
	128.7		o	128.7		o
	129.4		k	129.4	129.4	f,k
	129.6	130.0	f			
	132.4		p	132.5		p
	134.9		m	134.8		m
	141.4		l	141.1	139.2, 143.7	l,c,e
	154.0	154.3	h	154.4	153.8	h
	160.6		i	160.9		i
	79.7		a	79.8		a
	82.4		b	82.4		b
				117.8		d
				117.9		j
	118.2		j	118.3		j
	121.1		g	121.1		g
	123.4		d	123.4		d
	124.4		c	124.4		c
				128.5		n
	128.6		e	128.7		e
	129.6		k	130.1		k
	130.0		f	130.7		f
	135.7		l	136.6		l,m
	154.6		h	155.2		h
				160.4		
	161.1		i	161.4		i

^aFor X \neq H; p = i; n = k; o = j; m = l.^bMeasured from CDCl_3 and converted to TMS scale by $\sigma_{\text{CDCl}_3} - \sigma_{\text{TMS}} = 76.91$.

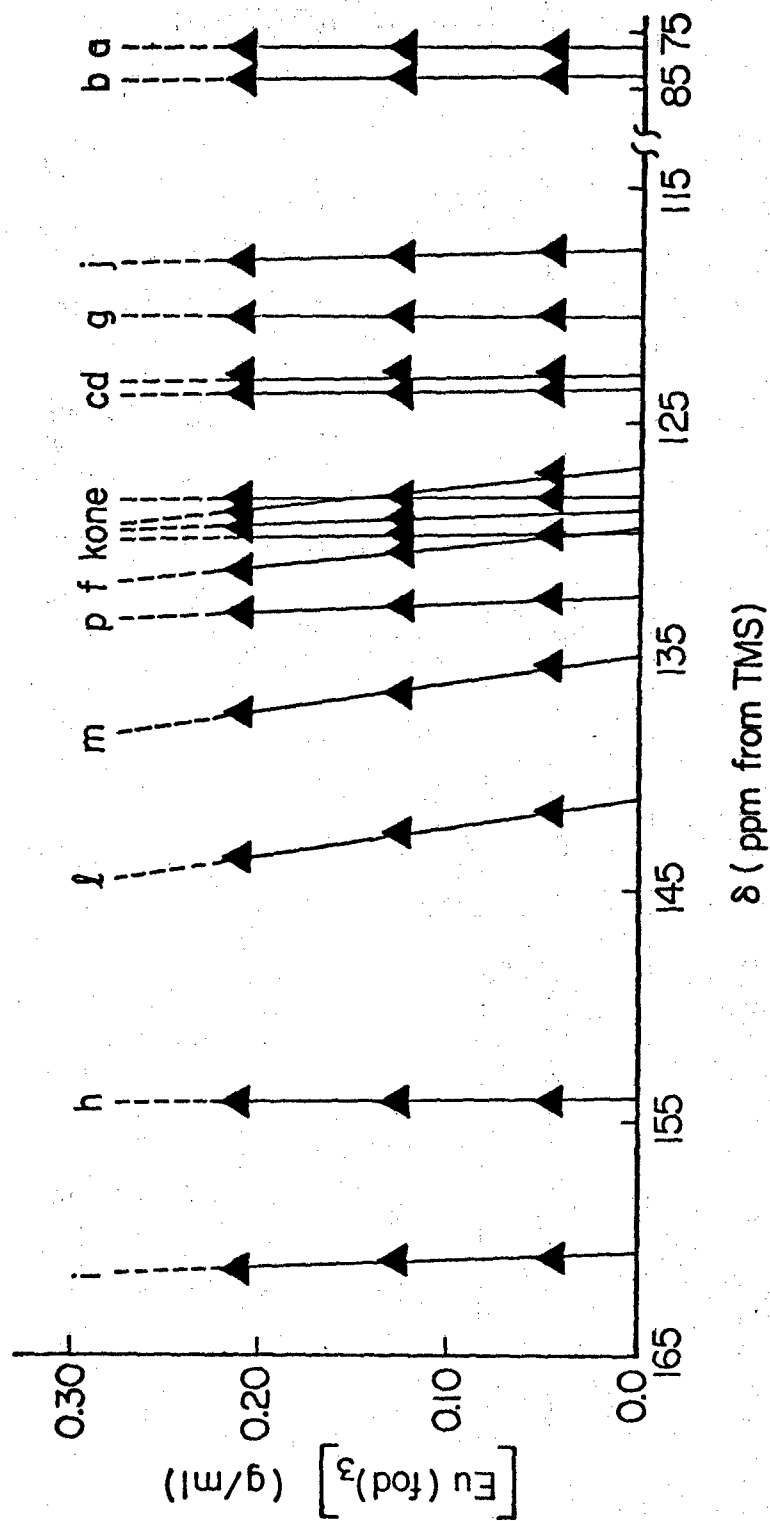
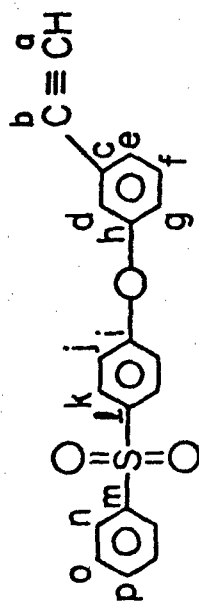


Fig. 11 ^{13}C Spectrum for Oligomer (II), δ vs $[\text{Eu}(\text{fod})_3]$.

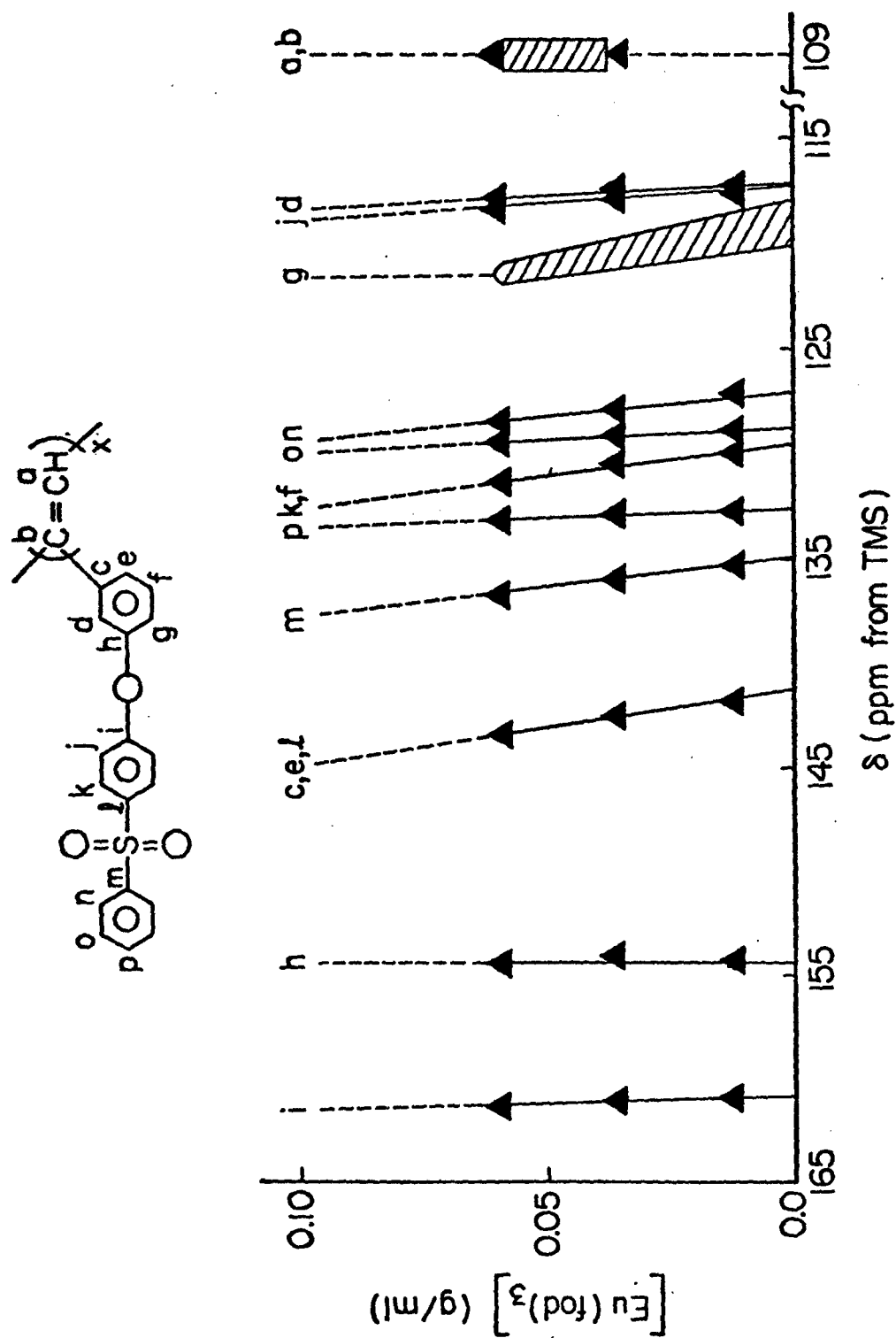


Fig. 12. ^{13}C Spectrum for Polymer (II), δ vs $[\text{Eu}(\text{fod})_3]$.

In the spectrum of polymer (II), the aromatic carbon formally assigned to the 119.9-ppm line in the oligomer is broadened and extends over the range 118-120 ppm, as indicated by the hatched area in Fig. 12. In addition, a broad resonance in the region expected for olefinic carbons was observed in the spectra obtained for the polymer solutions containing 0.04 to 0.06 M Eu(fod)_3 . The chemical shifts of α - and β -carbons in substituted styrenes are reported to occur in the range 133-150 and 109-120 ppm, respectively, relative to TMS [8].

DSC Kinetics

Figure 13 illustrates the reaction exotherms, i.e., dq/dt vs T , obtained from the dynamic DSC measurements for three of the five heating rates for the thermal reaction of bis[4-(3-ethynylphenoxy)phenyl]sulfone. In order to evaluate the temperature dependence of the rate data, Eq. (4) was rearranged to obtain

$$\log \left(\frac{d\alpha}{dt} \right) = \frac{-E}{2.303R} \left(\frac{1}{T} \right) + \log A (1 - \alpha)^n \quad (6)$$

At constant conversion, and assuming A and n constant, Eq. (6) should yield a linear relation between $\log (d\alpha/dt)$ and T^{-1} . Thus, the apparent activation energies, E_{ap} , were determined from the slope of Eq. (6) for each level of conversion. Representative rate data for oligomer (I) are summarized in Table 5. An Arrhenius plot for Eq. (6) using the data of Table 1 determined from the exotherms shown in Fig. 13 is given in Fig. 14. In Fig. 14 the data points obtained at each conversion level fall essentially on lines with the same line slope, thus indicating that E_{ap} is independent of the extent of reaction.

In order to evaluate the reaction order and A factor, Eq. (3) was rearranged to obtain

$$\log AF(\alpha) = \log A(1-\alpha)^n = n \log(1-\alpha) + \log A \quad (7)$$

Average values of $AF(\alpha)$ were calculated from the conversion data at each heating rate. The reaction order, n , and the A factor were obtained from the slope and intercept, respectively, from a least-squares analysis based on Eq. (7). Over the range 20-60% conversion, the reaction order was determined to be substantially less than unity, with $n = 0.33$.

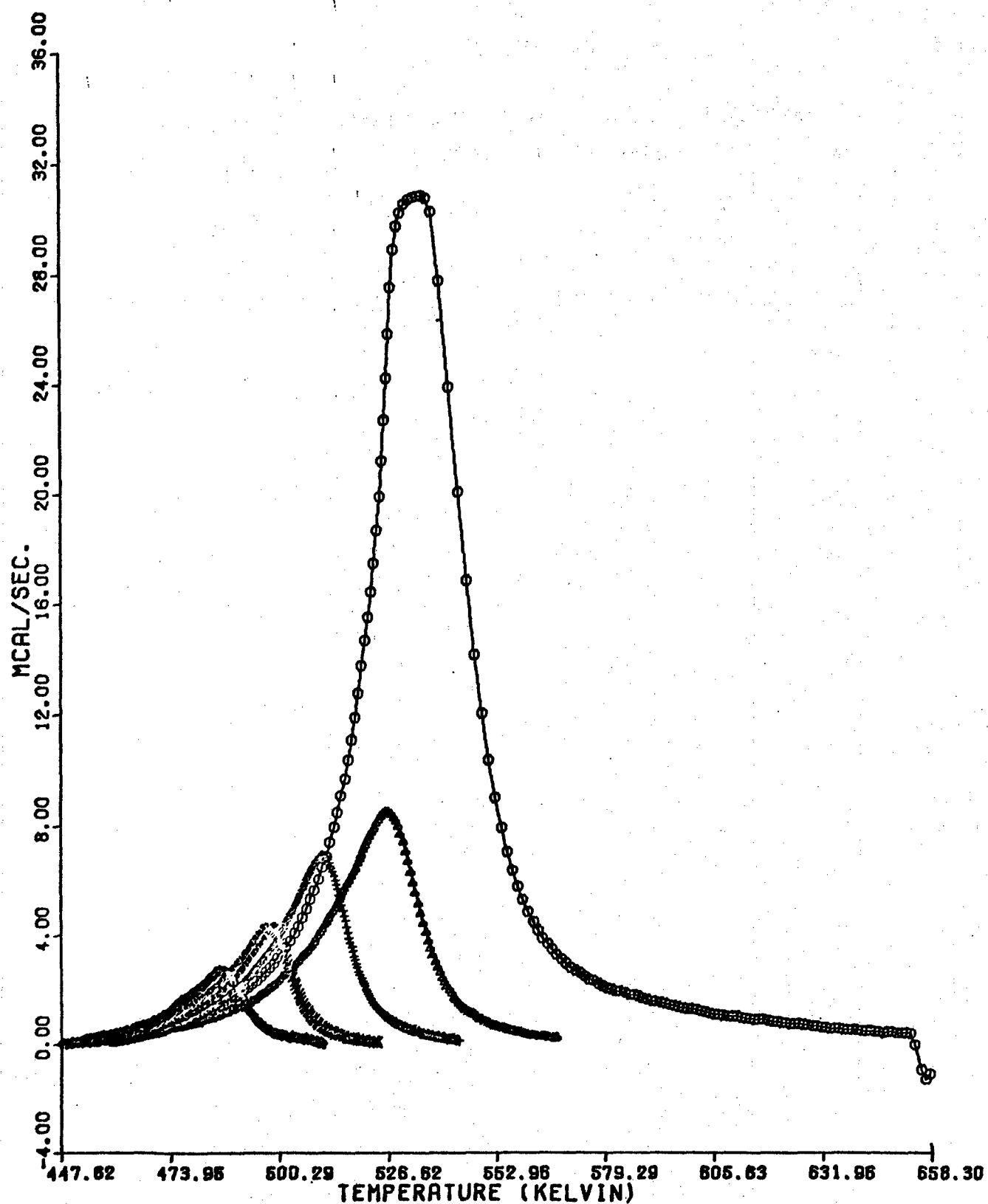


Fig. 13. Dynamic DSC Exotherms for Bis[4-(3-Ethynylphenoxy)Phenyl] Sulfone. Heat Rate in (K/min): o, 80; Δ, 40; +, 20; x, 10; □, 5.

TABLE 5

SUMMARY OF DYNAMIC DSC DATA FOR THE THERMAL POLYMERIZATION
OF BIS[4-(3-ETHYNYLPHENOXY)PHENYL] SULFONE

Heat Rate	W_0 (mg)	α	T (K)	$\frac{d\alpha}{dt} \times 10^4$ (s ⁻¹)	Total Data Pt.
80	5.49	10	511	79.0	61
		20	520	168.0	
		30	524	243.3	
		40	527	322.0	
		50	530	369.0	
		60	533	376.0	
40	3.01	10	495	42.0	57
		20	507	82.7	
		30	513	118.0	
		40	518	153.1	
		50	521	181.9	
		60	524	205.0	
20	4.55	10	486	30.4	161
		20	494	52.3	
		30	500	71.9	
		40	504	93.7	
		50	507	112.5	
		60	509	127.5	
10	5.35	10	475	17.3	66
		20	482	28.3	
		30	487	39.2	
		40	491	50.1	
		50	494	60.6	
		60	496	70.4	
5	6.43	10	467	9.70	58
		20	473	16.2	
		30	478	23.8	
		40	480	28.6	
		50	483	34.1	
		60	485	38.4	

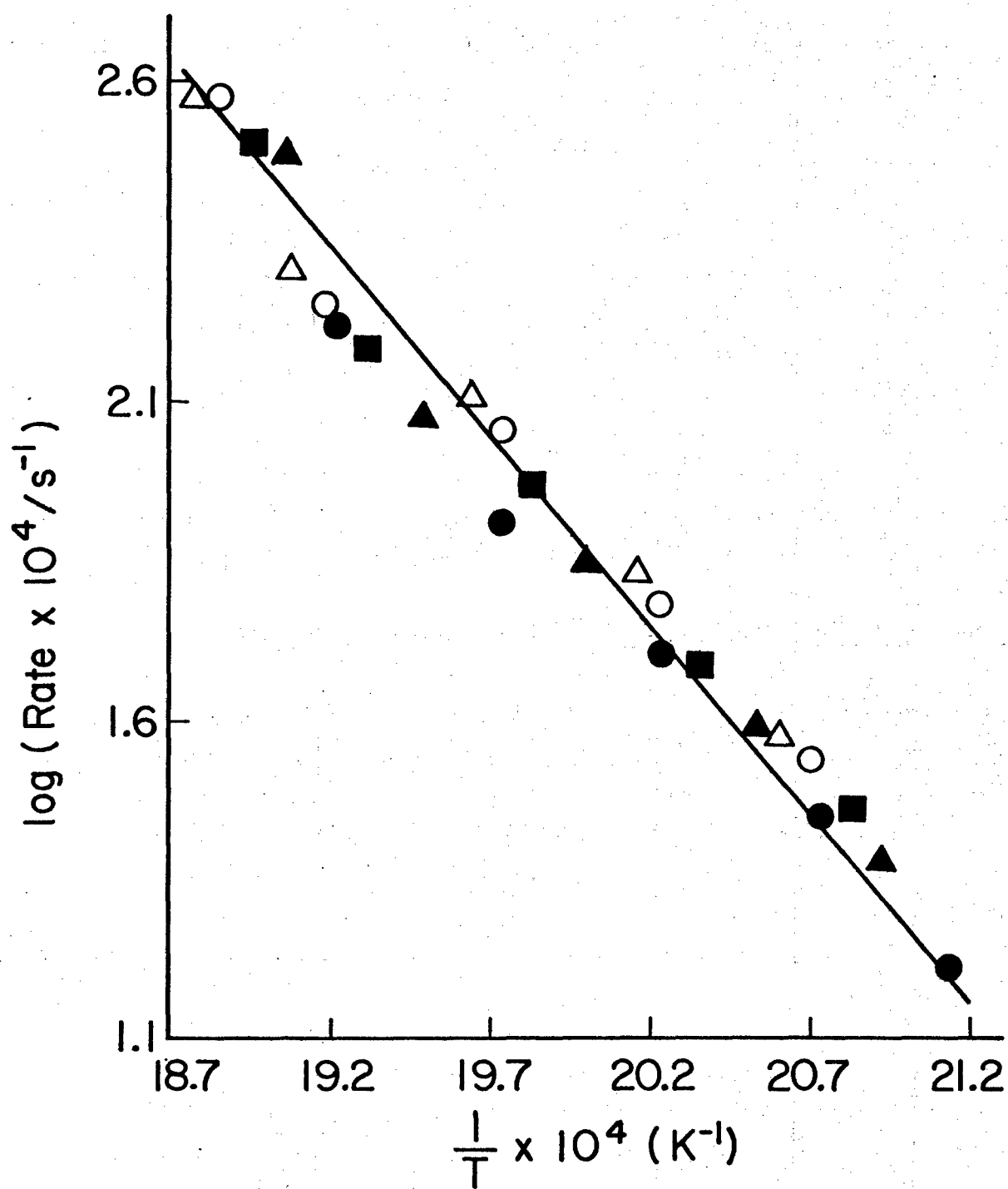


Fig. 14. Arrhenius Plot for Thermal Reaction of Bis[4-(3-Ethynylphenoxy) Phenyl]Sulfone from 467 to 533 K.

Least-squares analysis of the rate data such as summarized in Table 1, resulted in

$$\log (k_{ap}/s^{-1}) = (8.5 \pm 0.5) - (24.2 \pm 1)/\theta \quad (8)$$

where the uncertainties correspond to one standard deviation. The logarithm of the observed A factor compares favorably with those previously reported for simple arylacetylenes [9,10]; namely, phenylacetylene ($\log A/s^{-1} = 8.1 \pm 0.5$) and (3-phenoxyphenyl)acetylene ($\log A/s^{-1} = 7.6 \pm 0.5$).

The heats of reaction, calculated from each heating rate using Eq. (4), are summarized in Table 6. These data were averaged to obtain the enthalpy of polymerization, $\Delta H_p = -55 \pm 6$ kcal/mol.

Effect of Reaction Variables on Molecular Weight

The representative cumulative differential molecular-weight distributions determined by GPC analysis for the oligomer, bis[4-(3-ethynylphenoxy)phenyl]sulfone and the model compound, 4-(3-ethynylphenoxy)phenyl phenyl sulfone which were polymerized at 434 K, are illustrated in Fig. 15. Examination of Fig. 15 reveals clearly that both the oligomer and the model compound react to yield polymer as well as two lower-molecular-weight oligomeric fractions, which suggests that a common mechanism may be operative.

Figure 16 illustrates the effect of conversion upon the dispersion ratio, i.e., M_w/M_n , for the polymerization of bis[4-(3-ethynylphenoxy)phenyl] sulfone. As shown in Fig. 16, results of the GPC analyses indicate that $M_w/M_n \approx 1.5$ up to 30% conversion. Under conditions where α exceeds 0.3, the ratio M_w/M_n diverges rapidly as the reaction approaches the gel point. Intersection of tangents drawn along each of the linear branches in Fig. 16 implies that the critical conversion for gel formation exceeds 35%.

TABLE 6
HEAT OF POLYMERIZATION OF
BIS[4-(3-ETHYNYLPHENOXY)PHENYL]SULFONE

<u>Heat Rate</u> (K/min)	<u>-ΔH_p</u> (kcal/mol)
80	67.1
40	59.7
20	51.6
10	48.5
5	<u>48.2</u>
	av 55 ± 6

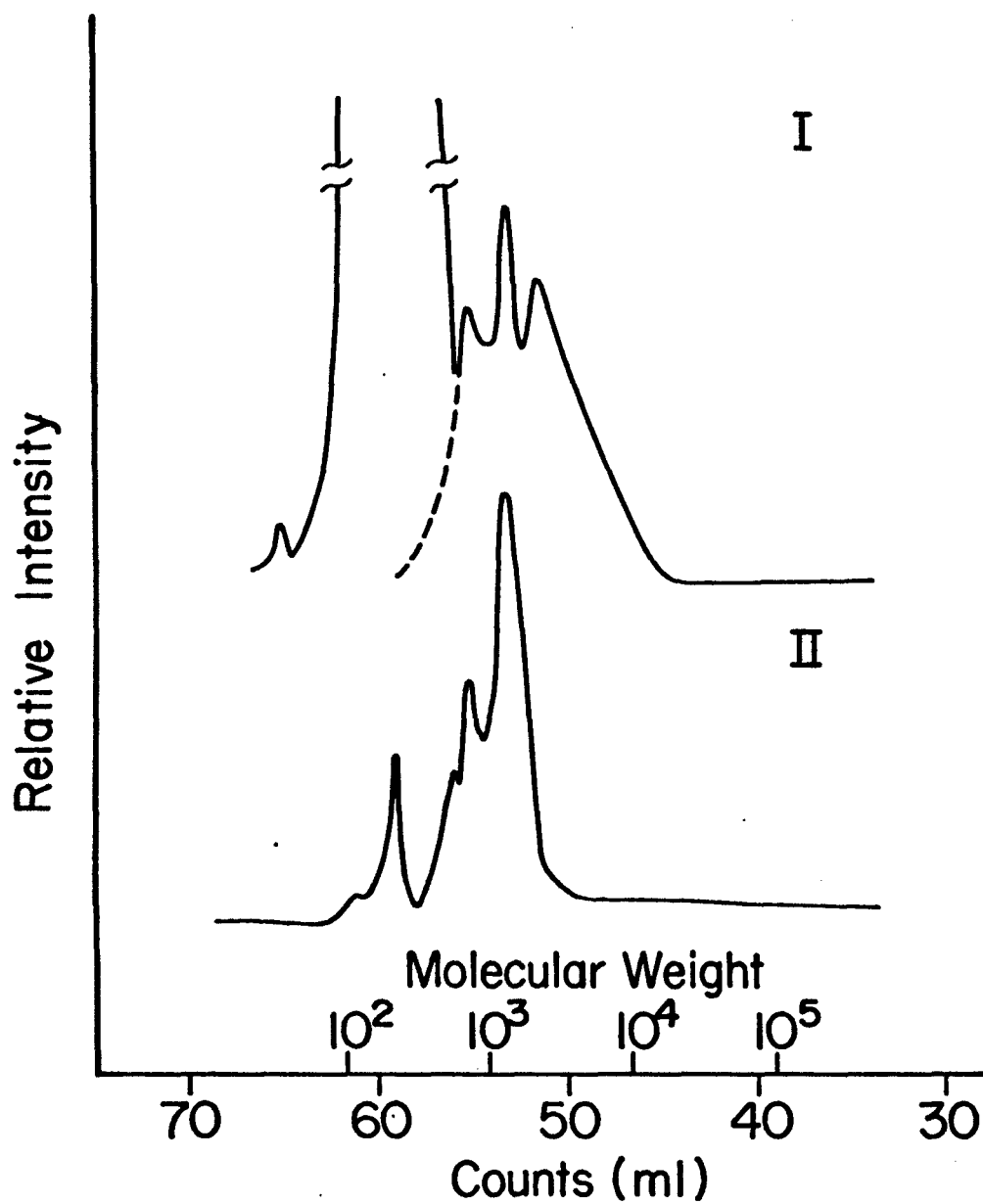


Fig. 15. Cumulative Differential Molecular-Weight Distributions for Thermal Polymerizations of Oligomers at 434 K. (a) Oligomer (I); (b) Oligomer (II).

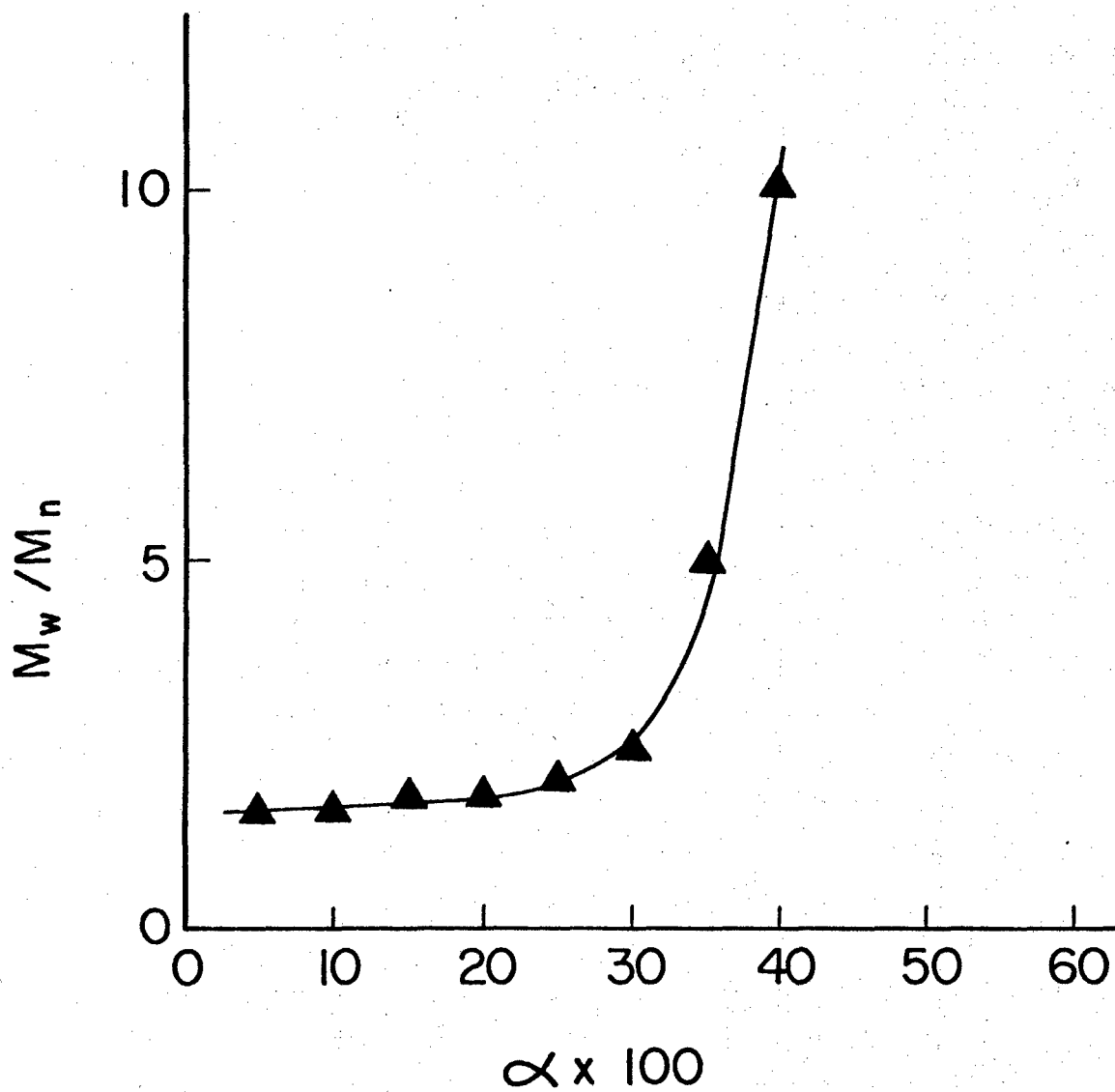


Fig. 16. Influence of Conversion upon the Ratio M_w/M_n at 434 K for Bis[4-(3-Ethynylphenoxy)Phenyl]Sulfone.

The influence of temperature upon the number-average molecular weight at 25% conversion in the range 390 to 510 K is shown in Fig. 17, and the data are summarized in Table 7. Although the data are somewhat scattered, M_n exhibits a small but significant exponential temperature dependence. For a conventional free-radical mechanism controlled by second-order termination, one expects a sizeable temperature dependence for the polymer molecular weight since the kinetic chain length is inversely proportional to the square root of the rate of initiation [10]. The small temperature variation shown in Fig. 17 suggests that in the pre-gel stage of polymerization, molecular weight is governed by a first-order termination.

Proposed Reaction Mechanism

The sum of the experimental data, in particular the polymer-characterization data, indicates a polymer structure consistent with a low-molecular-weight polyene. The possibility of a simple condensation or step-growth mechanism in the pre-gel stages of reaction can be ruled out on the basis of the dispersion data since a high-molecular-weight polymer, i.e., a polymer with $DP_n \geq 10$, would not be expected until attainment of high conversion. This observation along with the similarity of the kinetics to simple arylacetylenes [9,10] suggests that a free-radical chain mechanism is operative.

While the uncertainty associated with the determination of the dispersion ratio, M_w/M_n , from GPC probably is too large to draw definitive conclusions pertaining to the termination mechanism, the absence of a significant temperature dependence for number-average molecular weight strongly implies a first-order termination process as the major factor governing the kinetic and molecular chain lengths. Thus, the free-radical mechanism illustrated in Fig. 18 is proposed for the pre-gel stage of the thermal polymerization of Bis[4-(3-ethynylphenoxy)phenyl]sulfone.

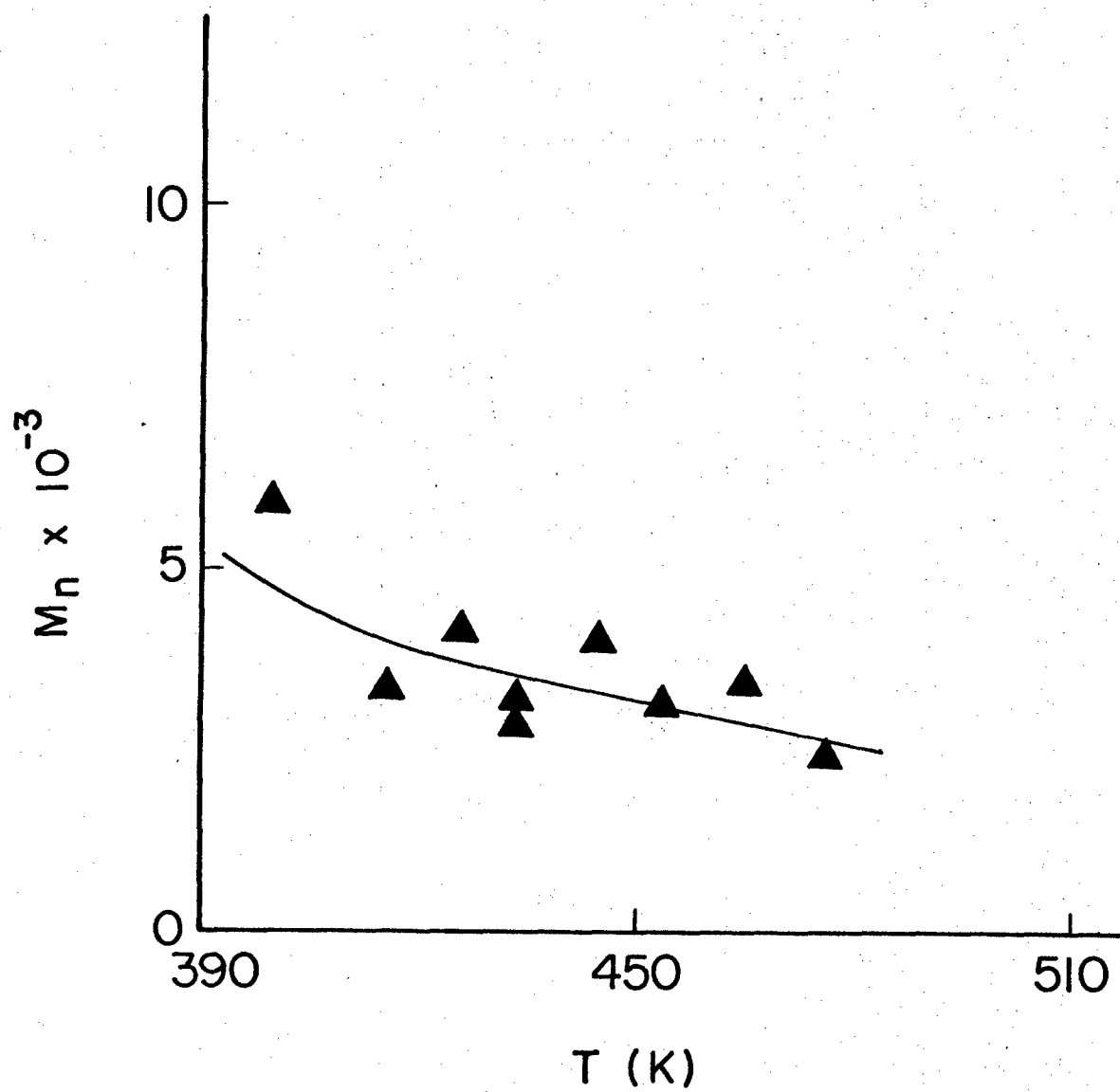


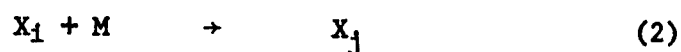
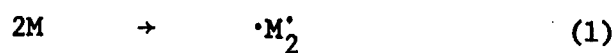
Fig. 17. Temperature Dependence of Number-Average Molecular Weight at 25% Conversion.

TABLE 7
EFFECT OF TEMPERATURE UPON
NUMBER-AVERAGE MOLECULAR WEIGHT AT CONSTANT CONVERSION

<u>TEMP</u> (K)	<u>M_w^a</u>
400	5898
416	3293
426	4175
434	3117
434	2827
445	4023
465	3457
476	2357

^a Measured via GPC with $\alpha \approx 0.25$.

REACTION MECHANISM



.

.

.

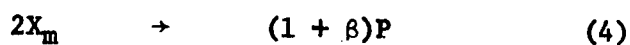
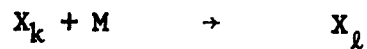
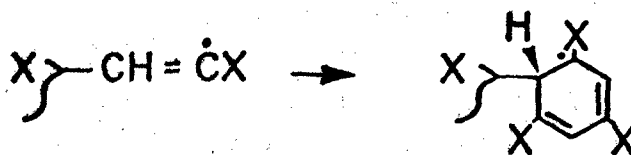


Fig. 18. Proposed Reaction Mechanism for Thermal Polymerization of Bis[4-(Ethynylphenoxy)Phenyl]Sulfone.

In the proposed mechanism, $\cdot M_2$ is the biradical, X_i , X_j , X_k , and X_l are growing polymer radicals, P represents the polymer, and β is an unknown variable which represents the fraction of polymer formed by disproportionation. Reaction (3), which represents a first-order deactivation of the growing polymer chain X_l , is consistent with the observation that the number-average molecular weight is only marginally dependent upon the polymerization temperature.

In reaction (1) of Fig. 18, the rate-determining step of initiation involves the tail-to-tail addition of two monomer units to yield a trans-biradical. Propagation is assumed to occur with equal probability at each radical site in the biradical; however, it is conceivable that one of the centers could be deactivated and initiation would result from a monoradical or psuedo-monoradical source. Reactions (2) and (3) are assumed to exert major control over the molecular weight, whereas reaction (4) does not.

While the nature of reaction (3) is not known with certainty, it is of interest to comment on two possibilities. First, in the absence of steric restrictions, reaction (3) could involve an intramolecular chain cyclization;



where X represents pendant 3-[4-[[4-(3-ethynylphenoxy)phenyl]sulfone]phenyl]-phenyl substituents attached to the polymer backbone. The proposed cyclohexadienyl species could then undergo unimolecular elimination to yield a cyclic trimer and a new active radical. The new radical center would disappear by radical coupling and/or disproportionations in reaction (4) or re-initiate the kinetic chain.

The second possibility is that the propagation is strongly size-dependent and that after achieving a certain critical chain length, the reaction

ceases. The free-radical site could be deactivated by steric restrictions or conceivably be transferred to the interior of the polymer chain. The deactivated radicals ultimately disappear through reaction (4). In this case, the formation of the trimer could arise from ring closure after addition of one monomer unit to the biradical formed in reaction (1) by head-to-tail addition.

If reaction (3) is identified with the first-order termination step, then application of the steady-state hypothesis assuming short kinetic chains leads to

$$-\frac{dM}{dt} = R_i \left\{ 1 + \frac{k_p}{k_t} M \right\} \quad (9)$$

for the net disappearance of monomer, where M is the monomer concentration, R_i is the rate of initiation, and k_p and k_t are specific rate constants for propagation and termination, respectively.

Under steady-state conditions the number-average degree of polymerization, DP_n , is related to the kinetic chain length, $\lambda = (dM/dt)/R_i$, by $DP_n = 2\lambda/(1+\beta)$, where β is the fraction of the polymer formed by disproportionation. If k_p/k_t and M are expressed as $A_p/A_t 10^{-(E_p - E_t)/\theta}$ and $M_o(1-\alpha)/(1+\Delta V/V_o)$, respectively, where ΔV is the volume change of polymerization and V_o and M_o refer to the volume and molarity of the neat monomer, then Eq. (9) may be rearranged to obtain

$$\log \left\{ DP_n - 2/(1+\beta) \right\} = - \frac{E_p - E_t}{2.303R} \left(\frac{1}{T} \right) + \log \left\{ \left(\frac{2}{1+\beta} \right) \frac{A_p}{A_t} \left[\frac{M_o(1-\alpha)}{1+\Delta V/V_o} \right] \right\} \quad (10)$$

For constant conversion, the decrease associated with $M_0/(1+\Delta V/V_0)$ will be offset by an expected increase in A_p/A_t ; therefore, within a reasonable approximation, the right-hand side of Eq. (10) involving $(1+\Delta V/V_0)$ should be invariant with temperature. Consequently, a plot of $\log \{DP_n - 2/(1+\beta)\}$ as a function of the reciprocal of absolute temperature should be linear, having a slope equivalent to $(E_p - E_t)/(2.303R)$.

The value of β is unknown; however, variation of β from zero to unity, while producing a small perturbation to the intercept of Eq. (10), would have a negligible effect upon the magnitude of $(E_p - E_t)/(2.303R)$. Therefore, β was equated to the average value of 0.5 and the molecular weight data in Table 7 plotted according to Eq. (10) in Fig. 19 were subjected to least-squares analysis to yield

$$\log \{DP_n - 4/3\} = (-1.0 \pm 0.6) + \frac{(3.6 \pm 1.3)}{\theta} \quad (11)$$

over the range 400 to 476 K. In Eq. (11) the difference in activation energies for propagation and termination indicates that E_t is approximately 4 kcal/mol larger than E_p . Also, from the intercept it may be inferred that A_t exceeds A_p by an order of magnitude. These parameters are qualitatively consistent with those expected from semi-empirical thermochemical estimates [10], and the agreement adds support to the proposed mechanism.

In the post-gel stage of the polymerization, subsequent reactions of the polymer chains, excess monomer, and the cyclic trimer would then result in additional chain extension and cross-linking to yield a large network resin. The incorporation of the trimer into the polymer chain is consistent with recent ^{13}C magic-angle spectra on cured samples of the acetylene-terminated polyimide, thermid, which indicates that less than 30% of the ethynyl groups react by cyclotrimerization [11].

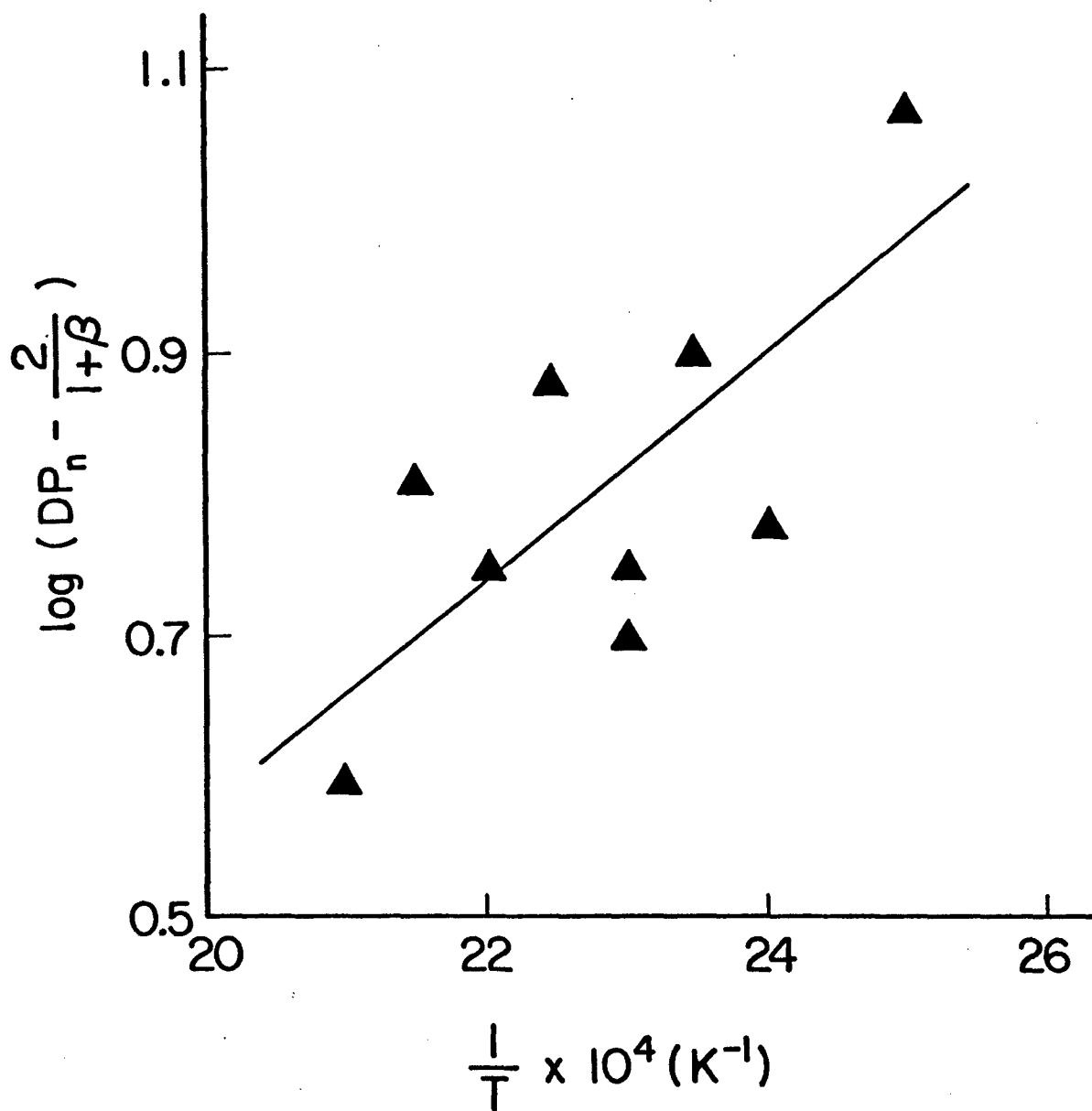


Fig. 19. Temperature Dependence of the Number-Average Degree of Polymerization at Constant Conversion.

SECTION 4
SUMMARY, CONCLUSION, AND RECOMMENDATIONS

SUMMARY AND CONCLUSIONS

A summary of results for TGMS analyses of a series of acetylene-terminated and related oligomers is presented. Sample weight loss and volatile gas evolution during programmed heating of polymers are correlated in order to assess thermal stabilities and obtain qualitative information concerning the mechanism of polymer degradation.

Thermal polymerization of a key oligomer, bis[4-(3-ethynylphenoxy)phenyl] sulfone, and an associated model compound, 4-(3-ethynylphenoxy) phenyl phenyl sulfone, were examined using combined techniques of DSC, GPC, IR, ^1H NMR, and ^{13}C NMR. Based upon the total data, a general mechanism for the polymerization of acetylene-terminated oligomers was devised. A more extensive discussion of the mechanistic implications is given in the publications in the accompanying Appendix.

The following points are pertinent for the proposed reaction mechanism:

- (1) Initiation results from a monoradical or psuedo-monoradical source in which the rate-determining step is governed by biradical formation arising from tail-to-tail addition of two monomer units.
- (2) In the pre-gel stage of the reaction, the kinetic and molecular chain lengths are controlled by a first-order termination which may involve cyclization of the growing polymer chain. Subsequent polymer formation results from radical coupling and/or disproportionation.
- (3) In the post-gel stages of the reaction, coupling of the primary polymer chains and additional chain extension arising from competing reactions of the trimer and residual monomer result in the formation of an infinite network.

RECOMMENDATIONS

It is recommended that future work involve the following:

- (1) Investigation of the rate of initiation using deuterium kinetic isotope effects to identify specific mechanisms that may lead to production of monoradicals.
- (2) Investigation of the kinetics of gel-formation in solution and bulk using a polymer with a well-defined primary molecular weight distribution.

REFERENCES

1. R. F. Kovar, G. F. L. Ehlers, and F. E. Arnold, J. Polym. Sci. Chem. Ed., 15, 1081 (1977).
2. I. J. Goldfarb and A. C. Meeks, Kinetic Analysis of Therogravimetry, AFML-TR-68-181 (Air Force Materials Laboratory, Wright-Patterson Air Force Base, OH, 1968).
3. J. P. Phillips, Spectra-Structure Correlation, (Academic Press, NY, 1964), p. 47.
4. J. P. Phillips, Op. Cit. pp. 94, 130.
5. C. I. Simionescu, V. Percec and S. Dumitrescu, J. Polym. Sci. Chem. Ed., 15, 2497 (1977).
6. F. W. Wehrli and T. Whirthlin, Interpretation of Carbon-13 NMR Spectra (Heyden, London, 1978), p. 47.
7. C. F. Poranski, W. B. Moniz, and T. W. Giants, Coatings and Plastics Preprints, 38, 605 (1978).
8. K. S. Dhami and J. B. Strothers, Can. J. Chem., 43, 510 (1965).
9. G. N. Bantysrev, I. M. Scherbokova, M. I. Cherkashin, I. D. Kalikhman, A. N. Chirgir, and A. A. Berlin, Izv. Akad. Nauk. SSSR, Ser Khim, 1848 (1969); Eng. Transl. Bull. Acad. Sci., USSR, 8, 1661 (1970).
10. J. M. Pickard, E. G. Jones, and I. J. Goldfarb, Macromolecules, 12, 895 (1979).
11. M. D. Sefcik, E. O. Stepkal, R. A. McKay, and J. Schaefer, Macromolecules, 12 423, (1979).

APPENDIX

**PRESENTATIONS AND PUBLICATIONS UNDER CONTRACT F33615-77-C-5175
FOR PERIOD JUNE 1978 - JUNE 1979**

THE KINETICS AND MECHANISM OF THE BULK THERMAL
POLYMERIZATION OF (3-PHENOXYPHENYL)ACETYLENE

By

J. M. Pickard* and E. G. Jones
Research Applications Division
Systems Research Laboratories, Inc.
2800 Indian Ripple Road
Dayton, Ohio 45440

and

I. J. Goldfarb
Air Force Materials Laboratory
Air Force Wright Aeronautical Laboratories
Air Force Systems Command
Wright-Patterson Air Force Base
Ohio 45433

Macromolecules 12, 895 (1979)

ABSTRACT

The kinetics of the high-temperature bulk polymerization of (3-phenoxyphenyl)-acetylene were examined over the temperature range 400 to 600 K using differential scanning calorimetry. Analyses of samples polymerized over a wide range of temperature using gel permeation chromatography revealed that the polymer molecular weight is invariant with temperature. The absence of an observable temperature correlation for polymer molecular weight is examined in terms of a biradical mechanism in which the kinetic and molecular chain lengths are controlled by a first-order termination step involving cyclization of the growing polymer chain. Based upon the observed data and semi-empirical thermochemical arguments, it is concluded that the molecular weight of poly(3-phenoxyphenyl)-acetylene is controlled predominantly by steric and thermochemical factors rather than the reaction energetics.

INTRODUCTION

The mechanisms for thermal polymerization of arylacetylenes are of interest from both theoretical and technological viewpoints. These compounds, in particular phenylacetylene and its simple derivatives, polymerize spontaneously in the range 400 to 600 K, and initiation may involve biradical formation [1,2]. Also, the molecular weight of the resultant polymer is rather insensitive to polymerization temperature [3,4]. The lack of an appreciable temperature dependence for molecular weight has been interpreted in the past as arising from degradative chain transfer [5,6] and more recently as being the result of a size-dependent first-order deactivation of the polymer chains [4,7].

The 3-phenoxyphenyl substituent in the related monomer, (3-phenoxyphenyl)acetylene, occurs frequently in complex acetylene-terminated oligomers [8] that are used in the synthesis of highly temperature-resistant polymers. Since (3-phenoxyphenyl)acetylene possesses a substituent present in the oligomers as well as a reactivity comparable to phenylacetylene [9], it represents a useful model compound to examine in order to gain insight into the mechanism of polymerization of the acetylene-terminated oligomers. In this paper, we wish to report the kinetics of the bulk polymerization of (3-phenoxyphenyl)acetylene and discuss the mechanistic implications.

EXPERIMENTAL

The monomer was obtained from Midwest Research Institute and purified by vacuum distillation prior to use. Analysis by IR spectroscopy and gel permeation chromatography (GPC) indicated that the monomer purity exceeded 99%.

For kinetic runs, conversion data were determined from isothermal and dynamic differential scanning calorimetry (DSC) measurements using a Perkin-Elmer DSC-II calibrated against lead and indium at heating rates of 80, 40, 20, 10, and 5 K/min. In addition, isothermal conversion data were obtained from near-IR measurements by observing the disappearance of the acetylenic C-H stretching motion at 3250 cm^{-1} .

DSC KINETICS

Dynamic DSC

For dynamic DSC, the disappearance of monomer was calculated from Eq. (i),

$$-\frac{1}{W_0} \left(\frac{dW}{dt} \right) = \frac{1}{Q} \left(\frac{dq}{dt} \right) = A 10^{-E/\theta} F(W), \quad (i)$$

where dq/dt is the differential power output in mcal/sec, Q is the total heat of reaction in mcal, W_0 is the initial weight of monomer, and W is the weight of residual monomer at time t . The parameters A and E are the usual Arrhenius parameters and $\theta = 2.303 RT$ kcal/mol.

The quantity $F(W)$ [10] in Eq. (i) represents a concentration variable and was assumed to have the form,

$$F(W) = (W/W_0)^n = (q/Q)^n = (1-\alpha)^n, \quad (\text{ii})$$

where n is the reaction order and α , the degree of conversion at time t , is $(1-W/W_0)$. The apparent rate constant, k_{ap} , is $A10^{-E/\theta}$; thus, Eqs. (i) and (ii) were combined to obtain

$$\frac{d\alpha}{dt} = k_{ap} (1-\alpha)^n. \quad (\text{iii})$$

The molarity of the reacting sample was defined as

$$M = \frac{X_0(1-\alpha)}{V_0 + \Delta V} = \frac{M_0(1-\alpha)}{1 + \Delta V/V_0} \quad (\text{iv})$$

where X_0 and M_0 are the initial moles and molarity of the neat monomer, respectively, V_0 is the initial volume, and ΔV is the volume change of the reaction. Density measurements for the pure monomer and solutions of polymer in monomer corresponding to 10% conversion indicated that ΔV approached 14% for 100% conversion.

The enthalpy of polymerization, ΔH_p , in kcal/mol was derived from

$$\Delta H_p = \Delta H_s \left(\frac{A_m}{A_s} \right) \left(\frac{W_s}{W_m} \right) \quad (v)$$

where ΔH_s is the heat of fusion of the standard, A_m and A_s are areas of the exotherms, and W_m and W_s are weights of monomer and standard.

In a typical dynamic DSC run, a sample of the freshly degassed monomer (2-4 mg) was transferred to a standard DSC pan and scanned under nitrogen at the appropriate heating rate. Data reduction and analysis were obtained with computer programs described previously [11].

Isothermal DSC

For isothermal DSC runs, a sample of the monomer was rapidly heated (heat rate = 320 K/min) to the desired temperature and the total output, dq/dt , was monitored continuously until apparent completion of the exotherm. At this time, the sample was rescanned to establish a baseline, the rate being given by the difference between the baseline and total output. The partial heat of reaction at time t_i was determined by step-wise integration using

$$q_i = (M_m / W_m) \Sigma (dq/dt) \Delta t \quad (vi)$$

where M_m is the molecular weight of monomer and Δt is the observation time.

GPC analysis of these samples indicated the presence of residual monomer;

therefore, conversions were calculated from Eq. (vi) by normalization with the total heat, Q , determined from the dynamic analysis.

IR MEASUREMENTS

Additional isothermal experiments were conducted by monitoring the disappearance of the monomer by IR spectroscopy. In these runs samples of the monomer were weighed into DSC pans, which in turn, were placed in $10 \times 1/4$ in. polymerization tubes. The polymerization tubes were purged with nitrogen and placed in a silicone oil bath maintained at 500 ± 0.2 K. At periodic intervals the tubes were removed from the oil bath and the reaction was quenched by submersion of the tubes in liquid nitrogen. The contents of the DSC pans were dissolved in carbon tetrachloride and the residual monomer was determined from IR at 3250 cm^{-1} .

MOLECULAR WEIGHTS

Molecular weight data were obtained with a Waters Model 244 Liquid Chromatograph using 10^4 , 10^3 , $2 (5 \times 10^2)$, and 10^2 Å μ -STYRAGEL columns. The GPC columns were standardized against low-molecular-weight polystyrene standards as well as isolated fractions of poly(3-phenoxyphenyl)acetylene. All samples used for the GPC calibration were standardized against benzil with a Mechrolab Vapor Phase Osmometer. Weight- and number-average molecular weights as functions of temperature and conversion were determined from the areas of the GPC curves.

RESULTS AND DISCUSSION

DSC KINETICS

Dynamic DSC

Figure 1 illustrates the reaction exotherms obtained for the dynamic DSC runs for three of the five heating rates. Representative rate data in the range 10 to 60% conversion and the total number of data points obtained from each exotherm are summarized in Table I. The temperature dependence of the rate data was evaluated by combining Eqs. (i) and (iii) to obtain

$$\log \left(\frac{d\alpha}{dt} \right) = \frac{-E}{2.303R} \left(\frac{1}{T} \right) + \log A(1-\alpha)^n. \quad (\text{vii})$$

At constant conversion, and assuming A and n constant, Eq. (vii) should yield a linear relation between $\log (d\alpha/dt)$ and T^{-1} . Therefore, the apparent activation energy, E, may be obtained from the slope of Eq. (vii) at each level of conversion. An Arrhenius plot of Eq. (vii) for the data of Table I is shown in Fig. 2. In Fig. 2, the data obtained at each of the different conversion points fall essentially on lines of the same slope and indicate that E is independent of conversion. In order to evaluate A and n, Eqs. (i) and (iii) were combined to derive

$$\log AF(W) = \log A(1-\alpha)^n = n \log (1-\alpha) + \log A. \quad (\text{viii})$$

Values of $AF(W)$, calculated from the average activation energy and the rate data at each heating rate, were combined with the conversion data and n and A were determined from the slope and intercept of Eq. (viii). The order plot derived from Eq. (viii) is shown in Fig. 3. Over the interval of 400 to 600 K from 20 to 60% conversion, the reaction was determined to be approximately first-order ($n = 1.09$), and least squares analysis of the rate data resulted in

$$\log (k_{ap}/s^{-1}) = (7.6 \pm 0.5) - (23.2 \pm 1)/\theta \quad (ix)$$

where $\theta = 2.303 RT$ kcal/mol. The error estimates correspond to one standard deviation.

The enthalpy of polymerization, ΔH_p , calculated for four of the five exotherms of the dynamic DSC data from Eq. (v) are summarized in Table II. The agreement between the values of ΔH_p obtained at each heating rate indicates that the reaction is independent of the heating rate.

Isothermal DSC

Conversion-versus-time data obtained from the isothermal DSC measurements over the temperature range 480 to 540 K as well as that obtained at 500 K from IR measurements are plotted in Fig. 4. The excellent agreement between these two techniques for the runs at 500 K confirms that the exothermicity of the reaction is associated with the loss of the acetylenic moiety.

Reaction order plots based upon the logarithmic form of Eq. (iii) for the isothermal data up to 70% reaction are shown in Fig. 5 where the indicated slopes were chosen to reflect the best overall fit to the observed data. Over the first 50% of reaction, least squares analysis resulted in reaction orders of 2.5, 2.9, 2.9, and 2.3 at 480, 500, 520, and 540 K, respectively. The reason for the disparity between these observations and the apparent first-order monomer dependence obtained from the dynamic method is unknown, although it may be related to a difference in the activity of the monomer at higher conversion associated with the dynamic experiments.

Rate data determined from the initial slopes of the conversion plots in Fig. 5 are summarized in Table III. These data were subjected to least squares analysis to obtain

$$\log (k_{ap}/s^{-1}) = (7.9 \pm 0.6) - (24.0 \pm 1.3)/\theta \quad (x)$$

which is in good agreement with the preferred result, Eq. (ix), obtained from the dynamic measurements.

The observed activation energies, $E = 23.2 \pm 1$ and 24.0 ± 1.3 kcal/mol from the dynamic and isothermal DSC analyses, respectively, are in good agreement with those expected from data previously reported for similar monomers [2], namely, phenylacetylene ($E = 26.2 \pm 1$ kcal/mol) and 2-methyl-5-ethynylpyridine ($E = 20.4 \pm 1$ kcal/mol).

A representative cumulative differential molecular weight distribution obtained from GPC analysis at 243 nm for monomer polymerized at 480 K is shown in Fig. 6. The total reaction products were dissolved in chloroform, and the major components consisting of fractions (1-2) were isolated by precipitation with methanol. The IR and ^1H NMR spectra of these fractions were similar to those previously reported for the trans-cisoidal isomer of polyphenylacetylene [12-14]. Low-pressure reduction of fraction (1) with a Pd/charcoal catalyst resulted in uptake of 4.6 moles H_2 /mole of polymer based upon a VPO molecular weight of 2300. For a polyene structure of the same molecular weight, one would expect an absorption of ≈ 11 moles of hydrogen for a quantitative reduction. For comparison, a sample of polyphenylacetylene ($M_n \approx 2000$) prepared under identical conditions absorbed 4.3 moles of H_2 /mole of polymer. Based on these data, it is concluded that the polymer is a polyene with a trans-cisoidal conformation.

Fractions (3-5) were all soluble in methanol, and resolution was achieved from repetitive collections of the GPC fractions. The ^1H NMR spectrum relative to TMS of the major methanol-soluble component, fraction (3), exhibited a complex multiplet centered at 7.2 ppm and a singlet at 7.9 ppm with intensity ratios consistent with that expected for the trimer, 1,3,5-tris(3-phenoxyphenyl)benzene. Mass-spectral analysis revealed that fraction (4) was dimer. The GPC retention volume of fraction (5) was identical to that of the monomer.

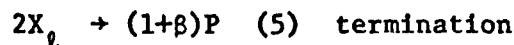
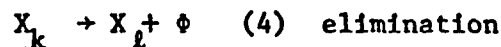
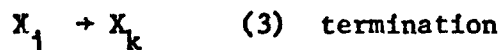
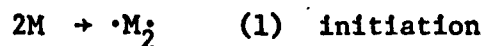
Molecular weights of the polymer distribution consisting of fractions (1-4) at several conversions and temperatures determined from the GPC analyses are

summarized in Table IV. For second-order termination, M_w/M_n should vary from 1.5 to 2.0, depending upon the amount of polymer formed by disproportionation. All of the data in Table IV exhibit $M_w/M_n \approx 1.2$ and are similar to those observed for polyphenylacetylene [7]. In view of the uncertainty associated with the GPC analysis of the ratio, M_w/M_n , it seems inappropriate to draw conclusions related to the termination mechanism from these measurements. On the other hand, the number-average molecular weights exhibit, at best, only a marginal temperature dependence. This observation strongly implies that the kinetic and molecular chain lengths are governed by a first-order termination step, as opposed to a second-order mechanism which would be reflected by a sizeable temperature dependence for molecular weight.

In addition to the data given in Table IV, two samples of monomer diluted with o-xylene ($M \approx 1.8$) were polymerized at 400 K. The average molecular weights of these samples were not significantly different from those obtained in bulk; thus, chain transfer can be excluded as a significant factor in controlling molecular weight.

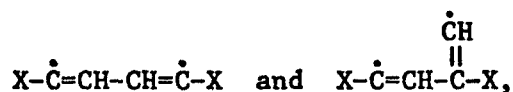
PROPOSED REACTION MECHANISM

Based upon the sum of our experimental data and the combined observations of Erhlich, *et al.*, [7] for the azobisisobutyronitrile-initiated reaction of phenylacetylene and those of Berlin and co-workers [2] for the corresponding thermal reaction, we propose the simple biradical mechanism shown below for (3-phenoxyphenyl)acetylene.



In the proposed mechanism, $\cdot M_2$ is a biradical; X_1 and X_j are growing polymeric radicals, X_k is a cyclic radical formed by intramolecular cyclization of radical X_j ; X_ℓ is an open-chain radical formed by unimolecular elimination of a cyclic trimer, ϕ , from species X_k ; P is polymer, and β is an unknown factor that may vary from zero to unity which represents the fraction of polymer formed by disproportionation.

Two possible structures for the biradical consist of the trans-1,4-di(3-phenoxyphenyl)-1,3-butadien-1,4-diyl and the cis-1,3-di(3-phenoxyphenyl)-1,3-butadien-1,4-diyl species,

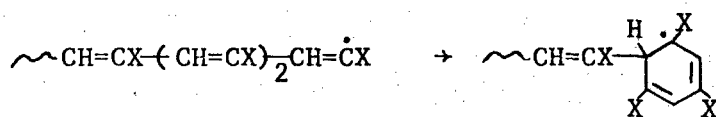


where X is identified with the 3-phenoxyphenyl substituent. While thermodynamic and structural considerations favor the trans species formed by tail-to-tail addition of monomer as the preferred structure, the cis-1,3-biradical obtained from head-to-tail addition should not be totally excluded.

Propagation is assumed to occur from a monoradical or pseudo-monoradical source. The initiating species could result from either subsequent reactions which produce simple monoradicals or from steric and/or conformational effects associated with one of the radical sites in $\cdot M_2$. However, in either case, one would still expect the rate-determining step of the reaction to be dominated by formation of the biradical, $\cdot M_2$.

Reactions (2), (3), and (4) are assumed to exert major control over the kinetic and molecular chain lengths, while reaction (5) does not. Reaction (3), first proposed for polymerization of phenylacetylene [7], represents first-order termination of the growing polymer chain. This is consistent with the polymer characterization data and the fact that the polymer molecular weight is rather insensitive to the polymerization temperature.

If propagation is exclusively head-to-tail, then reactions (3) and (4) may be represented as

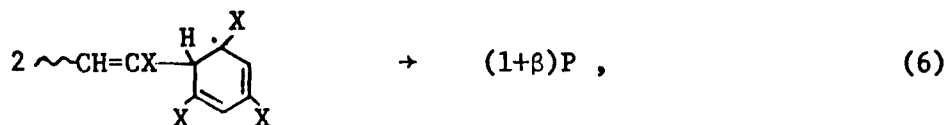


and

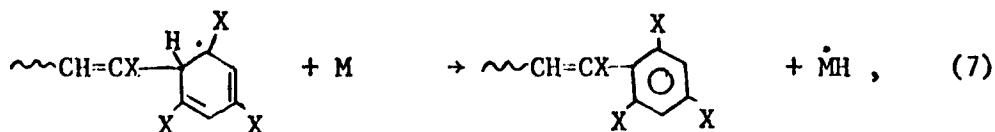


respectively. The conjugated radical, X_2 , formed by reaction (4) could then re-initiate the kinetic chain or disappear through reaction (5) by radical recombination and disproportionation.

The significance of competing termination steps involving the proposed cyclohexadienyl radicals, for example, by either the second-order reaction,



or the monomer transfer reaction,



may be assessed from consideration of appropriate relative rates. With respect to reaction (4), the relative rates of reactions (6) and (7) are $R_4/R_6 = k_4/(2k_6[X_k])$ and $R_4/R_7 = k_4/(k_7[M])$. From related thermochemistry [15], it is likely that $k_4 \geq k_6 = k_7$; therefore, the relative rates simplify to $R_4/R_6 \geq (2[X_k])^{-1}$ and $R_4/R_7 \geq [M]^{-1}$. Reaction (6) may be excluded from further consideration since this would require an unusually large molar concentration for X_k . i.e., $[X_k]$ would vary from 0.05 to 0.5, in order for the relative rate to be in the reasonable range of $0.1 \leq R_6/R_4 \leq 1$. Competition between reactions (4) and (7) is more feasible since $R_7 = R_4$ when $[M] = 1$; however, reaction (7) can still be excluded from the mechanism since appreciable chain transfer with o-xylene was not observed. Thus, the sequence of reactions (3-5) in the proposed mechanism would account for the observed product distribution, which consists primarily of linear polymer and cyclic trimer, as well as the marginal temperature dependence observed for the polymer molecular weight.

EVALUATION OF THE RATIO, k_p/k_t

Application of the usual steady-state hypothesis to the proposed mechanism assuming short kinetic chains leads to

$$-\frac{dM}{dt} = R_i \left\{ 1 + \frac{k_p}{k_t} M \right\}, \quad (\text{xi})$$

where R_i is the rate of initiation and k_p and k_t are specific rate constants for propagation and termination. Equation (xi) represents the net disappearance of monomer but simplifies to the more common long-chain approximation, i.e., $-dM/dt \approx (k_p/k_t)R_i M$, when $(k_p/k_t)M > 1$.

Since the kinetic chain length, λ , is $(-dM/dt)/R_i$, Eq. (xi) may be rearranged to obtain

$$\lambda = 1 + \frac{k_p}{k_t} M. \quad (\text{xii})$$

From Eq. (xii), one would expect a small temperature dependence for the kinetic chain length since k_p and k_t could have similar activation energies. The kinetic chain length is related to the number-average degree of polymerization, DP_n , by

$$DP_n = \frac{2}{(1+\beta)} \left\{ 1 + \frac{k_p}{k_t} M \right\}. \quad (\text{xiii})$$

Replacing M in Eq. (xiii) by Eq. (iv) yields

$$DP_n = \frac{2}{(1+\beta)} \left\{ 1 + \frac{k_p}{k_t} \left[\frac{M_0 (1-\alpha)}{1 + \Delta V/V_0} \right] \right\}, \quad (xiv)$$

which relates the number-average degree of polymerization at steady-state conditions to the extent of reaction and the volume contraction.

At ordinary temperatures, formation of polymer in reaction (5) would be expected to occur predominantly by radical combination. On the other hand, considering the rather high temperatures used to induce polymerization [16], one would infer similar size distributions for the intermediates and the resultant polymer. Thus, the unknown fraction, β , was equated to the average value of 0.5 and the molecular weight and conversion data in Table IV were combined in Eq. (xiv) to obtain the data for k_p/k_t summarized in Table V.

Examination of the block of data in Table V obtained at 500 K reveals a small correlation for k_p/k_t and the extent of reaction as expected from consideration of Eq. (xiv). Comparison of the average of the data at 500 K to the other entries over the entire temperature range indicates a negligible correlation with temperature.

The lack of an observable temperature correlation for k_p/k_t is not inconsistent with the suggestion based upon Eq. (xii) that the kinetic and molecular chain lengths might exhibit a small temperature coefficient arising from similar

activation energies for propagation and termination. For the related monomer, phenylacetylene, Erhlich and co-workers [4,7] have suggested that the temperature independence of the polymer molecular weight is due to a size-dependent electronic rearrangement rather than an exponential temperature dependence of rate constants. While this suggestion would apply equally to (3-phenoxyphenyl)-acetylene, we believe that the temperature independence of the molecular weight for both polymers may also be rationalized from kinetic and thermochemical arguments outlined below.

Entropy changes for both propagation and termination vary as $\overline{\Delta C_p^\circ} \ln(T/298)$, where $\overline{\Delta C_p^\circ}$ is the average heat capacity change of the reaction and T is absolute temperature. Changes in $\overline{\Delta C_p^\circ}$ are usually small, for example, thermochemical considerations [17] suggest that $\overline{\Delta C_p^\circ}$ for propagation is close to zero. In contrast, however, for termination (see Appendix) an additional increment arises from the loss of hindered internal rotation about carbon-carbon sigma bonds of the polyene chain in formation of the cyclohexadienyl species in reaction (4) which results in $\overline{\Delta C_p^\circ} = -3.5$ cal/K-mol. Therefore, the temperature dependence of the entropy change for termination should exceed that for propagation as determined by $\overline{\Delta C_p^\circ} \ln(T/298)$.

Since the magnitude of A_p/A_t is governed by the difference in entropy changes of propagation and termination, i.e., $\Delta S_p^\circ - \Delta S_t^\circ$, the latter considerations suggest that A_p/A_t should increase at higher temperature [18]. From the thermodynamic data of Table VI, the thermochemical considerations outlined in the Appendix, and assuming tight or product-like transition states [19] for propagation and termination, one can estimate that $\log (A_p/A_t/M^{-1}) = (-1.8 \pm 0.5) + 0.8 \ln(T/298)$ over the range 298 to 800 K.

Combining the estimate of $\log (A_p/A_t)$ with the average value, $k_p/k_t = 1.5 \text{ M}^{-1}$, from Table V at 500 K leads to

$$\log \left(\frac{k_p}{k_t} \text{M}^{-1} \right) = (-1.8 + 0.81 \ln(T/298) \pm 0.5) + (3.6 \pm 1)/\theta \quad (\text{xv})$$

for the predicted explicit temperature dependence of k_p/k_t .

The suggested temperature dependence of A_p/A_t would be negligible at ordinary temperatures for a polymerization consisting of long chains; however, it would be quite significant at high temperature when $\lambda \leq 10$. In fact, from the simple model given in the Appendix used to derive Eq. (xv), one expects A_p/A_t to increase by a factor of 1.4 over the range 450 to 540 K. In order for k_p/k_t to remain constant, a change in $E_p - E_t$ on the order of 0.2 kcal/mol would be required, which is well within the experimental uncertainty of the data of Table V. The predicted increase in A_p/A_t would effectively cancel the decrease associated with $(E_p - E_t)/\theta$ at higher temperature so that k_p/k_t remains essentially unchanged over the entire temperature range. Thus, it follows that $DP_n = 6 \pm 2$ estimated from Eq. (xiv) using k_p/k_t evaluated from Eq. (xv) over the range 450 to 540 K compares favorably with $DP_n = 5 \pm 0.5$ determined by the molecular weight data given in Table IV. Similar arguments might also account for the temperature independence of the molecular weight of polyphenylacetylene.

The proposed first-order termination step, reaction (4), is analogous to intramolecular propagation; therefore, the predicted temperature dependence for k_p/k_t

given by Eq. (xv) should be comparable to cyclization ratios for monomers that cyclopolymerize by competing inter- and intramolecular propagation. This is supported experimentally by

$$\log \left(\frac{k_p}{k_c} / M^{-1} \right) = (-3.5 \pm 0.8) + (2.3 \pm 1.2)/\theta \quad (\text{xvi})$$

for methacrylic anhydride [20], where k_c is the specific rate constant for intramolecular propagation. The similarities of the ratios of the pre-exponential factors as well as the observed activation energy differences in Eqs. (xv) and (xvi) provide additional support that termination involves intramolecular cyclization. Furthermore, this comparison is in accord with the expectation that A_t is greater than A_p , which suggests that the steric requirements for continued propagation exceed those for termination even though the activation energy for termination may be greater than that expected for propagation. This leads us to conclude that the kinetic and molecular chain lengths of poly(3-phenoxyphenyl)-acetylene are influenced more by steric and thermochemical effects than those associated with reaction energetics.

SUMMARY

The kinetics of the high-temperature bulk polymerization of (3-phenoxyphenyl)-acetylene were studied with isothermal and dynamic differential scanning calorimetry, gel permeation chromatography, and infrared spectroscopy. The apparent heat of polymerization at a mean temperature of 535 K was determined to be $\Delta H_p = -36.4 \pm 1$ kcal/mol. Least squares analysis of the rate data was used to obtain the activation energy, $E = 23.2 \pm 1$ kcal/mol, and the pre-exponential factor, $A = 10^{7.6 \pm 0.5} \text{ s}^{-1}$.

GPC analyses of samples polymerized over a wide range of temperature indicated that the polymer molecular weight ($M_n = 1007 \pm 68$) is insensitive to the polymerization temperature. This was discussed in terms of a simple biradical mechanism in which molecular weight is controlled by a first-order termination step involving cyclization of the growing polymer chains.

Analysis of the molecular weight data, based upon the proposed mechanism, resulted in $k_p/k_t = 1.5 \pm 0.5 \text{ M}^{-1}$. The lack of an observable temperature correlation for k_p/k_t is consistent with a small but nonetheless significant temperature dependence for A_p/A_t estimated from semi-empirical thermochemical considerations. It was suggested that the temperature dependence of A_p/A_t would cancel the decrease at higher temperature associated with $(E_p - E_t)/\theta$ so that k_p/k_t remains essentially unchanged over the entire temperature range.

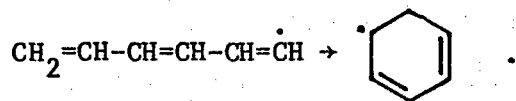
Based upon the internal consistency obtained by combining k_p/k_t with the semi-empirical estimate of A_p/A_t and the favorable comparison to kinetic data for a similar monomer, it was concluded that the kinetic and molecular chain lengths of poly(3-phenoxyphenyl)acetylene are controlled primarily by steric and thermochemical factors.

ACKNOWLEDGMENTS

Two of us, J. M. Pickard and E. G. Jones, gratefully acknowledge support of this work by the Air Force Systems Command, Air Force Materials Laboratory, Wright-Patterson Air Force Base, OH 45433 under Contract No. F33615-77-C-5175.

APPENDIX

The entropy change for termination was estimated for a model reaction of a polyene chain from group additivity [21] with the assumption that the entropy change is independent of the kinetic chain length and the nature of the pendant groups attached to the polymer backbone. Since the entropy change for termination depends largely upon the loss of hindered internal rotation about carbon-carbon sigma bonds, termination may be approximated as



The thermodynamic properties of the radicals, for example, entropy, were obtained by the difference method [22] using

$$S^\circ(\dot{\text{R}}) = S^\circ(\text{RH}) + \Delta S^\circ_{\text{vib}} + \Delta S^\circ_{\sigma} + \Delta S^\circ_{\text{e}} + \Delta S^\circ_{\text{conj}} \quad (\text{A1})$$

where $S^\circ(\dot{\text{R}})$ is the entropy of the radical and $\Delta S^\circ_{\text{vib}}$, ΔS°_{σ} , $\Delta S^\circ_{\text{e}}$, and $\Delta S^\circ_{\text{conj}}$ are corrections to the hydrocarbon entropy, $S^\circ(\text{RH})$, for changes associated with vibrational degrees of freedom, symmetry, electronic state, and resonance, respectively, arising from the loss of a hydrogen atom in the parent hydrocarbon. The additional corrections associated with mass, barrier heights, and overall rotation were neglected. The model compounds consisted of 1,3-cyclohexadiene and 1,3,5-hexatriene.

Corrections for symmetry were taken as $R \ln \sigma$, where σ is the product of the total independent symmetry axes within the molecule. Electronic states were assumed to be doubly degenerate and ΔS°_e was approximated as $R \ln(2S+1)$ where S is the net electron spin. For both radicals, $\Delta S^\circ_{\text{vib}}$ was associated with the loss of three vibrational degrees of freedom at 3000, 1150, and 700 cm^{-1} , while delocalization of the odd electron in the 1,3-cyclohexadienyl radical was equated to a 3-electron torsion at 500 cm^{-1} . Appropriate corrections for $\Delta S^\circ_{\text{vib}}$ and $\Delta S^\circ_{\text{conj}}$ were obtained from tables tabulated by Benson and O'Neal [22].

Gas phase thermodynamic properties of the parent model compounds and the radicals are summarized in Table VI. The absolute entropy change at 298 K, ΔS°_{298} , for the ideal gas state at one atmosphere is related to that at higher temperature by

$$\Delta S^\circ_T = \Delta S^\circ_{298} + \overline{\Delta C^\circ_p} \ln(T/298) \quad (\text{A2})$$

where ΔS°_T is the entropy change at temperature T and $\overline{\Delta C^\circ_p}$ is the average reaction heat capacity change over the observed temperature range. From the data given in Table VI, Eq. (A2) yields

$$\Delta S^\circ_T = (-12.6 \pm 0.5) - (3.5) \ln(T/298) \text{ cal/K-mol} \quad (\text{A3})$$

for termination over the range 298 to 800 K. One should note that the mole change for termination is zero; therefore, the entropy change is independent of the standard state and should be unchanged in a condensed phase [23].

The result for $\log (A_p/A_t)$ was evaluated from the assumption of tight transition states, i.e., assuming $\Delta S^\ddagger = \Delta S^\circ$ [19], from

$$\log \left(\frac{A_p}{A_t} \right) = \frac{\Delta S_p^\circ - \Delta S_t^\circ - R \ln \Delta V}{2.303 R} \quad (\text{A4})$$

where ΔV (≈ 0.14) is the volume change of polymerization. The entropy for propagation is not known precisely; however, it should be similar to that for related vinyl monomers, $\Delta S_p^\circ \approx -25 \pm 2$ cal/K-mol [19]. With the latter assumptions, Eqs. (A3) and (A4) lead to

$$\log \left(\frac{A_p}{A_t} M^{-1} \right) = (-1.8 \pm 0.5) + 0.8 \ln(T/298) \quad (\text{A5})$$

over the range 298 to 800 K.

REFERENCES AND NOTES

1. P. S. Shantarovich and I. A. Shlypanikova, *Vysokomol. Soedin.*, 3, 363 (1961); *Eng. Transl. Polym. Sci. USSR*, 3, 103 (1962).
2. G. N. Bantsyrev, I. M. Scherbakova, M. I. Cherkashin, I. D. Kalikhman, A. N. Chigir, and A. A. Berlin, *Izv. Akad. Nauk. SSSR, Ser. Khim.*, 1848 (1969); *Eng. Transl. Bull. Acad. Sci. USSR*, 8, 1661 (1970).
3. B. Biyani, A. J. Campagna, D. Daruwalla, C. M. Srivastava, and P. Ehrlich, *J. Macromol. Sci., Chemistry*, A9, 327 (1975).
4. H. X. Nguyen, S. Amdur, and P. Ehrlich, *Amer. Chem. Soc., Div. Polym. Chem. Prepr.*, 18(1), 200 (1978).
5. I. M. Barkalov, A. A. Berlin, V. I. Goldanskii, and Go Min-Gao, *Vysokomol. Soedin.*, 5, 368 (1963); *Eng. Transl. Polym. Sci. USSR*, 4, 1025 (1963).
6. I. M. Barkalov, V. I. Goldanskii, L. M. Kotova, and S. S. Kuzmina, *Vysokomol. Soedin.*, 5, 373 (1963); *Eng. Transl., Polym. Sci. USSR* 4, 1031 (1963).
7. S. Amdur, A. T. Y. Cheng, C. J. Wong, P. Ehrlich, and R. D. Allendoerfer, *J. Polym. Sci. Chem. Ed.*, 16, 407 (1978).
8. R. F. Kovar, G. F. L. Ehlers, and F. E. Arnold, *J. Polym. Sci., Chem. Ed.*, 15, 1081 (1977).

9. J. M. Pickard, E. G. Jones, and I. J. Goldfarb, Amer. Chem. Soc., Div. Polym. Chem. Prepr., 19(2), 591 (1978).
10. E. S. Freeman and B. Carroll, J. Phys. Chem., 62, 394 (1968).
11. I. J. Goldfarb and A. C. Meeks, Kinetic Analysis of Thermogravimetry, AFML-TR-68-181, Air Force Materials Laboratory, Wright-Patterson Air Force Base, OH, 1968.
12. R. J. Kern, J. Polym. Sci. A, 7, 621 (1969).
13. C. I. Simionescu, V. Percec, and S. Dumitrescu, J. Polym. Sci. Chem. Ed., 15, 2497 (1977).
14. S. Dumitrescu, V. Percec, and C. I. Simionescu, J. Polym. Sci. Chem. Ed., 15, 2893 (1977).
15. S. W. Benson and R. Shaw, J. Amer. Chem. Soc. 89, 5351 (1967).
16. M. G. Chauser, Y. M. Rodionov, and M. I. Cherkashkin, Dokl. Akad. Nauk SSSR, 230, 1122 (1976); Eng. Transl., Dokl. Chem., Proc. Acad. Sci. USSR, 230, 642 (1976).

17. If variations in chain length are neglected, then $\overline{\Delta C_p^\circ}$ for propagation is given by the difference in heat capacity of the monomer and the repeat unit of the polyene chain. For polymerization of acetylene, group additivity considerations similar to those outlined in the Appendix yield $\overline{\Delta C_p^\circ} = + 0.08 \text{ cal/K-mol}$ over the range 298 to 800 K.

18. This is analogous to use of the modified Arrhenius equation, $k = A'T^n e^{-E'/RT}$. The variables A' and E' are related to the usual Arrhenius parameters A and E by $A = A'(eT)^n$ and $E = E' + nRT$, where n is a small positive or negative integer.

19. A. M. North, The Kinetics of Free Radical Polymerization, Vol. 17 of The International Encyclopedia of Physical Chemistry and Chemical Physics, Pergamon Press, London, 1966, p. 58.

20. O. Chiantore, G. Camino, A. Chiorino, and M. Guaita, Makromol. Chem., 178, 125 (1977).

21. S. W. Benson, Thermochemical Kinetics, 2nd Ed., John Wiley and Sons, Inc., NY, 1976, p. 26.

22. H. E. O'Neal and S. W. Benson, Int. J. Chem., Kinet., 1, 221 (1969).

23. P. E. M. Allen and C. R. Patrick, Kinetics and Mechanisms of Polymerization Reactions, John Wiley and Sons, Inc., NY, 1974, p. 12.

FIGURE CAPTIONS

- Fig. 1. Reaction exotherms for thermal reaction of (3-phenoxyphenyl)acetylene. Heat rate (K/min) ● 80; ▲ 40; ■ 20.
- Fig. 2. Composite Arrhenius plot for thermal reaction of (3-phenoxyphenyl)-acetylene from 467 to 557 K. α ; ● 10; ▲ 20; ■ 40; ○ 60.
- Fig. 3. Dynamic DSC reaction order plot for thermal reaction of (3-phenoxyphenyl)-acetylene from 467 to 557 K.
- Fig. 4. Isothermal conversion time curves for thermal reaction of (3-phenoxyphenyl)-acetylene. DSC; ● 480 K; ▲ 500 K; ■ 520 K; ○ 540 K; IR; Δ 500 K.
- Fig. 5. Isothermal reaction order plots for thermal reaction of (3-phenoxyphenyl)-acetylene. — 0 to 50% conversion; ● 480 K; ▲ 500 K; ■ 520 K; ○ 540 K.
- Fig. 6. GPC trace for thermal reaction of (3-phenoxyphenyl)acetylene at 480 K. (1), (2) polymer; (3) oligomer; (4) dimer; (5) monomer.

TABLE I. SUMMARY OF DYNAMIC DSC DATA FOR THERMAL
POLYMERIZATION OF (3-PHENOXYPHENYL)ACETYLENE

Heat Rate (K/min)	$\alpha \times 100$	T (K)	$\frac{d\alpha}{dt} \times 10^3$ (s ⁻¹)	Total Data Pt.
80	10	518	9.87	122
	20	530	15.4	
	30	538	19.8	
	40	545	23.0	
	50	551	23.3	
	60	557	22.4	
40	10	508	4.13	170
	20	520	7.46	
	30	527	9.45	
	40	534	11.5	
	50	539	11.9	
	60	545	11.7	
20	10	500	2.67	152
	20	510	4.59	
	30	516	5.47	
	40	522	6.18	
	50	528	6.34	
	60	533	5.95	
10	10	480	1.15	169
	20	490	1.97	
	30	498	2.58	
	40	504	2.96	
	50	509	3.19	
	60	515	3.10	
5	10	467	0.74	125
	20	476	1.21	
	30	482	1.50	
	40	487	1.70	
	50	492	1.79	
	60	497	1.76	

TABLE II. HEAT OF POLYMERIZATION OF
(3-PHENOXYPHENYL)ACETYLENE

Heat Rate (K/min)	T_{\max}^a (K)	$-\Delta H_p$ (kcal/mol)
80	552	35.4
40	542	36.7
20	532	37.0
10	514	<u>36.6</u>
		Av 36.4 \pm 1

a. T_{\max} is the temperature at the maximum of the exotherm.

TABLE III. SUMMARY OF ISOTHERMAL DSC DATA FOR THERMAL
POLYMERIZATION OF (3-PHENOXYPHENYL)ACETYLENE

T (K)	W ₀ (mg)	$\frac{d\alpha}{dt} \times 10^4$ (s ⁻¹)	Reaction Order
540	2.2	133	2.5
520	2.1	64.3	2.9
500	3.7	27.0	2.9
480	3.6	8.33	2.3

TABLE IV. INFLUENCE OF TEMPERATURE AND CONVERSION ON THE
MOLECULAR WEIGHT OF POLY(3-PHENOXYPHENYL)ACETYLENE

T (K)	M_o^a (M)	$(1 + \Delta V/V_o)$	$\alpha \times 100^b$	M_n	M_w
540	2.65	0.921	51	1113	1301
520	2.76	0.960	26	1008	1099
500	2.80	0.980	13	973	1043
		0.970	19	947	1107
		0.956	28	971	1155
		0.941	38	912	1064
		0.934	43	1120	1374
		0.923	45	1091	1246
480	3.00	0.956	26	973	1131
460	3.14	0.970	19	1034	1201
450	3.31	0.967	21	985	1097
		0.969	20	<u>960</u>	<u>1095</u>
				Av 1007 \pm 68	1159 \pm 101

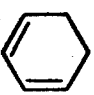

a. Bulk molarity of the monomer.

b. Determined from disappearance of the acetylenic
moiety at 3250 cm^{-1} .

TABLE V. INFLUENCE OF TEMPERATURE AND CONVERSION
ON THE RATIO, k_p/k_t

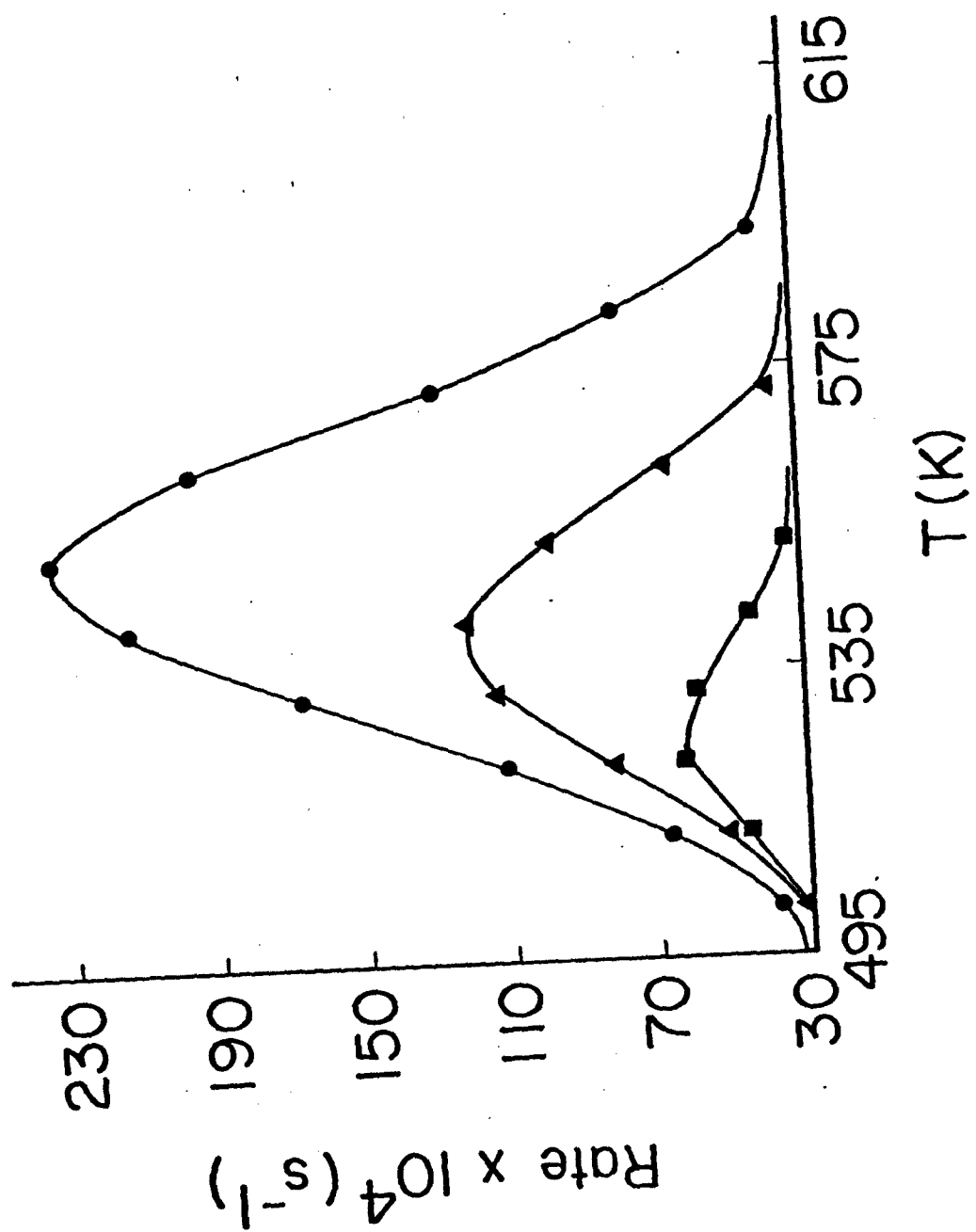
T (K)	$\alpha \times 100$	k_p/k_t (M ⁻¹)
540	51	2.4
520	26	1.4
500	13	1.1
	19	1.2
	28	1.3
	38	1.4
	43	2.1
	45	2.1
480	20	1.1
460	19	1.2
450	21	1.1
	20	<u>1.0</u>
		Av · 1.5 ± 0.5

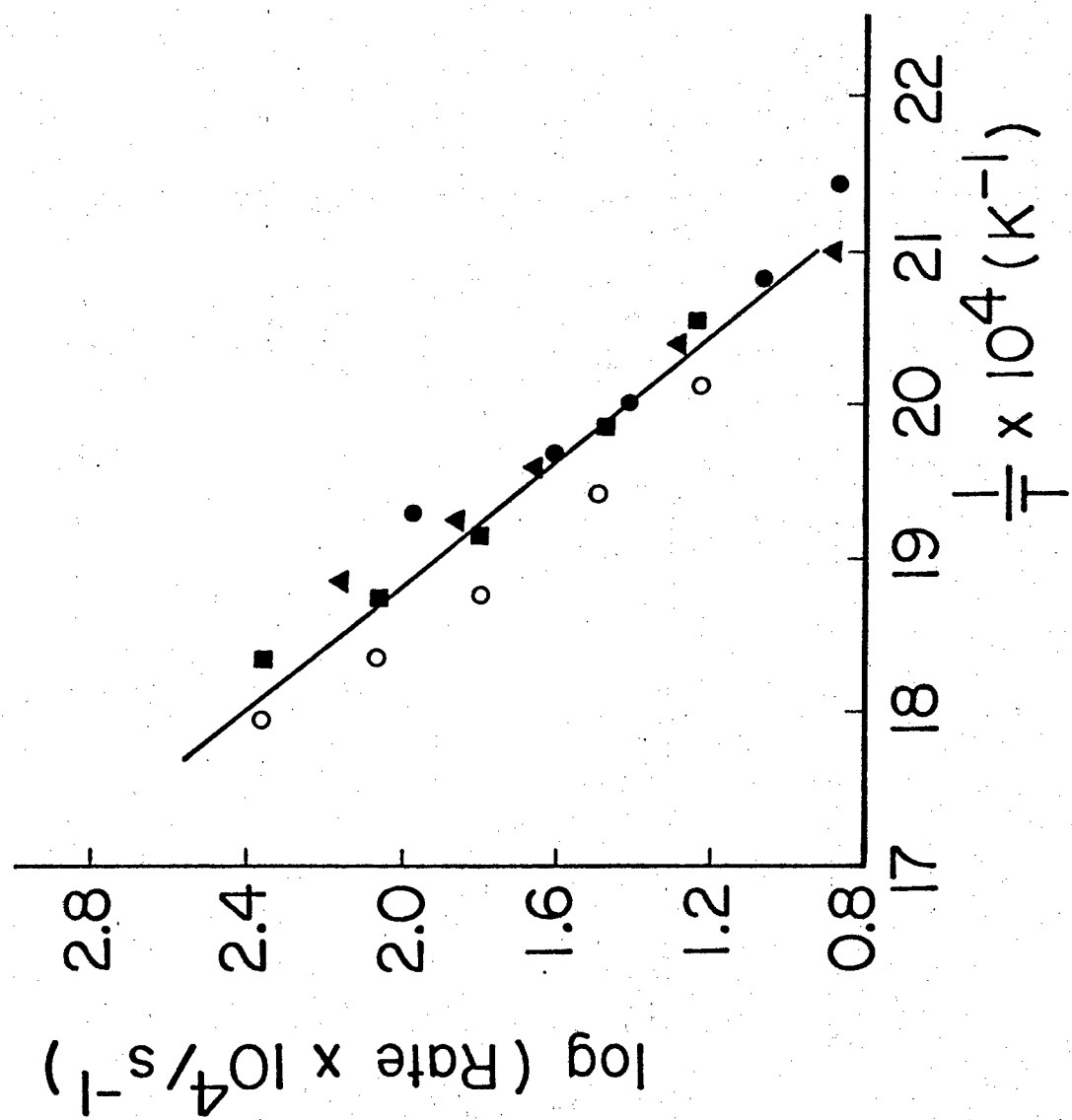
TABLE VI. SUMMARY OF IDEAL GAS THERMODYNAMIC PROPERTIES

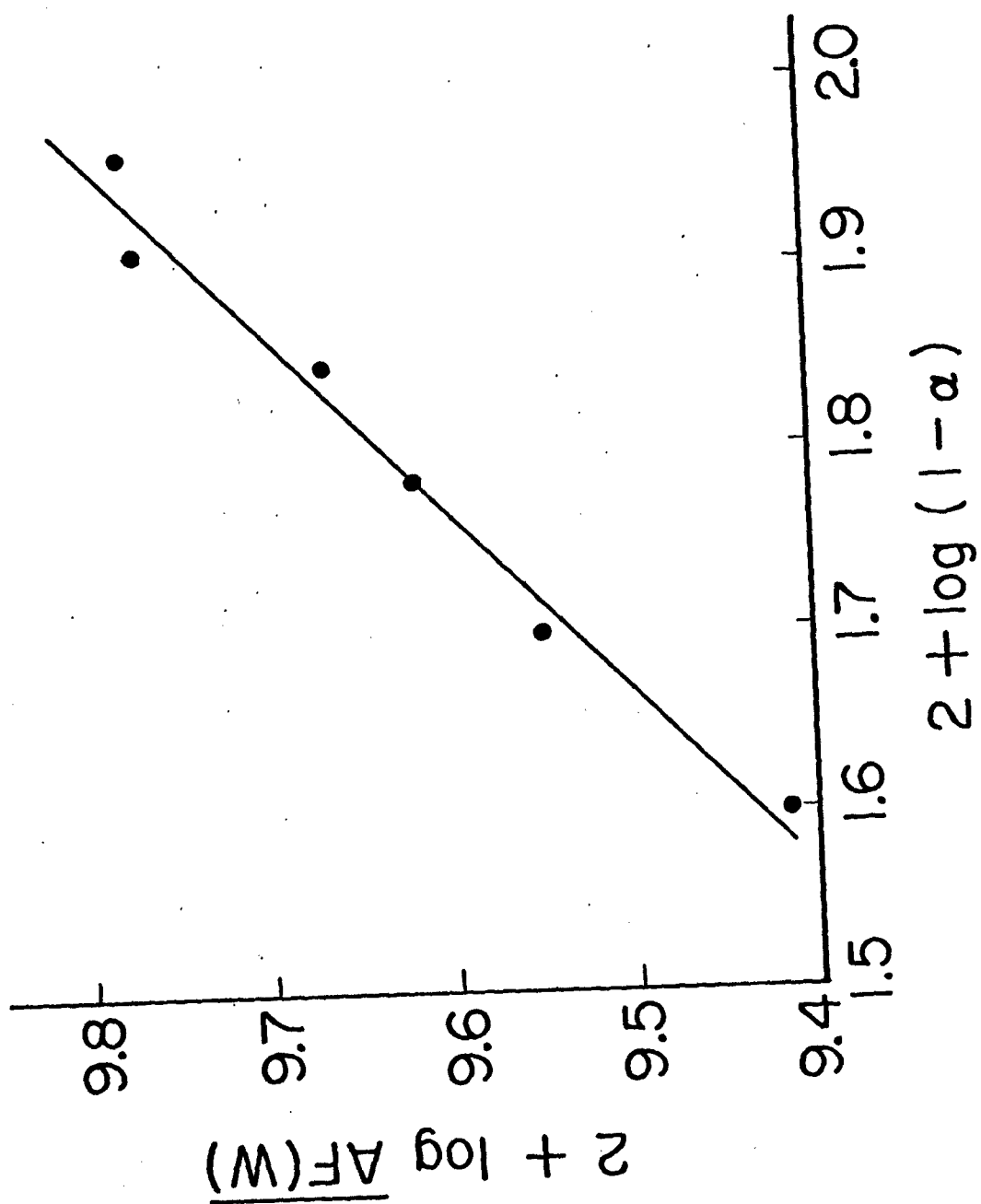
Species	Symmetry Number (σ)	S_{int}° ^a	C_p°	
		cal/K-mol	cal/K-mol	
		298 K	298 K	800 K
$\text{CH}_2=\text{CH}-\text{CH}=\text{CH}-\text{CH}=\text{CH}_2$	2	80.74	28.04	53.54
 ^b	2	67.40	23.08	51.42
$\text{CH}_2=\text{CH}-\text{CH}=\text{CH}-\dot{\text{C}}\text{H}$	1	79.02	26.90	50.09
	1	66.38	21.94	47.97

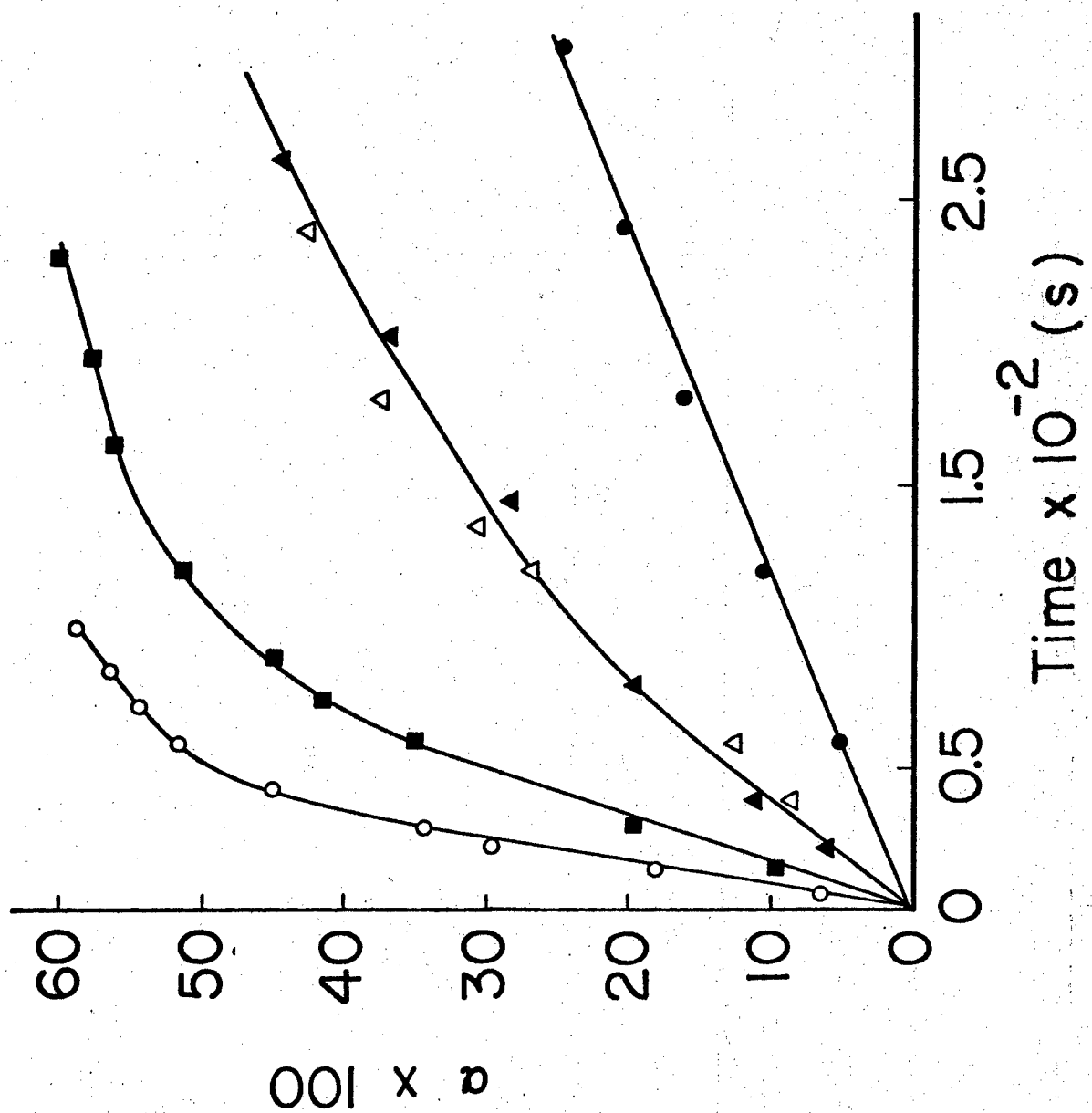
a. The intrinsic or symmetry-corrected entropy, S_{int}° , is related to absolute entropy by $S_{\text{int}}^{\circ} = S_{\text{abs}}^{\circ} + R \ln \sigma$.

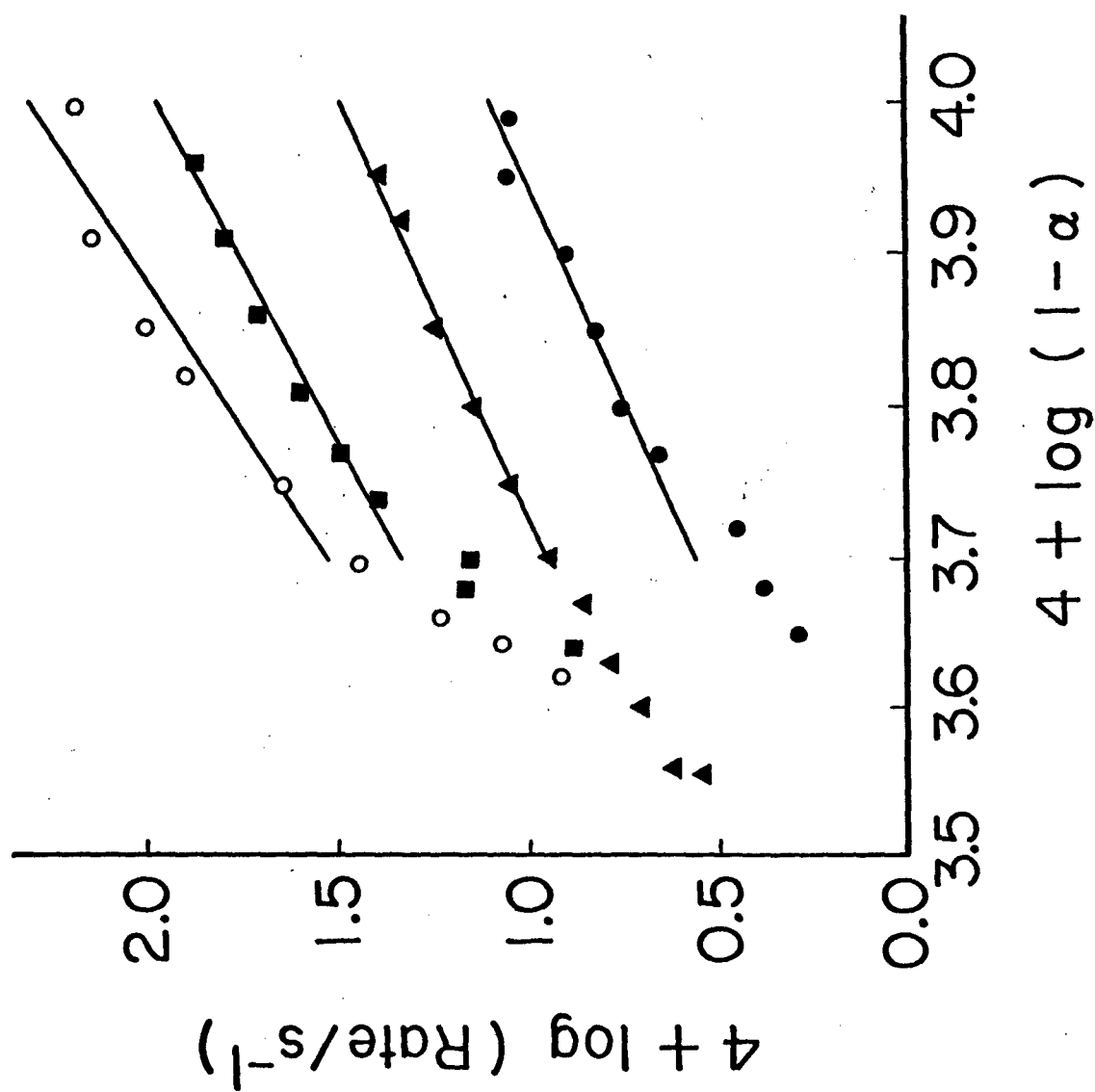
b. Estimated from $\text{CH}_3(\text{CH}_2)_4\text{CH}_3$ using Ref. [21], p. 68.

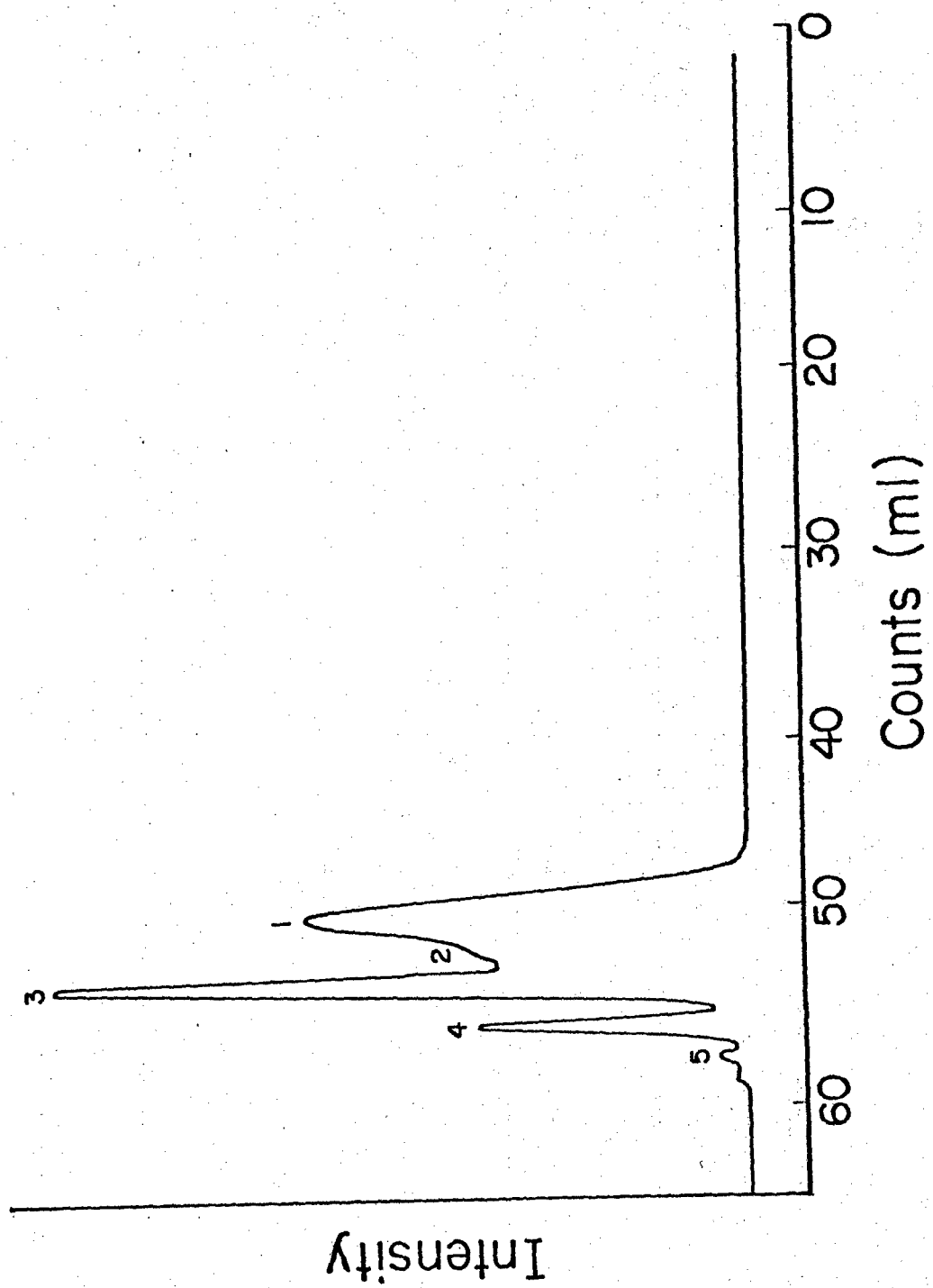












THE POLYMERIZATION OF BIS[4-(3-ETHYNYLPHENOXY)PHENYL]SULFONE AND 4-(3-ETHYNYLPHENOXY)-
PHENYL PHENYL SULFONE

<u>James M. Pickard</u>	Systems Research Laboratories, Inc.	x	x
<u>S. C. Chattoraj</u>	Research Applications Division		x
	2800 Indian Ripple Rd.		
	Dayton, Ohio 45440; phone 513-426-6000		
 M. T. Ryan	 Air Force Materials Laboratory		
	Air Force Wright Aeronautical Laboratories		
	Air Force Systems Command		
	Wright-Patterson Air Force Base, Ohio 45433		
	Systems Research Laboratories, Inc., 2800 Indian Ripple Rd., Dayton, OH 45440		
	Air Force Materials Laboratory, Wright-Patterson Air Force Base, OH 45433		
x	Macromolecules		none

THE POLYMERIZATION OF BIS[4-(3-ETHYNYLPHENOXY)PHENYL]SULFONE AND 4-(3-ETHYNYLPHENOXY)PHENYL PHENYL SULFONE. James M. Pickard and S. C. Chattoraj, Systems Research Laboratories, Inc., Research Applications Division, 2800 Indian Ripple Rd., Dayton, OH 45440; and M. T. Ryan, Air Force Materials Laboratory, Air Force Wright Aeronautical Laboratories, Air Force Systems Command, Wright-Patterson Air Force Base, OH 45433.

Thermal polymerization at 433 K of bis[4-(3-ethynylphenoxy)phenyl]sulfone (I) in the initial stages of reaction and of 4-(3-ethynylphenoxy)phenyl phenyl sulfone (II) up to 90% conversion was found to yield polymers with number-average molecular weights approaching 3000. The IR spectrum of polymer (I) contains a band at 3300 cm⁻¹, indicating the presence of free ethynyl moieties in the polymer. Both polymers exhibit weak bands in the region of 950 cm⁻¹, indicative of trans-unsaturation. The existence of trans-unsaturation in the polymer backbone is confirmed by ¹H NMR for both polymers and by ¹³C NMR for polymer (II) from analysis of spectral perturbations induced by the addition of a shift reagent, Eu(fod)₃. Assignments for ¹H NMR spectra were based upon a first-order analysis of multiplets, while those for ¹³C spectra were deduced from intensity effects and group additivity considerations. It is concluded that both polymers possess a trans-cisoidal structure.

Acknowledgement: Research sponsored in part by the Air Force Systems Command, Air Force Materials Laboratory, Wright-Patterson Air Force Base, OH 45433 under Contract No. F33615-77-C-5175.

THE POLYMERIZATION
OF BIS[4-(3-ETHYNYLPHENOXY)PHENYL]SULFONE
AND 4-(3-ETHYNYLPHENOXY)PHENYL PHENYL SULFONE

by

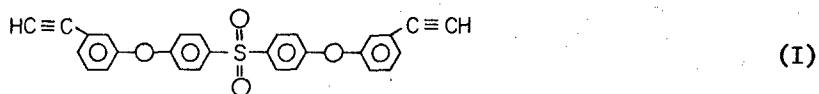
J. M. Pickard and S. C. Chattoraj
Systems Research Laboratories, Inc.
2800 Indian Ripple Rd.
Dayton, OH 45440

and

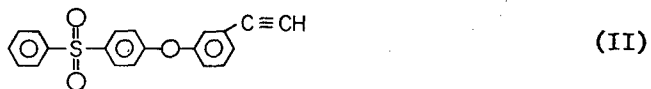
M. T. Ryan
Air Force Materials Laboratory
Air Force Wright Aeronautical Laboratories
Air Force Systems Command
Wright-Patterson Air Force Base, OH 45433

INTRODUCTION

In recent years, extensive research has been directed toward synthesis and characterization of acetylene-terminated oligomers consisting of sulfones, imides, and quinoxalines having potential for use as adhesives and composites in high-temperature aerospace environments [1]. The oligomers, for example, the sulfone



cure by the reaction of the terminal ethynyl moieties without evolution of volatile products, thereby avoiding the cavitation problem encountered with more conventional resin systems. Analogies drawn from the chemistry of simple arylacetylenes suggest that the pre-gel stage of the curing reaction may involve the formation of low-molecular-weight polyenes [2]. In this vein, oligomer (II)



would be expected to possess a reactivity comparable to that of simple arylacetylenes as well as that of the acetylene-terminated oligomer indicated by Structure (I). In this paper, IR, ^1H NMR, and ^{13}C NMR characterization data are presented which support the formation of polyene structures in the pre-gel stages of the bulk thermal polymerization of bis[4-(3-ethynylphenoxy)phenyl]sulfone (I) and 4-(3-ethynylphenoxy)phenyl phenyl sulfone (II).

EXPERIMENTAL

Polymer Synthesis

Polymerization was conducted in pyrex tubes under nitrogen atmosphere by heating in a silicone oil bath maintained at 433 ± 1 K. The reaction time for oligomer (I) was limited to 1 hr. ($\approx 40\%$ conversion) in order to minimize the formation of an insoluble cross-linked polymer. Oligomer (II) was reacted for 3 hr. to obtain a conversion approaching 90%. Reaction products for each oligomer were dissolved in CH_2Cl_2 , and the polymers were isolated by precipitation with methanol. Analysis of the reaction products by gel permeation chromatography revealed that, in

addition to the polymer, the reaction of both oligomers was accompanied by the formation of two lower-molecular-weight fractions. Analyses of the isolated polymers using vapor phase osmometry indicated that the number-average molecular weight of polymer (I) was 2785, while that of polymer (II) was 2620.

Polymer Characterization

Infrared spectra of the polymers and oligomers were obtained with a Perkin-Elmer 521 infrared spectrophotometer in either KBr matrices or as thin films on NaCl plates.

Nuclear magnetic resonance spectra were obtained with a Varian XL 100/15 NMR interfaced with a Varian VFT-100 computer and gyrocode decoupler. Proton spectra of the oligomers (0.2 M in CDCl_3) and polymers (0.05 g/ml in CDCl_3) as well as those obtained in the presence of 0.01 to 0.07 M concentrations of a shift reagent, $\text{Eu}(\text{fod})_3$, were recorded in the CW mode at 100.1 MHz. Chemical shifts were measured relative to internal TMS.

Pulsed FT ^{13}C spectra at 25.2 MHz for oligomer and polymer (I) were obtained in 1.7-mm tubes, while the spectra for oligomer and polymer (II) were obtained in 12-mm tubes. Proton-noise decoupled spectra of the oligomers were obtained using a 65° pulse and repetition time of 4.8 sec, while those of the polymers along with decoupled spectra were obtained with a 25° pulse and repetition time of 0.8 sec.

RESULTS AND DISCUSSION

IR spectra

Infrared spectra of the monomers and polymers are illustrated in Fig. 1. The structural complexity and inherent lack of high symmetry rule out the use of detailed group theoretical correlations; however, qualitative observations are easily discerned. The spectra of both oligomers, Figs. 1a and 1c, possess an intense band in the region of 3300 cm^{-1} and weak bands at 2100 cm^{-1} which are characteristic of the C-H and $\text{C}\equiv\text{C}$ stretching motions of the ethynyl groups, [3]. In polymer (II) the 3300 cm^{-1} band is absent, while in polymer (I) the intensity of this band has decreased to about one-half that observed in the initial oligomers, Figs. 1a and 1c.

The spectra of both oligomers and polymers exhibit weak bands at 3050 cm^{-1} , very intense bands at $1600\text{--}1500\text{ cm}^{-1}$, and strong bands at $700\text{--}600\text{ cm}^{-1}$ which are characteristic of C-H stretching, C=C stretching, and C-H deformation modes of the aromatic rings [4]. The positions of the intense bands in both polymers and monomers in the $1350\text{--}1200$ and $1150\text{--}1060\text{ cm}^{-1}$ regions associated with the symmetric and antisymmetric stretching motions of aryl ether and aryl sulfone moieties [5] are relatively unperturbed by polymerization. By analogy with simple polyarylacetylenes [2], both polymers exhibit weak bands around $960\text{--}940\text{ cm}^{-1}$ that may be indicative of trans-unsaturation. This observation and the existence of pendant ethynyl groups in polymer (I) are indications that both polymers possess trans-polyene structures.

^1H NMR Spectra

The proton spectra in the region 3-8 ppm for polymers (I) and (II) and changes induced by addition of the shift reagent, $\text{Eu}(\text{fod})_3$, are given in Figs. 2 and 3. Figures 2a and 3a both show characteristic broad absorption in the region 6-8 ppm which is analogous to the spectra of polyarylacetylenes [2].

Polymer (I) in Fig. 2a shows broad absorption at 7.9, 7.5 (CHCl₃ impurity), and 7.0 ppm with half-bandwidths, i.e., $\Delta\nu_{1/2}$, of 35, 10, and 35 Hz, respectively. The absorption at 7.0 ppm is asymmetric and decreases toward the baseline at 6.0 ppm. There is also a resonance with $\Delta\nu_{1/2} = 4$ Hz centered at 3.1 ppm, indicative of pendant ethynyl groups. The relative intensities of the ethynyl and aromatic protons are consistent with the proposed polyene structure for polymer (I). Polymer (II) in Fig. 3a exhibits broad absorption from 6 to 7.2 ppm, with $\Delta\nu_{1/2} \approx 80$ Hz, a sharp CHCl₃ impurity at 7.2 ppm, and broad absorptions with $\Delta\nu_{1/2} \approx 20$ Hz at 7.2 and 7.9 ppm. Assignments for the proton spectra based upon a first-order analysis of the multiplets are summarized in Table I.

Coordination of the shift reagent with the polymers would be expected to occur at the sulfone nucleus, which is supported experimentally by the spectral changes shown in Figs. 2b and 3b. Figure 3b for polymer (II) shows clearly that the aromatic protons shift downfield, revealing a broad resonance at 6.2 ppm. Similar behavior, but less intense due to more extensive line broadening, is observed in the spectrum of polymer (I) in Fig. 2b. The resonance in both polymers at 6.2 ppm is in the region reported for the olefinic protons of the trans-cisoidal isomer of polyphenylacetylene [2].

¹³C NMR Spectra

Assignments for ¹³C spectra were based upon intensity considerations and additivity rules for substituted benzenes [6,7]. In the oligomers, chemical shifts for the carbon atoms in the ethynylbenzene moiety were derived from substituent constants for a p-sulfonylphenoxy group and empirical parameters given for ethynylbenzene [6]. Chemical shifts for the aromatic carbons in the polymers, based upon parameters for phenylacetylene and styrene [6] were estimated from the chemical shifts of the oligomers and the assumption that the ethynyl group is converted to an ethene linkage by polymerization. The observed ¹³C spectra are summarized in Table II, and the reasonable agreement between the observed and estimated chemical shifts supports the polyene structure assumed for each polymer.

Changes in ¹³C spectra induced by the addition of Eu(fod)₃ to oligomer and polymer (II) are illustrated in Figs. 4 and 5, respectively. Figure 4 reveals that the largest downfield shifts of the aromatic carbons in the oligomer occur at positions l and m which are directly bonded to the sulfone nucleus. In Fig. 4 the ethynyl carbons at 78.3 and 82.2 ppm are unchanged by the addition of Eu(fod)₃.

In the spectrum of polymer (II), the aromatic carbon formally assigned to the 119.9-ppm line in the oligomer is broadened and extends over the range 118-120 ppm, as indicated by the hatched area in Fig. 5. In addition, a broad resonance in the region expected for olefinic carbons was observed in the spectra obtained for the polymer solutions containing 0.04 to 0.06 MEu(fod)₃. The chemical shifts of α - and β -carbons in substituted styrenes are reported to occur in the range 133-150 and 109-120 ppm, respectively, relative to TMS [8].

Additional work involving ¹³C spectra is in progress to further elucidate the polymer structures. It is anticipated that these experiments will provide additional information related to the stereochemistry of the polymer chains.

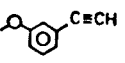
ACKNOWLEDGEMENTS

The authors wish to thank Dr. F. E. Arnold and Mr. B. A. Reinhardt of the Air Force Materials Laboratory for synthesis of oligomers. Research sponsored in part by Air Force Systems Command, Air Force Materials Laboratory, Wright-Patterson AFB, OH, under Contract. No. F33615-77-C-5175.

REFERENCES

1. R. F. Kovar, G. F. L. Ehlers, and F. E. Arnold, *J. Polym. Sci. Chem. Ed.*, **15**, 1081 (1977).
2. C. I. Simionescu, V. Percec, and S. Dumitrescu, *J. Polym. Sci. Chem. Ed.*, **15**, 2497 (1977).
3. J. P. Phillips, *Spectra-Structure Correlation*, Academic Press, NY, 1964, p. 47.
4. W. West, Ed., *Chemical Applications of Spectroscopy*, Vol. IX, *Technique of Organic Chemistry*, Interscience, NY, 1956, pp. 388, 392-94.
5. J. P. Phillips, *op. cit.*, pp. 94, 130.
6. F. W. Wehrli and T. Whithlin, *Interpretation of Carbon-13 NMR Spectra*, Heyden, London, 1978, p. 47.
7. C. F. Poranski, W. B. Moniz, and T. W. Giants, *Coatings and Plastics Chemistry Preprints*, **38**, 605 (1978).
8. K. S. Dhami and J. B. Strothers, *Can. J. Chem.*, **43**, 510 (1965).

Table I. SUMMARY OF ^1H NMR DATA

Oligomer ^a			Polymer	
X	Obs. δ (ppm)	Assign ^b	Obs. δ (ppm)	Assign ^b
H	7.9, 8.0	g, h	7.8	g, h
	7.5	i, e	7.5	i, c, l
	7.3	b, e	6.0-7.2	b, d, f, j, =CH
	7.2	d		
	7.0	f, j		
	3.1	a		
	7.9	g	7.9	g
	7.3	b, e	7.4	b, e
	7.1	d	7.1	c, d, f, =CH
	7.0	f, c	3.1	a
	3.1	a		

^aFor X \neq H, g=h, f=i

^bBased on first-order analysis of multiplets.

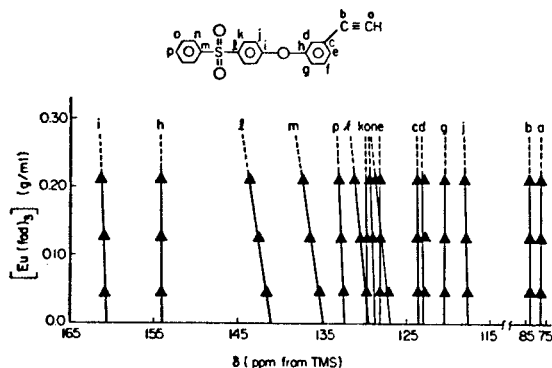


Fig. 4. ^{13}C Spectrum for oligomer (II), δ vs. $[\text{Eu}(\text{fod})_3]$.

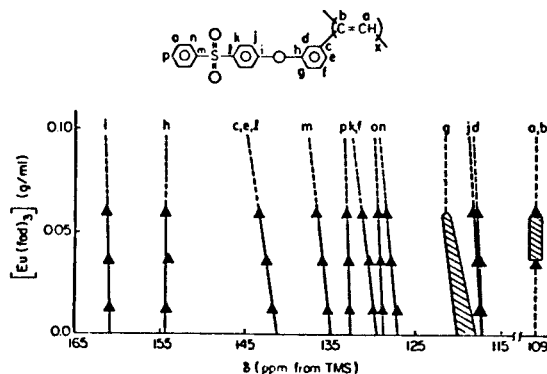


Fig. 5. ^{13}C Spectrum for polymer (II), δ vs. $[\text{Eu}(\text{fod})_3]$.

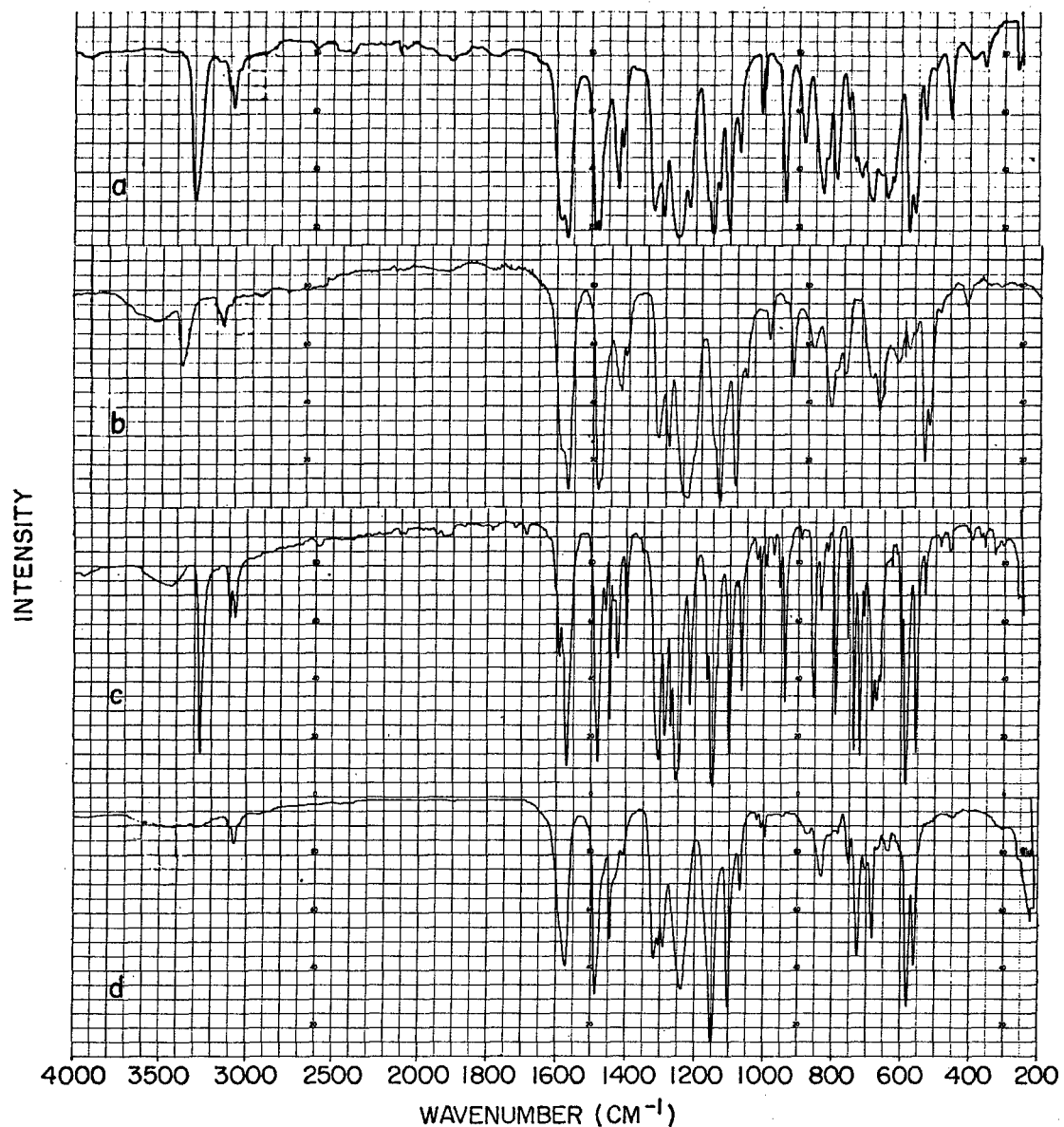


Fig. 1. IR spectra. (a) oligomer (I), (b) polymer (I), (c) oligomer (II), (d) polymer (II).

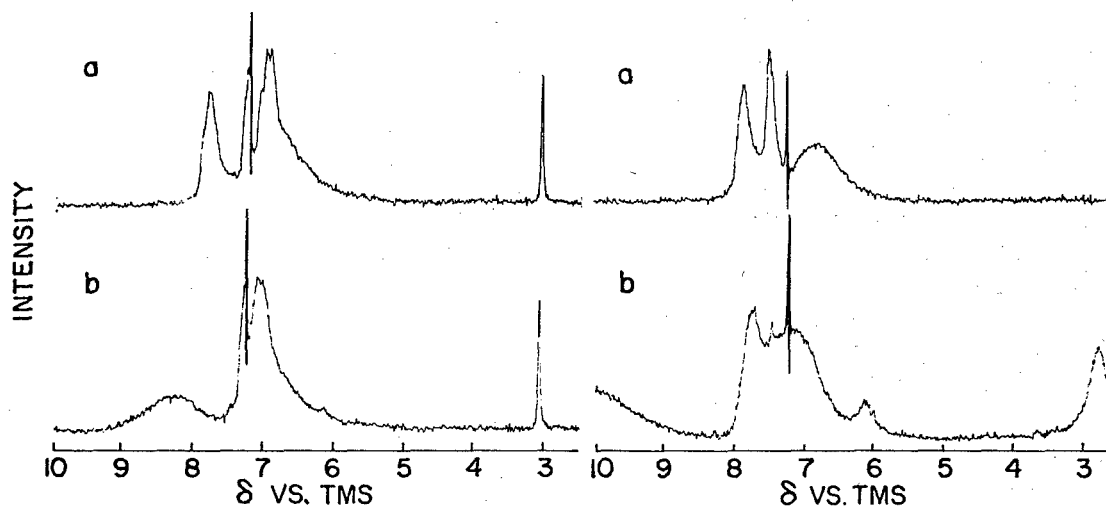
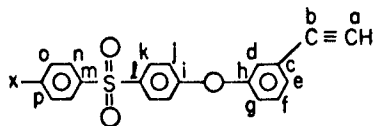
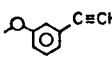


Fig. 2. ¹H NMR spectra. (a) polymer (I), (b) polymer (I) with Eu(fod)₃.

Fig. 3. ¹H NMR spectra, (a) polymer (II), (b) polymer (II) with Eu(fod)₃.

Table II. SUMMARY OF ^{13}C NMR DATA

$\frac{X}{H}$	Oligomer ^a			Polymer		
	Obs. δ^b (ppm)	Calc. δ (ppm)	Assign.	Obs. δ^b (ppm)	Calc. δ (ppm)	Assign.
	78.3		a	109		a,b
	82.2		b			
	117.5		j	117.2, 117.4	117.3	d j
	120.4	119.9	g	118-120	120.1	g
	123.1	123.9	d			
	123.6	123.5	c			
	126.9		n	126.9		n
	128.1	128.3	e			
	128.7		o	128.7		o
	129.4		k	129.4	129.4	f,k
	129.6	130.0	f			
	132.4		p	132.5		p
	134.9		m	134.8		m
	141.4		l	141.1	139.2, 143.7	l,c,e
	154.0	154.3	h	154.4	153.8	h
	160.6		i	160.9		i
		79.7		a	79.8	
82.4			b	82.4		b
				117.8		d
				117.9		j
118.2			j	118.3		j
121.1			g	121.1		g
123.4			d	123.4		d
124.4			c	124.4		c
				128.5		n
128.6			e	128.7		e
129.6			k	130.1		k
130.0			f	130.7		f
135.7			l	136.6		l,m
154.6			h	155.2		h
				160.4		
161.1			i	161.4		i

^aFor $X \neq H$; $p = i$; $n = k$; $o = j$; $m = l$.

^b Measured from CDCl₃ and converted to TMS scale by $\sigma_{\text{CDCl}_3} - \sigma_{\text{TMS}} = 76.91$.

THE KINETICS AND MECHANISM OF THE BULK THERMAL POLYMERIZATION
OF BIS[4-(3-ETHYNYLPHENOXY)PHENYL]SULFONE

<u>James M. Pickard</u>	Systems Research Laboratories, Inc.	x	x
E. Grant Jones	Research Applications Division		
	2800 Indian Ripple Rd.		x
	Dayton, Ohio 45440; phone 513-426-6000		
Ivan J. Goldfarb	Air Force Materials Laboratory		
	Air Force Wright Aeronautical Laboratories		
	Air Force Systems Command		
	Wright-Patterson Air Force Base, Ohio 45433		
	Systems Research Laboratories, Inc., 2800 Indian Ripple Rd., Dayton, OH 45440		
	Air Force Materials Laboratory, Wright-Patterson Air Force Base, OH 45433		
X	Macromolecules		none

THE KINETICS AND MECHANISM OF THE BULK THERMAL POLYMERIZATION OF BIS[4-(3-ETHYNYLPHENOXY)PHENYL]SULFONE. James M. Pickard and E. Grant Jones, Systems Research Laboratories, Inc., Research Applications Division, 2800 Indian Ripple Rd., Dayton, OH 45440; and Ivan J. Goldfarb, Air Force Materials Laboratory, Air Force Wright Aeronautical Laboratories, Air Force Systems Command, Wright-Patterson Air Force Base, OH 45433.

The kinetics of the bulk thermal polymerization of bis[4-(3-ethynylphenoxy)phenyl]-sulfone were determined using differential scanning calorimetry over the range 450 to 510 K. Least squares analyses of the rate data were used to obtain an apparent activation energy, $E=24.2 \pm 0.7$ kcal/mol, and logarithm of the pre-exponential factor, $\log(A/s^{-1})=8.5 \pm 0.6$. In the pre-gel stages of polymerization at constant conversion, the number-average molecular weight of the polymer exhibited a small exponential temperature dependence. These data are examined in terms of a free-radical chain mechanism in which molecular weight is controlled by a first-order termination reaction.

Acknowledgement: Research sponsored in part by the Air Force Systems Command, Air Force Materials Laboratory, Wright-Patterson Air Force Base, OH 45433 under Contract No. F33615-77-C-5175.

THE KINETICS AND MECHANISM OF THE BULK THERMAL POLYMERIZATION
OF BIS[4-(3-ETHYNYLPHENOXY)PHENYL]SULFONE

by

J. M. Pickard and E. G. Jones
Research Applications Division
Systems Research Laboratories, Inc.
2800 Indian Ripple Rd.
Dayton, OH 45440

and

I. J. Goldfarb
Air Force Materials Laboratory
Air Force Wright Aeronautical Laboratories
Air Force Systems Command
Wright-Patterson Air Force Base, OH 45433

INTRODUCTION

During the past decade, acetylene-terminated oligomers which cure by the facile reaction of the terminal ethynyl groups have received considerable attention due to their use as adhesives and composites in high-temperature aerospace environments [1]. While several suggestions have been made that the curing reaction involves a polycondensation or aromatization of the ethynyl moieties which leads to diverse products consisting of tri-substituted benzenes, naphthalenes, and cyclooctatetrenes [2,3], apparently little effort has been directed toward elucidating the reaction mechanism. In a previous paper [4], evidence was presented which indicated that below 50% conversion, bis[4-(3-ethynylphenoxy)phenyl]-sulfone polymerizes in the range 400 to 500 K to yield a conjugated polyene having a molecular weight approaching 3000. These observations, which imply a reactivity comparable to that of simple arylacetylenes, suggest that the pre-gel stage of the curing reaction of the oligomers proceeds by conventional free-radical polymerization. In this paper, the kinetics of polymerization of bis[4-(3-ethynylphenoxy)phenyl]sulfone are presented, and evidence is offered in support of a free-radical chain mechanism in which molecular weight is governed by a first-order termination reaction.

EXPERIMENTAL

Kinetics

Rates of polymerization were determined by dynamic differential scanning calorimetry (DSC) using a Perkin-Elmer DSC-2 calibrated against lead and indium at heating rates of 5, 10, 20, 40, and 80 K/min. Rates of conversion, da/dt , were calculated from

$$\frac{da}{dt} = \frac{1}{Q} \left(\frac{dq}{dt} \right) = 10^{-E/\theta} F(\alpha), \quad (i)$$

where Q is the apparent heat of reaction (in mcal), dq/dt is the differential output (in mcal s^{-1}), A and E are the usual Arrhenius parameters, and $\theta = 2.303RT$ kcal/mol. The quantity $F(\alpha)$ is a concentration variable and is expressed as

$$F(\alpha) = (q/Q)^n = (1-\alpha)^n, \quad (ii)$$

where q is the partial heat of reaction at time t , α is conversion, and n is the reaction order. Equations (i) and (ii) are combined to obtain

$$\frac{d\alpha}{dt} = A 10^{-E/\theta} (1-\alpha)^n = k_{ap} (1-\alpha)^n \quad (iii)$$

where k_{ap} is the observed rate constant.

Molecular Weight Measurements

Molecular weight data were obtained with a Waters Model 244 Liquid Chromatograph (GPC) using 10^4 , 10^3 , $2(5 \times 10^2)$, and 10^2 Å μ -STYRAGEL columns with THF as the solvent at a flow rate of 1 ml/min. Calibration of the GPC columns was based upon isolated fractions of a polymer of known molecular weight determined by vapor phase osmometry. Examination of the GPC trace of the reaction products revealed the presence of the polymer as well as two oligomeric fractions. Weight- and number-average molecular weights of the product distribution, including the oligomeric fractions, were determined as functions of conversion and temperature from the areas of the GPC curves.

RESULTS AND DISCUSSION

DSC Kinetics

In order to evaluate the temperature dependence of the rate data, Eq. (iii) was rearranged to obtain

$$\log \left(\frac{d\alpha}{dt} \right) = \frac{-E}{2.303R} \left(\frac{1}{T} \right) + \log A (1-\alpha)^n. \quad (iv)$$

For constant conversion and assuming A and n to be constant, Eq. (iv) should yield a linear relation between $\log(d\alpha/dt)$ and the reciprocal of absolute temperature. Therefore, the apparent activation energy may be determined from the slope of a plot of Eq. (iv) obtained from different extents of conversion. A representative Arrhenius plot for data obtained for five heating rates in the range 10 to 60% is given in Fig. 1. Examination of Fig. 1 reveals that the data obtained at different extents of conversion and variable heating rates fall on lines having the same slope, thereby indicating that the activation energy is independent of both conversion and heating rate.

Taking the logarithm of Eq. (iii) yields

$$\log AF(\alpha) = \log A (1-\alpha)^n = n \log(1-\alpha) + \log A. \quad (v)$$

Values of $AF(\alpha)$, calculated from the average activation energy and rate data at each heating rate, were combined with conversion data and values for n and A were determined from the slope and intercept, respectively, using Eq. (v). From 463 to 504 K in the range 20 to 60% conversion, the reaction was found to be significantly less than first-order, with $n = 0.33$. Least squares analysis of the rate data in Fig. 1 was used to obtain the logarithm of the apparent rate constant,

$$\log(k_{ap}/s^{-1}) = (8.5 \pm 0.6) - \frac{(24.2 \pm 0.7)}{\theta}, \quad (vi)$$

where the uncertainties correspond to one standard deviation. The logarithm of the observed A factor compares favorably with values reported previously for bulk polymerization of simple arylacetylenes [5,6], namely, phenylacetylene ($\log A/s^{-1} = 8.1$) and (3-phenoxyphenyl)acetylene ($\log A/s^{-1} = 7.6$).

Values of Q obtained from the integral of the DSC exotherms were averaged to obtain the enthalpy of polymerization, $\Delta H_p = -55 \pm 6$ kcal/mol.

Effect of Reaction Variables on Molecular Weight

Figure 2 illustrates the variation of the dispersion ratio, i.e., the ratio of the weight- and number-average molecular weights, M_w/M_n , with conversion for samples of the oligomer polymerized at 434 K. Examination of Fig. 2 reveals that $M_w/M_n \approx 1.5$ up to approximately 30% conversion. Under conditions where conversion exceeds 30%, M_w/M_n rises rather rapidly as the reaction approaches the gel point. The intersection of tangents drawn along each of the linear branches in Fig. 2 implies that the critical conversion for gel formation exceeds 35%.

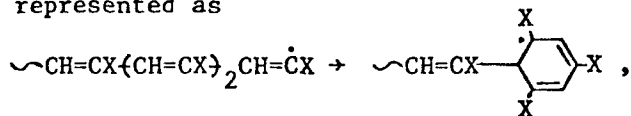
The influence of temperature upon the number-average molecular weight at 25% conversion in the range 390 to 510 K is shown in Fig. 3. Although the data are somewhat scattered, M_n exhibits a small but significant exponential temperature dependence. For a conventional free-radical mechanism controlled by second-order termination, one expects a sizeable temperature dependence for the polymer molecular weight since the kinetic chain length is inversely proportional to the square root of the rate of initiation. The small temperature variation shown in Fig. 3 suggests that in the pre-gel stage of polymerization, molecular weight is governed by a first-order termination.

Reaction Mechanism

If it is assumed that kinetic and molecular chain lengths are controlled by a first-order termination, then application of the steady-state hypothesis assuming short kinetic chains leads to

$$-\frac{dM}{dt} = R_i \left\{ 1 + \frac{k_p}{k_t} M \right\} \quad (\text{vii})$$

for the net disappearance of monomer, where M is the monomer concentration, R_i is the rate of initiation, and k_p and k_t are specific rate constants for propagation and termination, respectively. The suggested first-order termination most likely involves intramolecular cyclization [7] which may be represented as



where X corresponds to the pendant 3-[4-[[4-(3-ethynylphenoxy)phenyl]-sulfonyl]phenyl]phenyl substituents attached to the polymer backbone. The cyclohexadienyl radicals formed in the first-order termination reaction may disappear by several competing reaction pathways involving (a) aromatization via proton transfer to monomer, (b) unimolecular elimination of a cyclic trimer followed by radical combination and/or disproportionation, and (c) direct formation of the polymer through radical combination. Analogies drawn from the thermochemistry for simple free radicals would favor reaction (b); however, reactions (a) and (c) cannot be totally excluded. Reactions such as (a) and (c) provide a mechanism for introducing aromatic moieties into the polymer backbone and are qualitatively consistent with ^{13}C magic-angle measurements on acetylene-terminated polyimides by Sefcik and co-workers [8] which indicate that less than 30% of the ethynyl groups react by cyclotrimerization.

Under steady-state conditions the number-average degree of polymerization, DP_n , is related to the kinetic chain length, $\lambda = (-dM/dt)/R_i$, by $DP_n = 2\lambda/(1+\beta)$, where β is the fraction of the polymer formed by disproportionation. If k_p/k_t and M are expressed as $A_p/A_t 10^{-(E_p-E_t)/\theta}$ and $M_0(1-\alpha)/(1+\Delta V/V_0)$, respectively, where ΔV is the volume change of polymerization and V_0 and M_0 refer to the volume and molarity of the neat monomer, then Eq. (vii) may be rearranged to obtain

$$\log \left\{ DP_n - 2/(1+\beta) \right\} = - \frac{E_p - E_t}{2.303R} \left(\frac{1}{T} \right) + \log \left\{ \left(\frac{2}{1+\beta} \right) \frac{A_p}{A_t} \left[\frac{M_o(1-\alpha)}{1+\Delta V/V_o} \right] \right\}. \quad (\text{viii})$$

For constant conversion, the decrease associated with $M_o/(1+\Delta V/V_o)$ will be offset by an expected increase in A_p/A_t ; therefore, within a reasonable approximation, the right-hand side of Eq. (viii) involving $(1+\Delta V/V_o)$ should be invariant with temperature. Consequently, a plot of $\log \{ DP_n - 2/(1+\beta) \}$ as a function of the reciprocal of absolute temperature should be linear, having a slope equivalent to $(E_p - E_t)/(2.303R)$.

The value of β is unknown; however, variation of β from zero to unity, while producing a small perturbation to the intercept of Eq. (viii), would have a negligible effect upon the magnitude of $(E_p - E_t)/(2.303R)$. Therefore, β was equated to the average value of 0.5, and the molecular weight data plotted according to Eq. (viii) in Fig. 4 were subjected to least squares analysis to yield

$$\log \left\{ DP_n - 4/3 \right\} = (-1.0 \pm 0.6) + \frac{(3.6 \pm 1.3)}{\theta} \quad (\text{ix})$$

over the range 400 to 476 K. In Eq. (ix) the difference in activation energies for propagation and termination indicates that E_t is approximately 4 kcal/mol larger than E_p . Also, from the intercept it may be inferred that A_t exceeds A_p by an order of magnitude. These observations are qualitatively consistent with predictions derived from semi-empirical thermochemical estimates [9] and strongly imply that the kinetic and molecular chain lengths are governed by opposing thermodynamic factors which overshadow the otherwise favorable reaction energetics.

ACKNOWLEDGEMENTS

The authors express sincere appreciation to Dr. F. E. Arnold and Mr. G. A. Loughran of the Air Force Materials Laboratory for synthesis of the bis[4-(3-ethynylphenoxy)phenyl]sulfone. This research was sponsored in part by the Air Force Systems Command, Air Force Materials Laboratory, Wright-Patterson Air Force Base, OH 45433 under contract No. F33615-77-C-5175.

REFERENCES

1. R. F. Kovar, G. F. L. Ehlers, and F. E. Arnold, *J. Polym. Sci. Chem. Ed.*, **15**, 1081 (1977).
2. A. L. Landis, N. Bilow, R. H. Borchan, R. E. Lawrence, and T. J. Aponyi, *Polymer Preprints*, **15** (2), 537 (1974).
3. P. M. Hergenrother, G. F. Sykes, and P. R. Young, *J. Heterocyclic Chem.*, **13**, 993 (1976).
4. J. M. Pickard, S. C. Chatteraj, and M. T. Ryan, *Polymer Preprints*, preceding paper in this issue.
5. G. N. Bantseyrev, I. M. Scherbakova, M. I. Cherkashin, I. D. Kalikhman, A. N. Chirgir, and A. A. Berlin, *Izv. Akad. Nauk. SSSR, Ser Khim*, 1848 (1969); *Eng. Transl. Bull. Acad. Sci. USSR*, **8**, 1661 (1970).
6. J. M. Pickard, E. G. Jones, and I. J. Goldfarb, *Polymer Preprints*, **19** (2), 591 (1978).

7. S. Amdur, A. T. Y. Cheng, C. W. Wong, P. Ehrlich, and R. D. Allendoerfer, *J. Polym. Sci. Chem. Ed.*, **16**, 407 (1978).
8. M. D. Sefcik, E. O. Stejskal, R. A. McKay, and J. Schaefer, *Macromolecules*, in press.
9. J. M. Pickard, E. G. Jones, and I. J. Goldfarb, *Macromolecules*, submitted for publication.

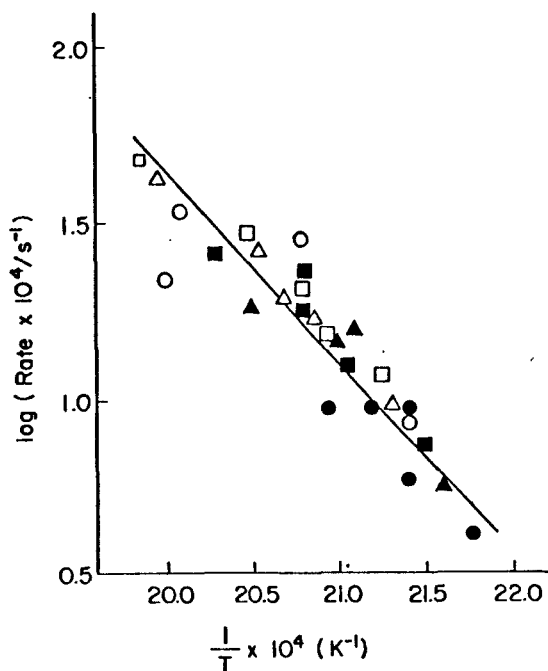


Fig. 1. Arrhenius plot for reaction of bis[4-(3-ethynylphenoxy)phenyl sulfone from 452 to 510 K $\alpha=0.1$ \bullet , 0.2, \blacktriangle ; 0.3, \blacksquare ; 0.4, \circ ; 0.5, \triangle ; 0.6, \square .

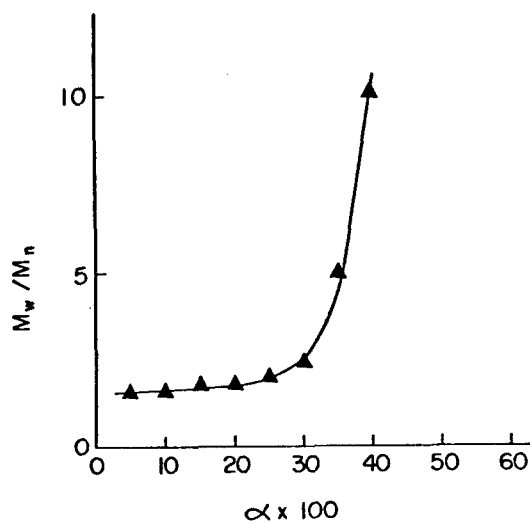


Fig. 2. Influence of conversion upon the dispersion ratio, M_w/M_n , at 434 K.

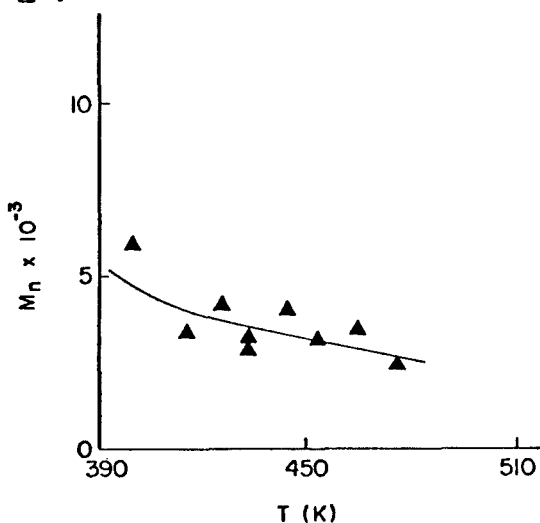


Fig. 3. Temperature dependence of number-average molecular weight at 25% conversion.

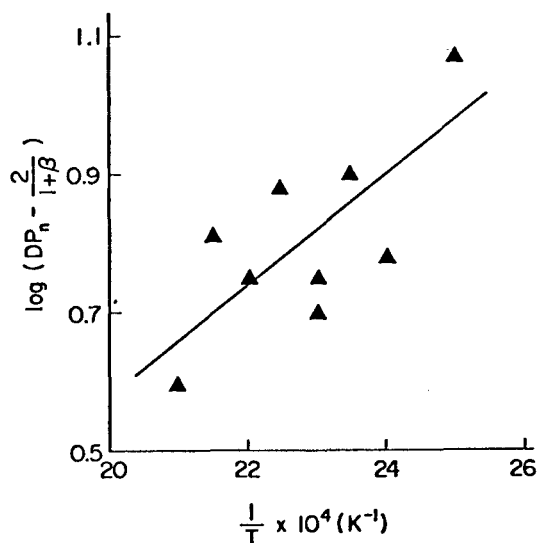


Fig. 4. Plot of Eq. (viii) at 25% conversion assuming $\beta=0.5$, — least squares fit.